MODERN RADIOLOGY eBook

Chest Imaging

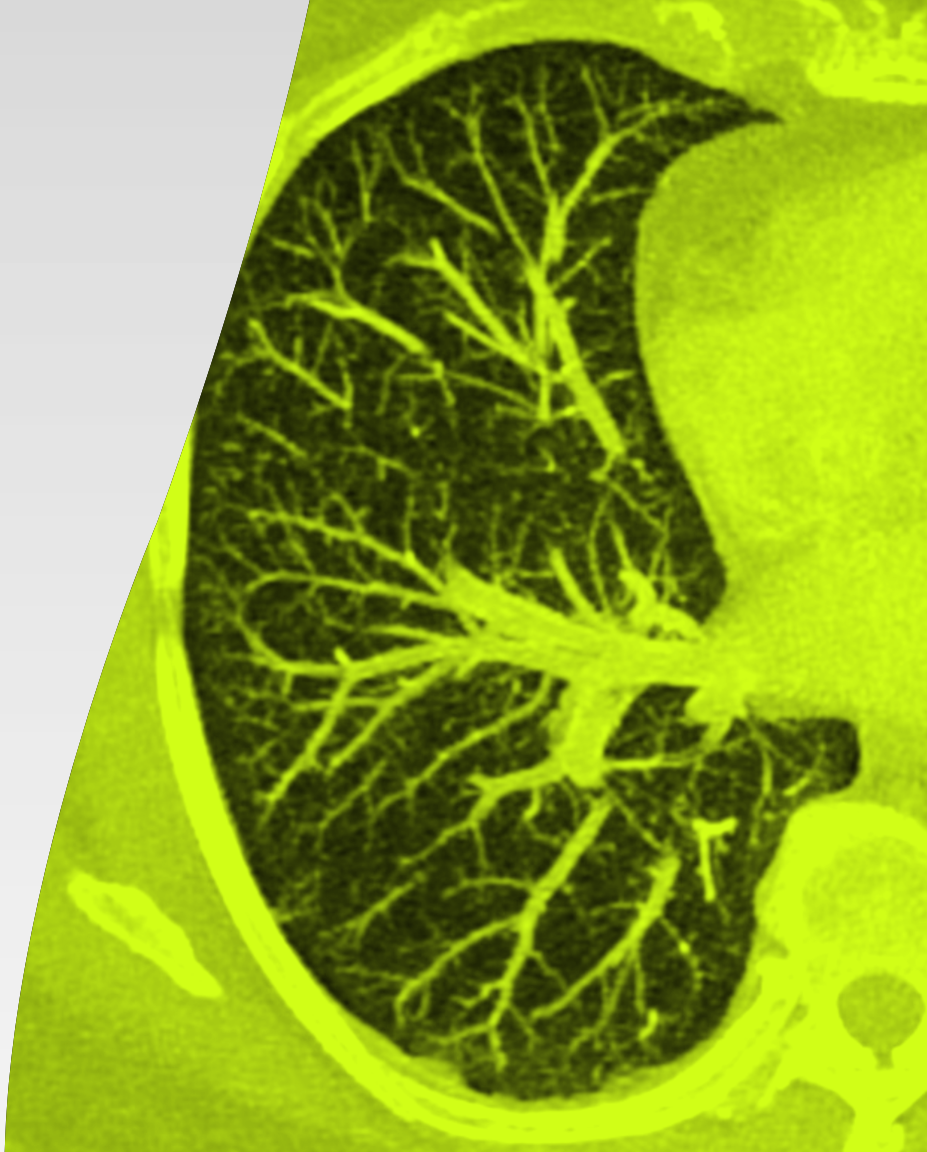

EUROPEAN SOCIETY OF RADIOLOGY

Preface

Modern Radiology is a free educational resource for radiology published online by the European Society of Radiology (ESR). The title of this second, rebranded version reflects the novel didactic concept of the *ESR eBook* with its unique blend of text, images and schematics in the form of succinct pages, supplemented by clinical imaging cases, Q&A sections and hyperlinks allowing to switch quickly between the different sections of organ-based and more technical chapters, summaries and references.

Its chapters are based on the contributions of over 100 recognised European experts, referring to both general technical and organ-based clinical imaging topics. The new graphical look showing Asklepios with fashionable glasses, symbolises the combination of classical medical teaching with contemporary style education.

Although the initial version of the *ESR eBook* was created to provide basic knowledge for medical students and teachers of undergraduate courses, it has gradually expanded its scope to include more advanced knowledge for readers who wish to 'dig deeper'. As a result, *Modern Radiology* covers also topics of the postgraduate levels of the *European Training Curriculum for Radiology*, thus addressing postgraduate educational needs of residents. In addition, it reflects feedback from medical professionals worldwide who wish to update their knowledge in specific areas of medical imaging and who have already appreciated the depth and clarity of the *ESR eBook* across the basic and more advanced educational levels.

I would like to express my heartfelt thanks to all authors who contributed their time and expertise to this voluntary, non-profit endeavour as well as Carlo Catalano, Andrea Laghi and András Palkó, who had the initial idea to create an *ESR eBook* and - finally - to the ESR Office for their technical and administrative support.

Modern Radiology embodies a collaborative spirit and unwavering commitment to this fascinating medical discipline which is indispensable for modern patient care. I hope that this *educational* tool may encourage curiosity and critical thinking, contributing to the appreciation of the art and science of radiology across Europe and beyond.

Minerva Becker, Editor

Chest Imaging

CHAPTER OUTLINE:

Copyright and Terms of Use

How to cite this work:

European Society of Radiology, Minerva Becker, Julien Cohen, Jean-François Deux, Annemiek Snoeckx (2025), ESR Modern Radiology eBook:

- **Chest Imaging. DOI 10.26044/esr-undergraduate-ebook-25**

CHAPTER OUTLINE:

Signage

CORE KNOWLEDGE

ATTENTION

HYPERLINKS

FURTHER KNOWLEDGE

COMPARE

REFERENCES

QUESTIONS

Chest Imaging

CHAPTER OUTLINE:

MODERN RADIOLOGY eBook

Based on the ESR Curriculum for Radiological Education

Chest Imaging

AUTHORS

Minerva Becker[1] | Julien Cohen[1] | Jean-François Deux[1] | Annemiek Snoeckx[2]

AFFILIATION

[1] Division of Radiology, Diagnostic Department, University Hospitals of Geneva, University of Geneva, Geneva, Switzerland

[2] Department of Radiology, Antwerp University Hospital and University of Antwerp, Antwerp, Belgium

<↑> HYPERLINK

Minerva.Becker@hug.ch
Julien.Cohen@hug.ch
Jean-François.Deux@hug.ch
Annemiek.Snoeckx@uza.be

CHAPTER OUTLINE:

Chapter Outline

Introduction

CHAPTER OUTLINE:

/ Introduction

Welcome to the basics of chest imaging!

Understanding the fundamentals of chest imaging is essential for accurately diagnosing a wide range of pulmonary and thoracic conditions. Chest imaging techniques include conventional chest X-rays (CXRs), computed tomography (CT), Positron Emission Tomography CT (PET CT), Magnetic Resonance Imaging (MRI) and ultrasonography (US).

CXRs serve as the cornerstone of thoracic imaging, providing a quick and cost-effective assessment of a variety of diseases. When interpreting CXRs, it's crucial to understand the standard radiographic views and to familiarise yourself with the normal chest anatomy. Developing a systematic approach to CXR interpretation will help you identify abnormalities efficiently and communicate findings effectively.

In addition to CXR, CT has become indispensable for evaluating complex thoracic pathology with greater detail and sensitivity. Understanding the basic CT anatomy and the key CT features of common chest diseases is essential not only for interpreting thoracic CT scans accurately but also for requesting the appropriate imaging investigation as a referring doctor.

The aims of this chapter are

- to briefly discuss relevant advantages and disadvantages of each imaging technique used to investigate chest pathologies
- to understand which is the most appropriate imaging investigation in a specific clinical scenario
- to outline a systematic approach to the interpretation of CXRs
- to introduce the reader to key CT features of common chest diseases

For didactic reasons, correlation of CXR findings with CT and PET CT findings is provided, whenever appropriate.

As chest pathologies are also discussed in other chapters of the ESR e-book, such as cardiac imaging, emergency radiology, vascular imaging or interventional radiology, you will be referred to the respective chapters, whenever necessary.

/ Chest Imaging

CHAPTER OUTLINE:

Diagnostic Imaging Techniques

CHAPTER OUTLINE:

/ Chest X-Ray (CXR)

Chest X-ray (CXR), a fundamental imaging modality in medical diagnostics, plays a pivotal role in evaluating various thoracic conditions. Its versatility, accessibility and cost-effectiveness contribute to its widespread use in clinical practice.

>|< COMPARE

ADVANTAGES:

One of the primary advantages of CXRs is their ability to provide quick and non-invasive visualisation of the thoracic cavity, including the lungs, heart, ribs and surrounding structures. This imaging technique is invaluable for diagnosing a wide range of respiratory conditions such as pneumonia, tuberculosis, chronic obstructive pulmonary disease (COPD) and lung cancer.

Additionally, CXRs are routinely used in the assessment of cardiac abnormalities, rib fractures and pleural effusions.

CXRs also offer the advantage of being readily available in most healthcare settings. The simplicity and speed of obtaining CXRs allow for rapid evaluation of patients presenting with respiratory symptoms or chest trauma, aiding in timely diagnosis and treatment decisions.

DISADVANTAGES:

Despite its numerous advantages, CXRs have limitations. One notable drawback is its lower sensitivity compared to computed tomography (CT) or magnetic resonance imaging (MRI). CXRs may not always detect subtle abnormalities or provide detailed anatomical information, necessitating further evaluation with complementary imaging studies.

Nevertheless, the widespread use of CXRs persists due to their cost-effectiveness, portability and familiarity among healthcare providers. In many clinical scenarios, CXRs serve as the initial imaging modality, guiding further diagnostic workup or treatment plans. Their role as a rapid and accessible tool for assessing thoracic pathology continues to make CXRs a cornerstone of modern medical imaging practice.

The standard radiographic views of CXRs include the erect posterior-anterior (PA) projection, the erect and sitting lateral projections, the supine and erect anterior-posterior (PA) projections.

The technical aspects of conventional X-ray imaging are described in the respective eBook chapter

/ Erect Posterior-Anterior (PA) Projection

<!> ATTENTION

/ The PA projection is the standard frontal radiograph acquired with the patient standing.

/ The image is viewed as if looking at the patient face-to-face

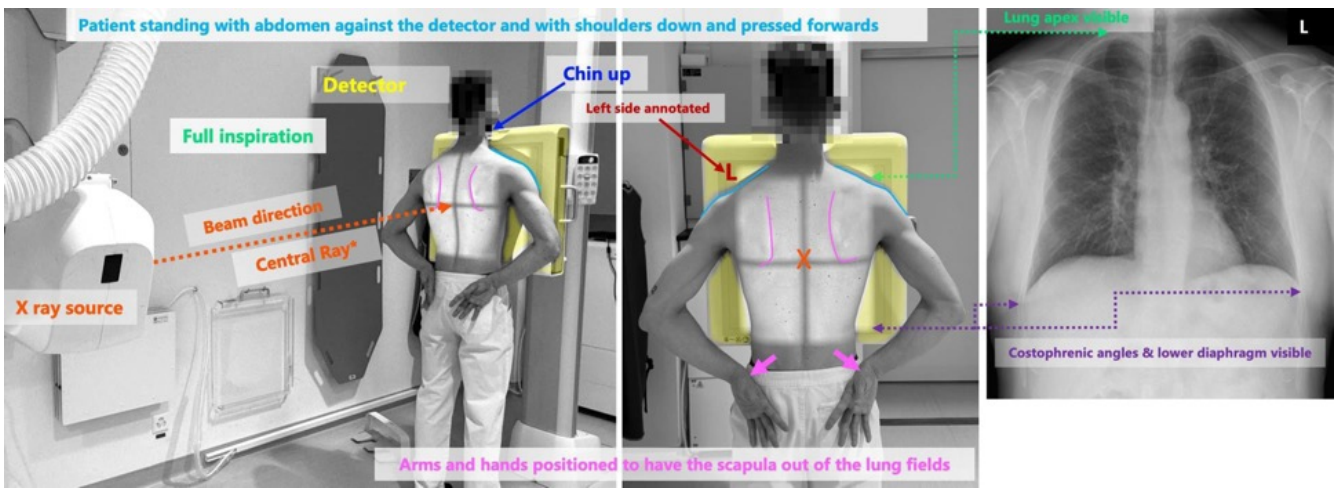

*The Central X-ray is perpendicular to the detector and centred on the midline at the level of the inferior scapula borders
** Digital detector or conventional film cassette.
The distance between the X-ray tube and the detector = 1.80m

Many thanks to Davide Cabral, Damien Locarnoni and Adrien Grobet from the Division of Radiology, Geneva University Hospitals for their contributions to creating this figure.

Technical quality criteria of a CXR PA projection include:

- The **patient identity (name and date of birth)** are indicated on the image
- The **date and hour** when the CXR was obtained are indicated
- The **left side** of the film is indicated and whether this is a **PA projection**
- The CXR should be in a **strict anterior view (no rotation)** > i.e., the distance between the right medial clavicle and the vertical line through the spinous processes of the dorsal spine (**a**) should be equal to the distance between the left clavicle border and the vertical line through the spinous processes of the dorsal spine (b).

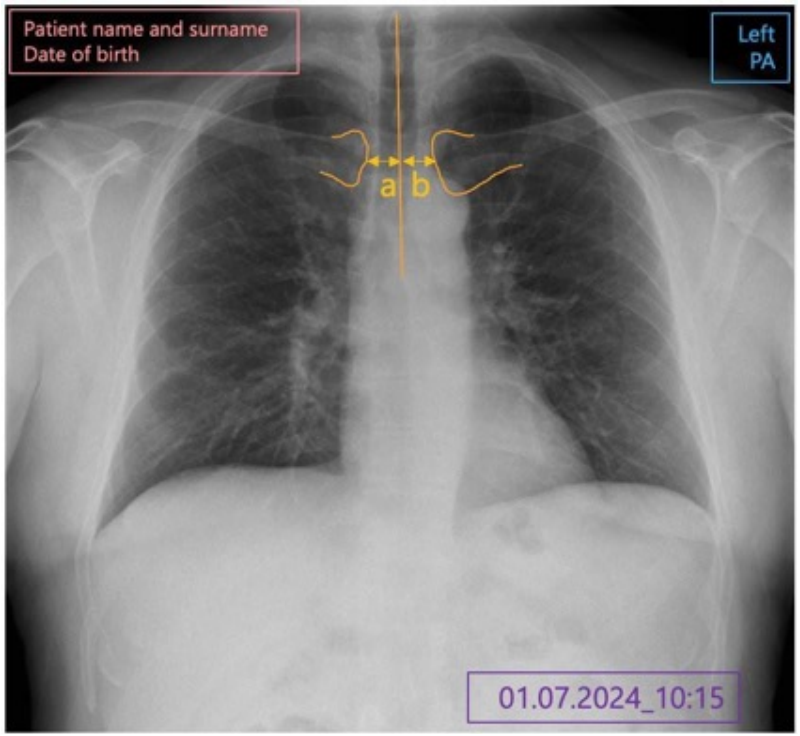

<!> ATTENTION

This is important as rotation may cause anatomical distortion and may result in erroneous image interpretation.

Further technical quality criteria include:

- **The trachea (yellow)** is centred
- Maximum inspiration, i.e., **at least 10 posterior ribs (pink)** should be visible above the **diaphragm (orange)** or 5-7 **anterior ribs (green)** at the **mid-clavicular line (blue)**.

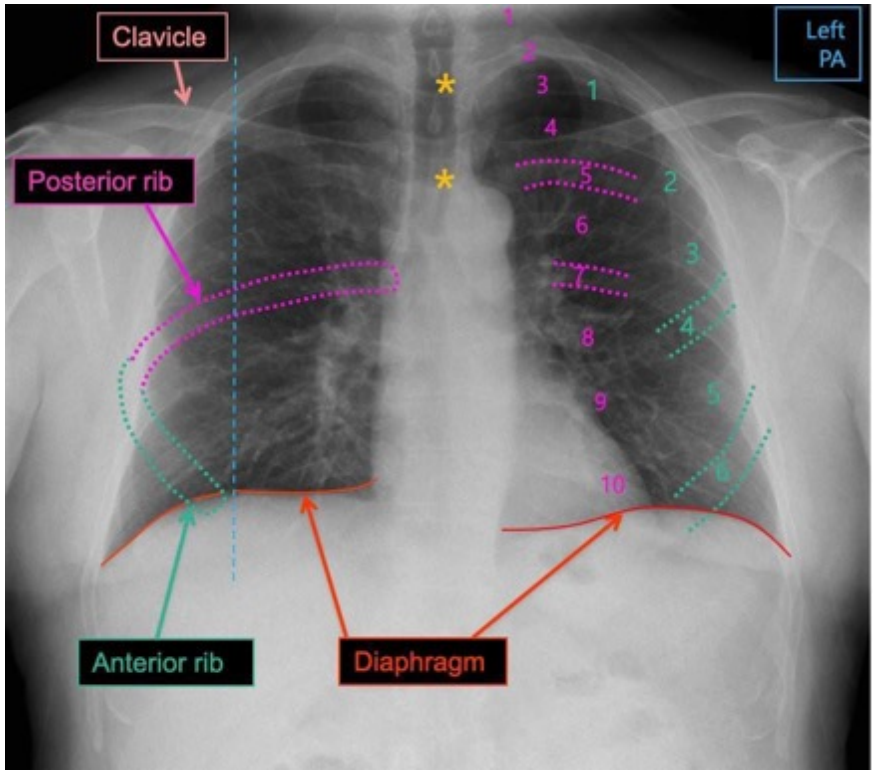

<!> ATTENTION

- To correctly count the ribs, note that the posterior rib portions are more horizontally oriented than the anterior ribs!
- < 5 anterior ribs: insufficient inspiration
- > 7 anterior ribs: lung
- hyperinflation

Finally, technical quality criteria of a CXR include:

- The **lung domes (blue)**, the **costophrenic angles (yellow)** and the **diaphragms (green)** should be clearly visible
- Exposure should be such that the **thoracic vertebrae (red ellipse)** should be slightly visible behind the heart and the **lung vessels (purple ellipse)** should be clearly seen
- The **scapulae (orange)** should be mostly outside the lung fields

<!> ATTENTION

Before making a diagnostic assessment, the technical quality of a CXR should be evaluated to avoid overdiagnosis.

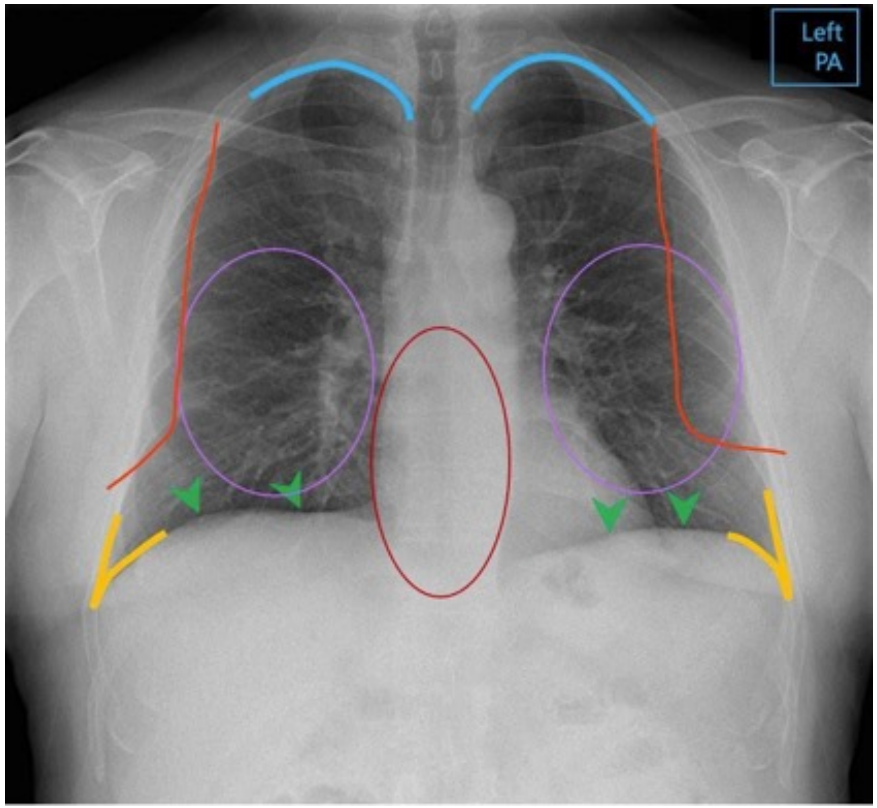

/ Lateral Projections (Erect and Sitting)

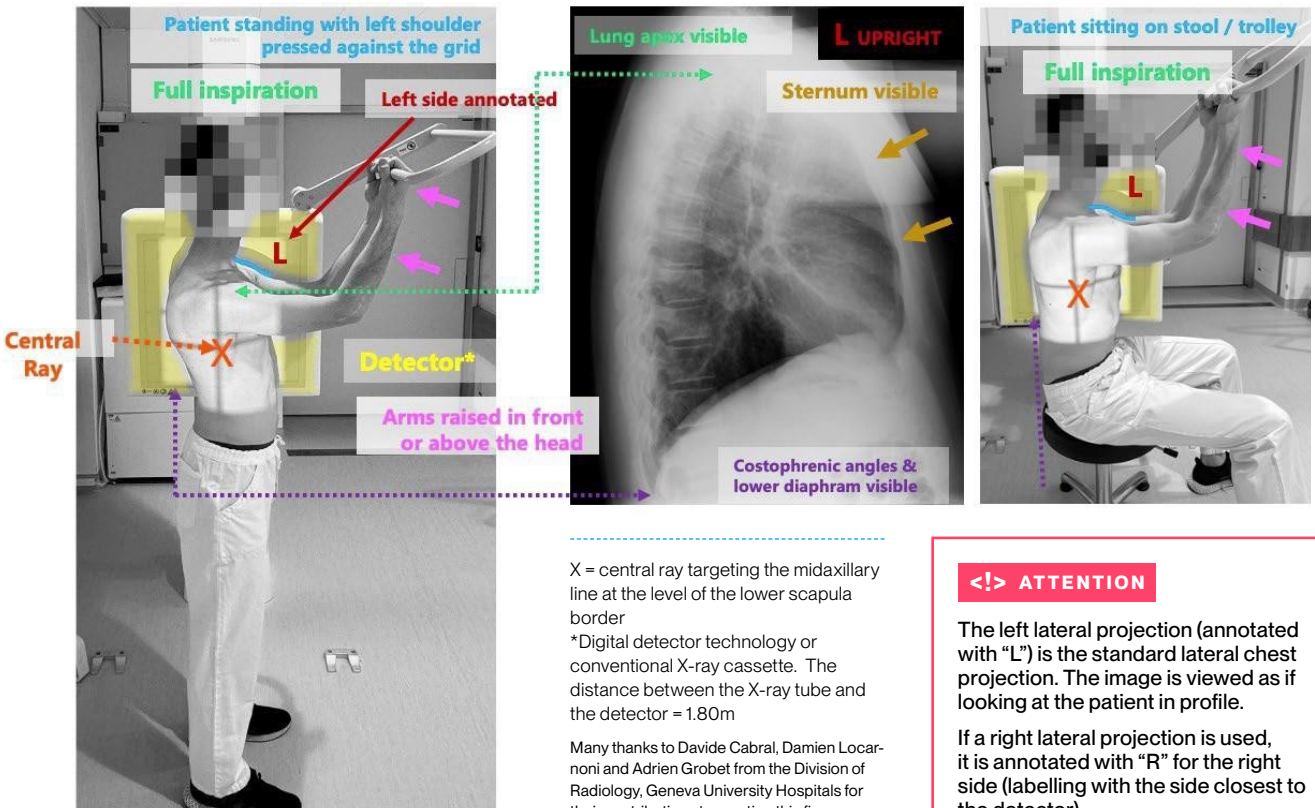

X = central ray targeting the midaxillary line at the level of the lower scapula border
*Digital detector technology or conventional X-ray cassette. The distance between the X-ray tube and the detector = 1.80m

Many thanks to Davide Cabral, Damien Locarnoni and Adrien Grobet from the Division of Radiology, Geneva University Hospitals for their contributions to creating this figure.

<!> ATTENTION

The left lateral projection (annotated with "L") is the standard lateral chest projection. The image is viewed as if looking at the patient in profile.

If a right lateral projection is used, it is annotated with "R" for the right side (labelling with the side closest to the detector)

The technical quality criteria of a lateral CXR include:

- The **lung apices (blue)**, the **costophrenic angles (yellow)** and the **diaphragms (green)** should be clearly visible
- The **sternum (pink)** should be seen

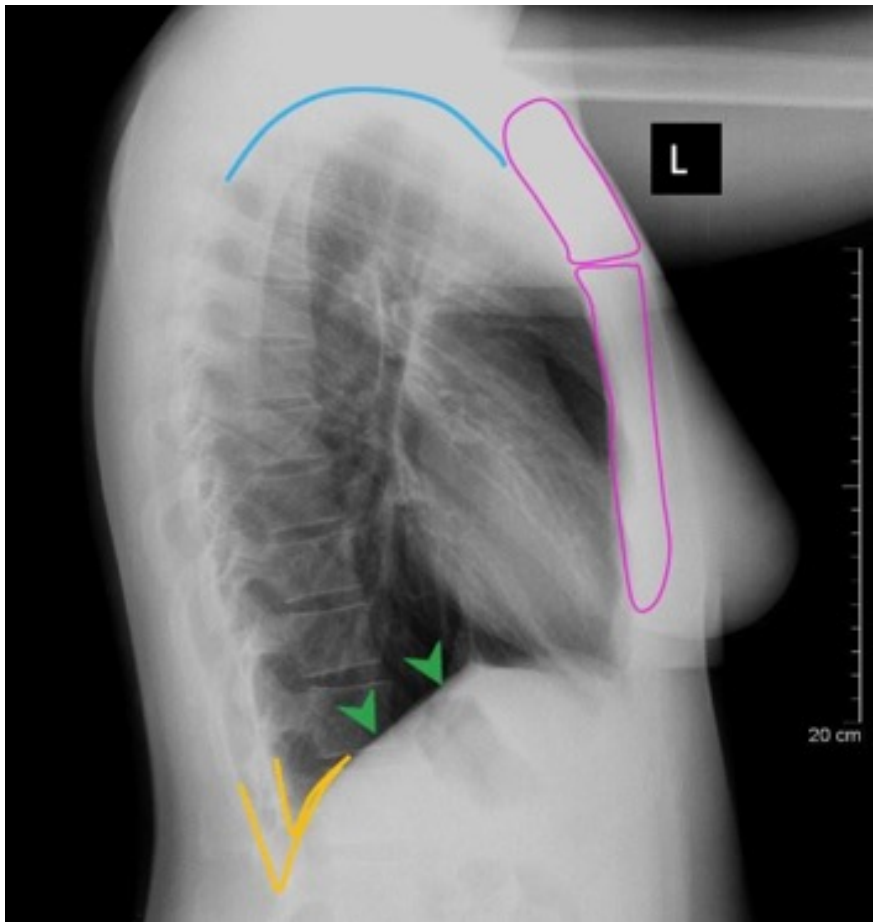

/ Anterior-Posterior (AP) Projections (Supine and Sitting)

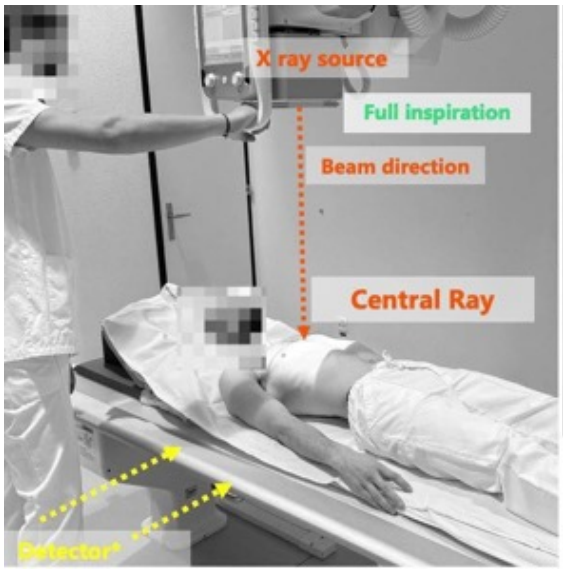

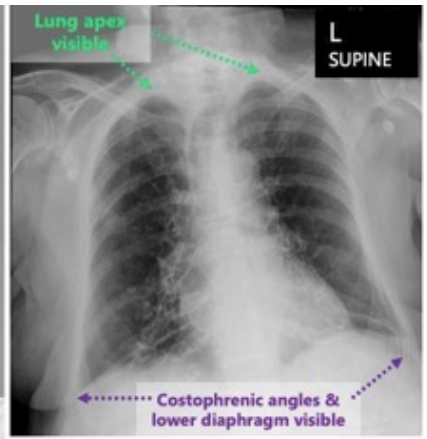

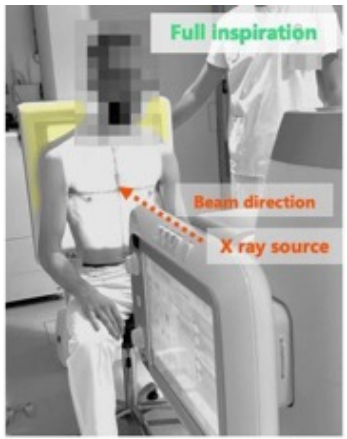

*Digital detector technology or conventional X-ray cassette. The distance between the X-ray tube and the detector should be ideally 1.80m. However, this is not always possible due to ceiling height. Therefore, 1.50m is sometimes used.

Many thanks to Davide Cabral, Damien Locarnoni and Adrien Grobet from the Division of Radiology, Geneva University Hospitals for their contributions to creating this figure.

<!> ATTENTION

The AP supine and the AP erect (in bed or on a stool) projections are used when the patient is too unwell to stand or to sit or when the patient cannot leave the hospital room (isolation).
The image is viewed as if looking at the patient face-to-face.

CHAPTER OUTLINE:

/ Digital Radiography

>|< COMPARE

ADVANTAGES:

Digital CXR offers numerous advantages over traditional film-based CXR. In this technique, X-ray images are captured electronically and viewed on computer screens, eliminating the need for physical film processing.

This digital approach presents several key benefits:

+ enhanced image quality and clarity compared to conventional CXR
+ the digital format allows for manipulation of image contrast, brightness and zoom levels, enabling better visualisation and interpretation of subtle abnormalities
+ lower radiation doses than film-based counterparts, reducing patients' exposure to ionising radiation - this is particularly advantageous for paediatric and pregnant patients, as well as those requiring frequent X-ray examinations
+ ease of storage and transmission. Digital images are stored electronically in picture archiving and communication systems (PACS), facilitating quick retrieval and comparison with previous studies.
+ dgital CXRs can be easily shared with referring physicians or specialists for consultation or further evaluation
+ digital CXRs streamline workflow and increase efficiency in radiology departments
+ no need for film processing or darkroom facilities, saving time and resources
+ images can be acquired, processed and interpreted rapidly, leading to faster diagnosis and treatment decisions

DISADVANTAGES:

Despite these advantages, digital radiography has certain limitations:

– initial cost of implementing digital radiography systems can be substantial compared to traditional film-based equipment

– digital systems require regular maintenance and upgrades to ensure optimal performance, adding to overall operational expenses

In terms of clinical use, digital CXRs are invaluable for diagnosing a wide range of thoracic conditions, as described in this eBook chapter. They are also commonly employed in preoperative evaluations, postoperative monitoring and routine health screenings.

While initial costs and maintenance requirements may present challenges, the numerous advantages (superior image quality, reduced radiation exposure, enhanced workflow efficiency and seamless data management compared to traditional film radiography) make digital CXRs indispensable in modern medical practice.

/ Difference between PA and AP Projections

>|< COMPARE

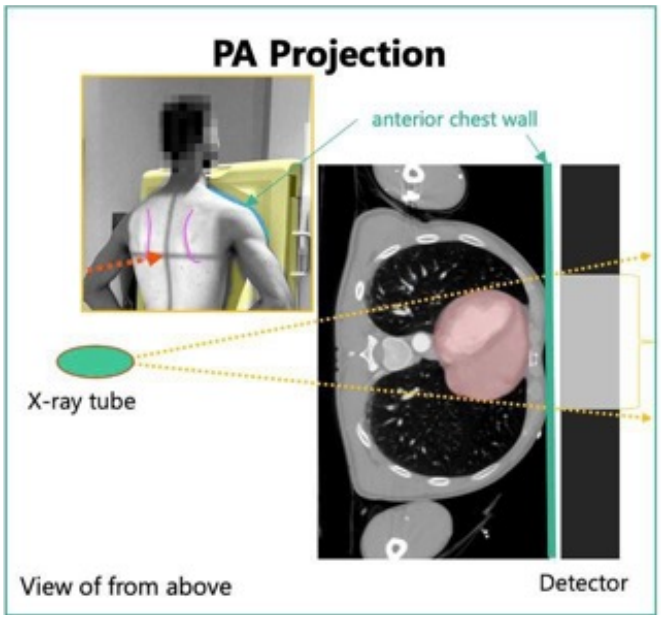

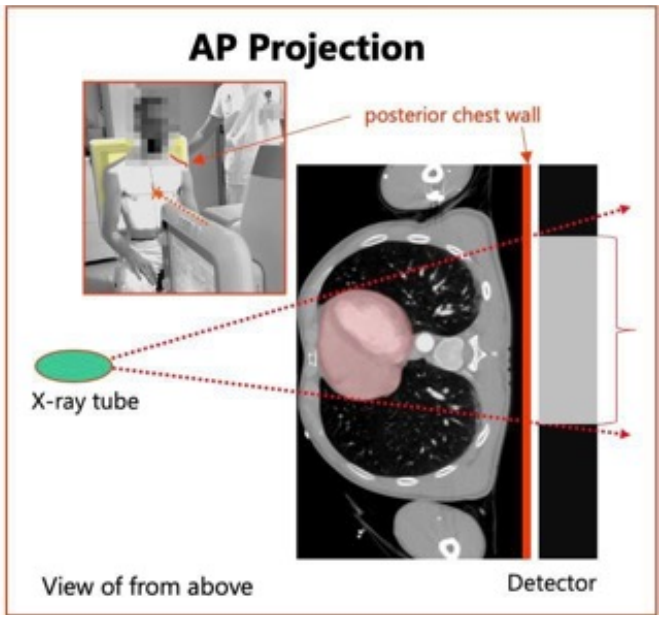

<!> ATTENTION

For the **chest PA** projection, the detector is close to the **anterior (green)** chest wall, therefore, closer to the heart.

For the **chest AP** projection, the detector is close to the **posterior (red)** chest wall, therefore, farther away from the heart.

Due to X-ray beam divergence, the heart appears **larger** on the AP CXR projection compared to the PA projection. The larger heart size on the AP CXR should not be misinterpreted as pathology.

/ Computed Tomography (CT)

Standard CT chest protocols involve intravenous contrast injection and the CT acquisition is started after approximately 20 seconds to visualise arterial structures. Images with **soft tissue (mediastinal, A)**, **bone (B)** and **lung window (C)** settings, as well as 2D reconstructions in the **coronal (D)** and **sagittal (E)** planes are obtained routinely.

Variations include CT angiography (CTA), CT pulmonary angiogram (CTPA), high-resolution CT (HRCT) with thin sections (continuous 1 - 1.5 mm slices) for detailed lung parenchyma evaluation and low dose CT (LD CT) with thin sections.

Indications range from assessing masses, nodules and lung cancer staging to diagnosing vascular and pleural diseases and emergencies like chest trauma or pulmonary embolism.

While chest CT offers quick access and detailed anatomical information, it comes with radiation exposure and some limitations in vascular assessment.

The technical aspects, advantages and disadvantages of CT are described in detail in the eBook chapter on CT. For CTA and CPA **> see eBook chapter on Vascular Imaging**

<!> ATTENTION

When performing a CT of the chest, it is of utmost importance to tailor the examination to the specific questions asked by the referring physician. Therefore, the appropriate clinical information is a must, especially regarding the timing of intravenous contrast delivery, e.g., the CT imaging protocol will be different in suspected lung embolism versus staging of lung cancer.

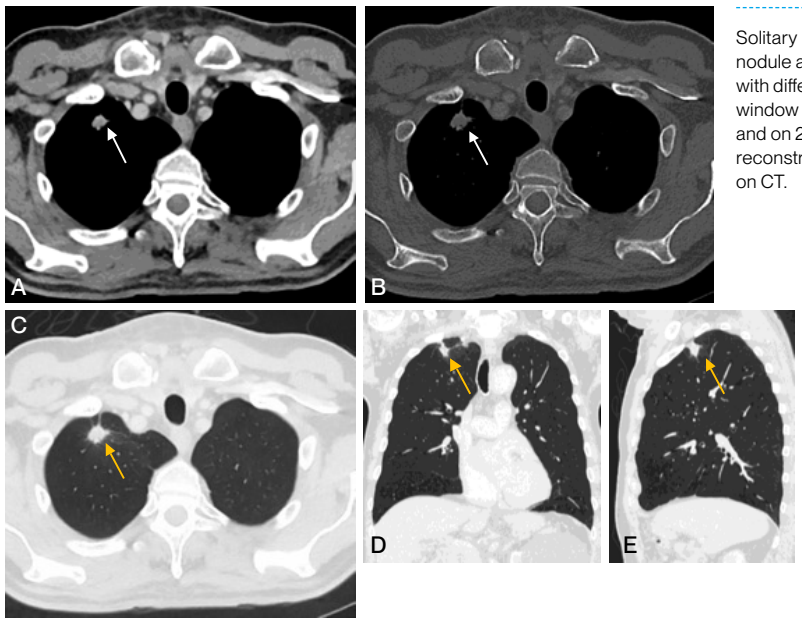

Solitary lung nodule as seen with different window settings and on 2D reconstructions on CT.

/ Ultrasonography (US)

The technical aspects of US are described in the eBook chapter on US.

Ultrasound (US) imaging has emerged as an additional, valuable, non- irradiating tool to evaluate chest pathology.

The main indications for chest ultrasound include:

- / detection and quantification of pleural effusions, guidance of thoracentesis and evaluation of loculated collections
- / diagnosing pneumothorax, particularly in critically ill patients
- / detecting pneumonia and providing monitoring
- / aiding in biopsy guidance of peripherally located chest masses

Contraindications of US are related to patient comfort and cooperation.

US may be limited in obese individuals or those with massive subcutaneous emphysema.

<!> ATTENTION

US is particularly beneficial when immediate assessment is needed, such as in emergency settings or when radiation exposure is a concern (pregnant women or children). Its portability allows bedside evaluation, making it invaluable in critical care settings.

Diagnostic US performance varies depending on the pathology being evaluated. For pleural effusions and pneumonia, US has high sensitivity and specificity. In diagnosing pneumothorax, the reported sensitivity is variable as it depends on pneumothorax size, however, the specificity is high.

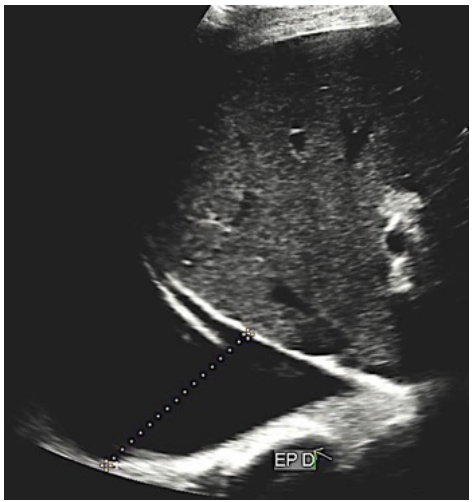

Right pleural effusion detected on US imaging.

<∞> REFERENCES

Lichtenstein DA. Ultrasound in the management of thoracic disease. Crit Care Med. 2007;35(5 Suppl):S250-S261. doi:10.1097/01.CCM.0000260670.67304.40

Volpicelli G, Elbarbary M, Blaivas M, et al. International evidence-based recommendations for point-of-care lung ultrasound. Intensive Care Med. 2012;38(4):577-591. doi:10.1007/s00134-012-2513-4

Abid I, Qureshi N, Lategan N, Williams S, Shahid S. Point-of-care lung ultrasound in detecting pneumonia: A systematic review. Can J Respir Ther. 2024 Jan 29;60:37-48. doi: 10.29390/001c.92182. PMID: 38299193; PMC10830142.

Jahanshir, A., Moghari, S.M., Ahmadi, A. et al. Value of point-of-care ultrasonography compared with computed tomography scan in detecting potential life-threatening conditions in blunt chest trauma patients. Ultrasound J 12, 36 (2020). https://doi.org/10.1186/s13089-020-00183-6

/ Magnetic Resonance Imaging (MRI)

The MRI technique, its advantages and disadvantages are described in the eBook chapter on MRI.

For the indications and utility of MRI in the assessment of cardiac pathology **> see eBook chapter on Cardiac Imaging.**

While CT scans are pivotal in noncardiac chest imaging, MRI is an equivalent or even superior alternative to CT in the following situations:

- / assessing the lung apices, diaphragm, spinal column and pleural pathology
- / characterising masses, which cannot be adequately characterised with CT, e.g., some cystic masses
- / determining neoplastic chest wall invasion and identifying blood vessel or mediastinal invasion
- / detecting metastatic invasion of bone marrow
- / providing functional data to improve treatment response evaluation in cancer

>|< COMPARE

+ MRI offers notable advantages > excellent tissue contrast, multiplanar imaging capability, sensitivity to blood flow and the absence of ionising radiation. Its radiation-free nature makes it particularly suitable for paediatric and pregnant patients, as well as those requiring ongoing monitoring.

– However, MRI is limited by signal loss from lung motion and lack of protons in the lung and magnetic field inhomogeneity due to air-tissue interfaces.

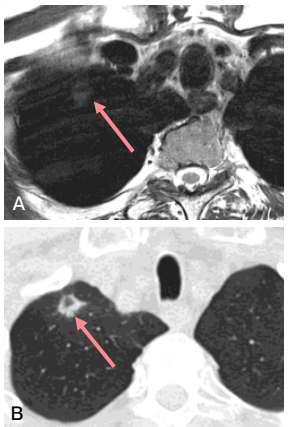

Follow-up MRI obtained in a patient with head and neck squamous cell carcinoma (HN SCC). A right upper lobe nodule was seen on the T2W sequence (A). CT (B) confirmed the presence of a solitary lung nodule. Biopsy revealed lung metastasis from HN SCC.

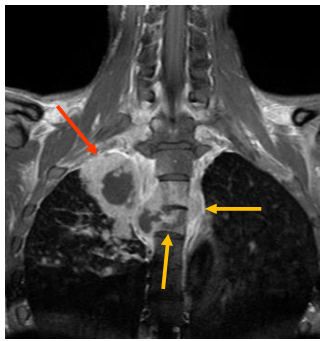

Spinal tuberculosis with a large apical empyema in a different patient. Contrast-enhanced T1W MR image reveals a large **spinal and paraspinal mass with osseous destruction (yellow)** extending into the **right lung apex (red)**.

<∞> REFERENCES

Sim AJ et al. A review of the role of MRI in diagnosis and treatment of early stage lung cancer. Clin Transl Radiat Oncol. 2020 Jun 6;24:16-22. doi: 10.1016/j.ctro.2020.06.002. PMID: 32596518; PMCID: PMC7306507.

Koyama H, Ohno Y, Seki S, Nishio M, Yoshikawa T, Matsumoto S, Sugimura K. Magnetic resonance imaging for lung cancer. J Thorac Imaging. 2013 May;28(3):138-50. doi: 10.1097/RTI.0b013e31828d4234. PMID: 23549390.

/ Positron Emission Tomography CT (PET CT)

The PET CT technique, its advantages and disadvantages are described in the eBook chapter on nuclear imaging.

PET CT plays an important role in the diagnosis, staging and monitoring of tumours in the chest, including lung cancer, oesophageal cancer and lymphomas.

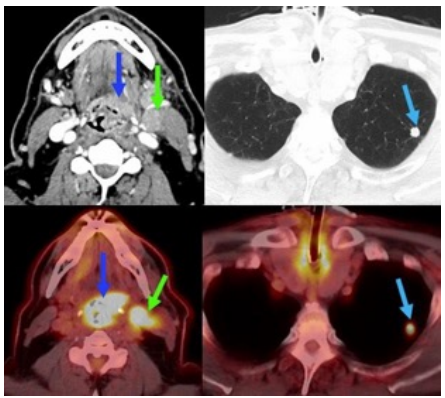

FDG PET CT images of a patient with a histologically proven **primary adenocarcinoma of the lung (light blue)** and a synchronous **primary squamous cell carcinoma of the oropharynx (dark blue)** with **ipsilateral lymph node metastasis (green)**. There were no other metastatic lymph nodes nor distant metastases.

>|< COMPARE

\+ One significant advantage of PET CT is its ability to detect metabolic changes associated with malignancy at an early stage, sometimes before structural changes are evident on CT scans. In selected cases, PET CT may be superior to contrast enhanced CT for the delineation of tumours associated with post- obstructive extensive atelectasis. Although PET CT is of limited value for the T classification of lung cancer, it increases the diagnostic accuracy for the N and M classification. Compared to standalone CT, PET CT offers superior sensitivity and specificity for detecting extra-thoracic metastatic disease, especially osseous and adrenal lesions.
Additionally, PET CT can help differentiate between benign and malignant lesions, reducing the incidence of false positives and unnecessary invasive procedures. PET CT also allows detection of occult primary tumours and second primary cancers, guiding treatment decisions and facilitating therapeutic approaches.
Moreover, PET CT is valuable for monitoring treatment response and detecting disease recurrence, allowing clinicians to adapt treatment strategies accordingly. Its ability to assess both the extent of disease and its metabolic activity provides valuable prognostic information, aiding in patient management and improving outcomes.

– However, PET CT has some limitations, such as its relatively high cost compared to other imaging modalities, which may limit its accessibility in some healthcare settings. Additionally, PET CT involves exposure to ionising radiation, although advances in technology have reduced radiation doses while maintaining image quality.

<∞> REFERENCES

Farsad M. FDG PET/CT in the Staging of Lung Cancer. Curr Radiopharm. 2020;13(3):195-203. doi: 10.2174/1874471013666191223153755. PMID: 31868151; PMCID: PMC8206197.

Kitajima, K., Doi, H., Kanda, T. et al. Present and future roles of FDG-PET/CT imaging in the management of lung cancer. Jpn J Radiol 34, 387–399 (2016). https://doi.org/10.1007/s11604-016-0546-2

Groheux D, Quere G, Blanc E, Lemarignier C, Vercellino L, de Margerie-Mellon C, Merlet P, Querellou S. FDG PET-CT for solitary pulmonary nodule and lung cancer: Literature review. Diagn Interv Imaging. 2016 Oct;97(10):1003-1017. doi: 10.1016/j.diii.2016.06.020. Epub 2016 Aug 24. PMID: 27567555.

/ **Chest** Imaging

CHAPTER OUTLINE:

How to Read a Chest X-Ray (CXR)

CHAPTER OUTLINE:

/ Difference between Tissues: Basic Concepts

The amount of X-ray absorption by tissues depends on their atomic number (Z). It rises with the 3rd power of Z. The absorbed amount defines the density of tissues on an X-ray images

> see eBook chapter on Conventional X-Ray Imaging!

The denser the tissue, the more X-rays are attenuated. Because calcium has a high atomic number, it absorbs X-rays most; therefore, bone appears "whitish" while air appears as "black" areas. Soft tissues, water and fat appear in different shades of grey. As metals have even higher Z, they appear as "white" areas on conventional X-rays.

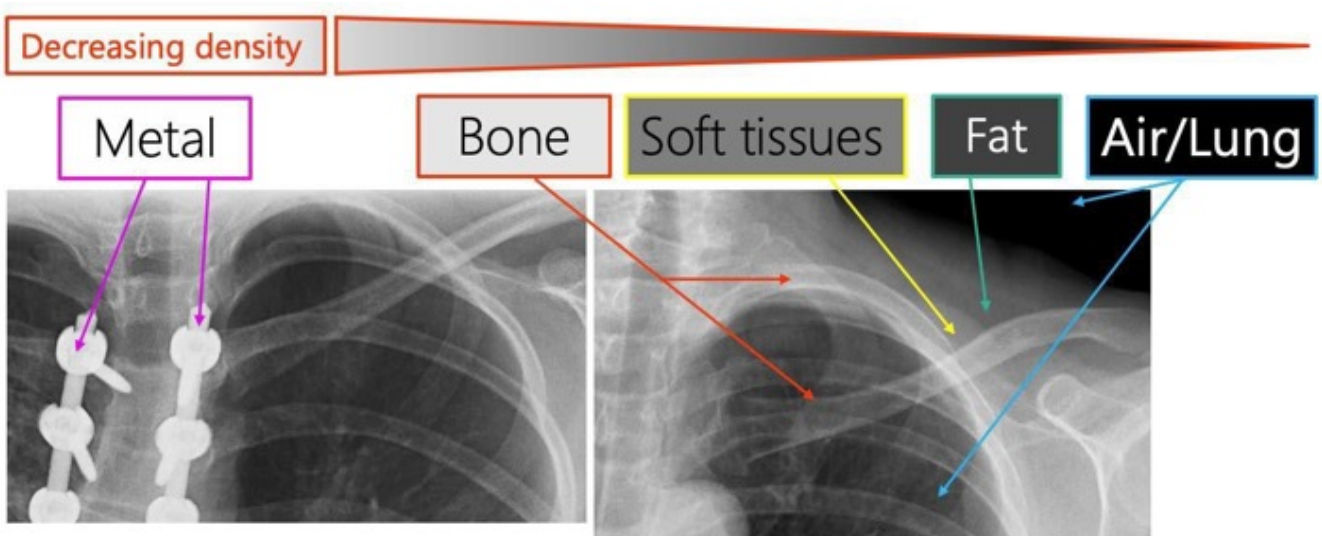

/ A Systematic Approach Is a Must!

There are many different ways to read a CXR, e.g., following the ABCDEFGHI approach (mnemonic chest radiograph assessment mainly used in the English literature):

- Airway
- Bone & soft tissue
- Cardiac
- Diaphragm
- Effusion
- Fields, fissures, foreign bodies
- Great vessels
- Hila & lung
- Impression

Alternatively, a CXR can be read from the **periphery of the CXR image to the centre (red)** (i.e., starting with the soft tissues of the chest wall and bones and then continuing with the pleural spaces, lung contours (mediastinal margins, diaphragm), lungs and pulmonary blood vessels, hila, mediastinum and ending with the heart). Vice-versa a CXR can be read from the **centre of the image to its periphery (green)**.

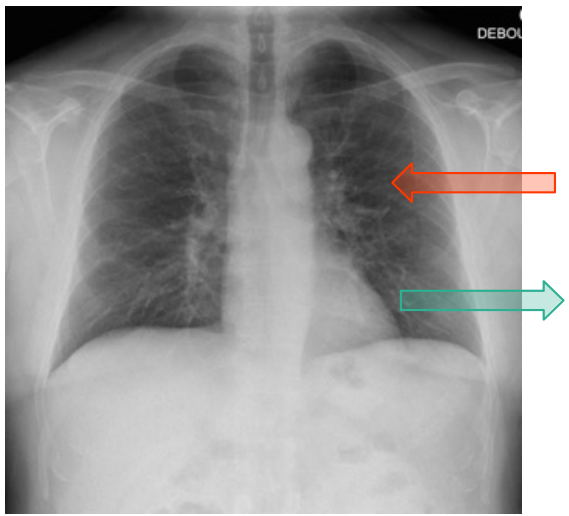

<!> ATTENTION

Independently on how a CXR image is read, one should follow a logical or easy to remember approach. All anatomic structures should be evaluated and the same reading sequence should be followed to avoid missing out lesions! A checklist approach is very useful for the detection of relevant findings. It is advisable to begin with the technical image quality.

The Normal Chest X-Ray (CXR)

CHAPTER OUTLINE:

/ Soft Tissues

In general, the soft tissues of the chest wall, breasts and neck tend to be symmetric. However, some degree of breast asymmetry is very common. As breast tissue can obscure parts of the lungs, asymmetry of lung zones should not be mistaken for underlying lung pathology.

The nipples can sometimes be seen on the PA CXR and they should not be confounded with lung nodules. Metallic nipple markers can be used to indicate the nipple position. This allows to distinguish a nipple shadow from a lung nodule on a CXR.

The normal fat planes between the muscles of the chest wall and the neck are smooth.

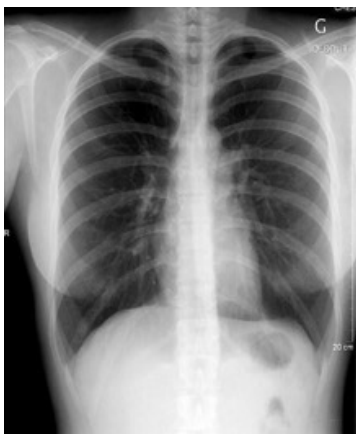

PA CXR with symmetric soft tissues.

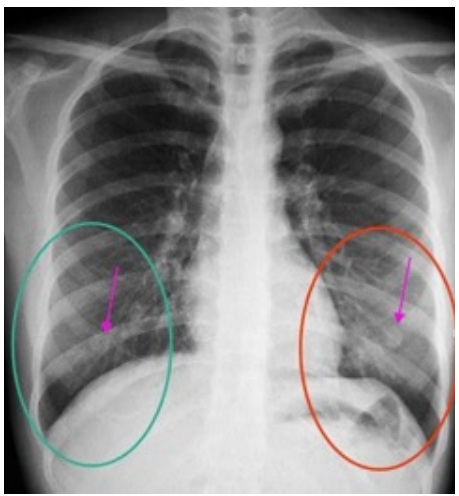

PA CXR with asymmetric soft tissues. The **left lower lung zone (red circle)** appears denser than **the right lower lung (green circle)** zone because of asymmetric breast tissue. **Nipple projections (pink arrows).**

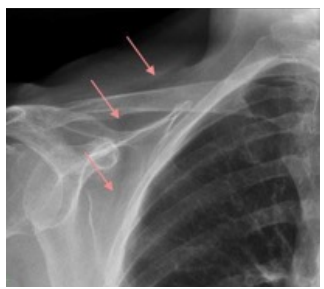

Close-up of a PA CXR shows the **normal fat planes (arrows),** which are less dense than muscles.

/ Bones

The clavicles, scapulae, humeri, ribs, the vertebral column and the sternum are seen on CXRs.

Normal bones have a **dense cortex (blue arrows)** and a **marrow cavity (pink asterisks)** composed of spongy bone, which appears less dense. The **vertebral bodies (green line)** have a regular almost rectangular shape. The spinal processes of the dorsal spine form a **straight line (yellow dashed line)** on the PA CXR. On a lateral CXR, there is **some minor degree of kyphosis curvature** (however, there are large differences in the normal population - **pink dashed line**).

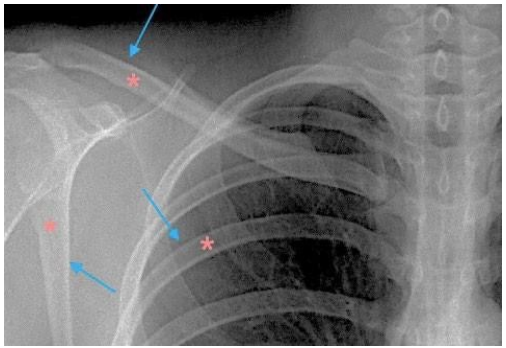

Detail from a PA CXR showing the normal anatomy of the clavicles, scapula, ribs and veretebral bodies.

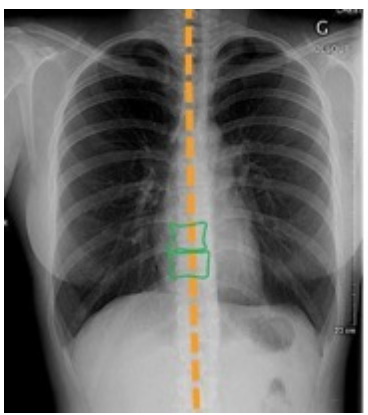

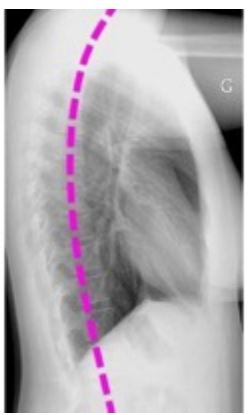

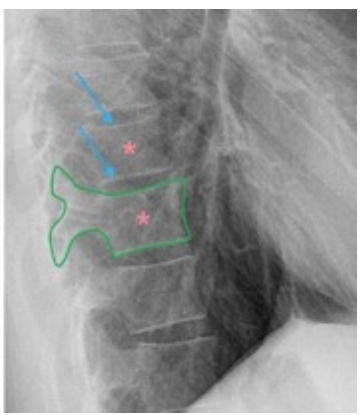

Detail from a lateral CXR showing the normal anatomy of the veretebral bodies.

<!> ATTENTION

CXRs are not very sensitive to bone pathology, which can be easily overlooked as findings can be very subtle.

/ Pleura and Pleural Cavity

The pleura is a serous membrane that encloses the lungs and lines the thoracic cavity. It folds back on itself forming the pleural space or pleural cavity. There is no connection between the right and left pleural space.

The pleural cavity is located between the visceral pleura (attached to the lungs) and the parietal pleura (attached to the opposing chest wall, the exposed thoracic diaphragm surface and the lateral aspect of the mediastinum).

The pleural cavity contains a very small amount of serous fluid which acts as a lubricant and allows for easy lung movement and inflation/deflation during breathing. Under normal circumstances, the visceral and the parietal pleura are in contact with each other. Therefore, the pleural cavity is regarded as a potential space.

The pleural fissures are formed by the visceral pleura surrounding the different lung lobes.

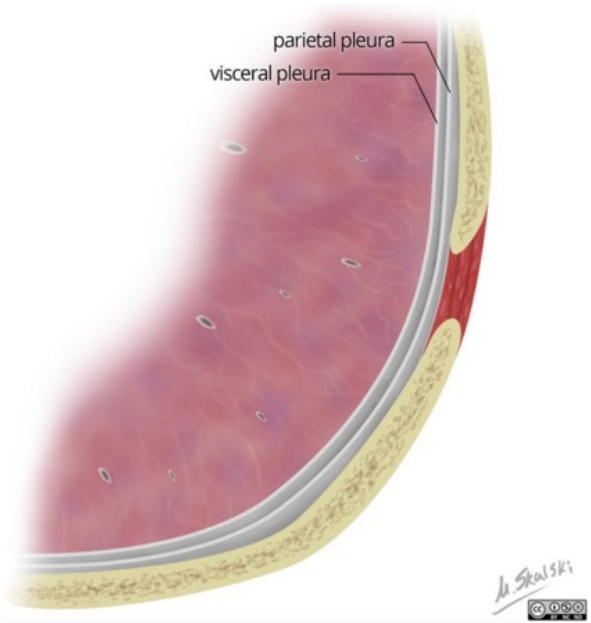

Case courtesy of Matt Skalski, https://radiopaedia.org/?lang=us, Radiopaedia.org. From the case https://radiopaedia.org/cases/53333?lang=us rID: 53333

CHAPTER OUTLINE:

The pleural cavity is clearly seen on CXRs only if it is abnormal.

On a normal CXR, the lung markings should be seen up to the chest wall. The contours of the **left (blue line)** and **right (yellow line)** pleural cavity around the lung edges form a thin line.

The **left (green line)** and **right (light green line)** hemidiaphragm dome cannot be distinguished from the pleural cavity located along the domes. The right hemidiaphragm is either higher or at the same level as the left hemidiaphragm.

The normal **right and left lateral (pink circles)**, **right and left posterior (purple circles)** and the **anterior (blue circle)** costophrenic recesses are seen as the lateral, anterior and posterior costophrenic angles.

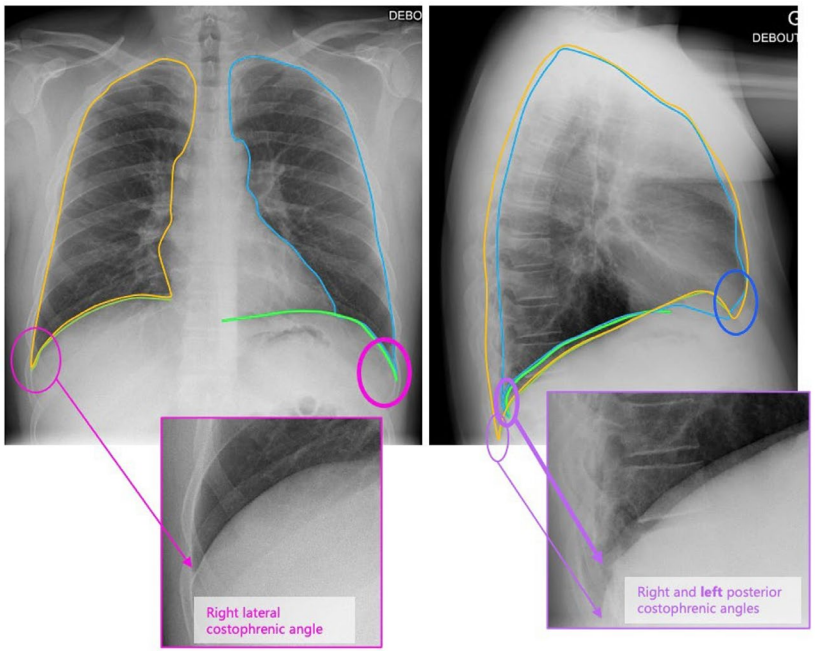

<!> ATTENTION

The costophrenic angles should always be acute and sharply delineated.

On a left lateral CXR, the **right posterior** costophrenic recess appears larger than the **left posterior** recess because it is farther away from the detector/film.

The normal fissures are often not seen on CXRs. However, when visible, they appear as subtle, thin lines in typical locations as described below.

The **horizontal fissure (pink arrows)**, which can be occasionally seen on an PA /AP and lateral CXR, appears as a horizontal line located at the level of the right hilum. It divides the upper right lobe from the middle lobe.

The **main or oblique fissures (blue arrows)** cannot be seen on a PA/AP CXRs because they have an oblique orientation. However, they can be occasionally identified as very thin lines with an oblique posterior-superior towards anterior-inferior orientation on lateral CXRs.

The right oblique fissure divides the right upper and middle lobe from the inferior lobe. The left oblique fissure divides the left upper lobe from the inferior lobe.

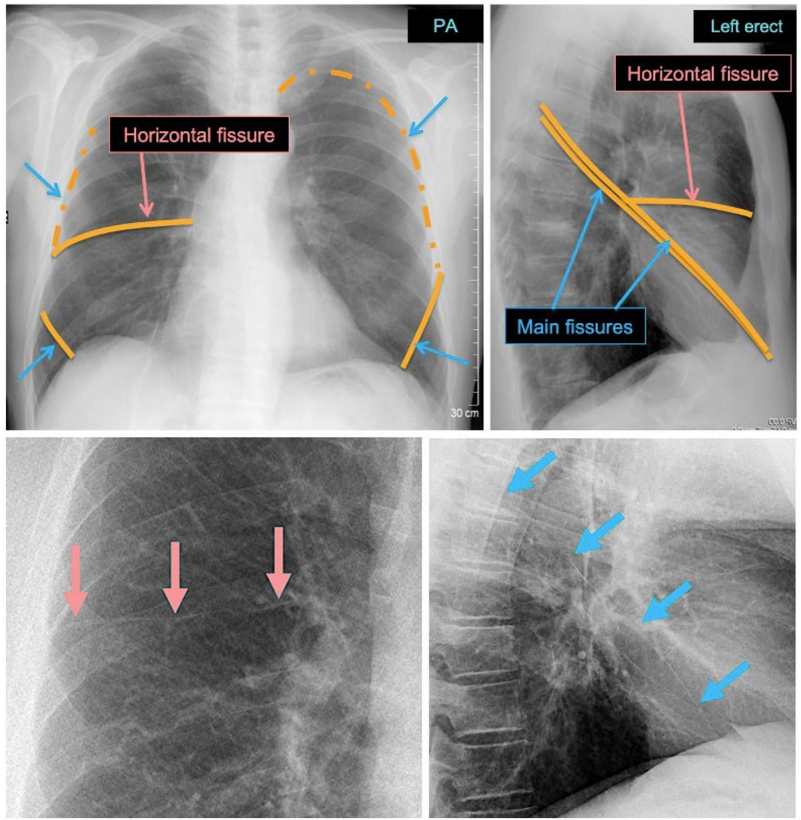

/ Mediastinum

The mediastinum is a space in the midline of the chest located between the left and right lung, the sternum and the vertebral column and between the upper chest aperture and the diaphragm. It contains the heart and great vessels, the internal mammary vessels, part of the azygos system, the thoracic duct, the trachea, the right and left main bronchi, nerves (phrenic, vagus branches), the thymus and many lymph nodes.

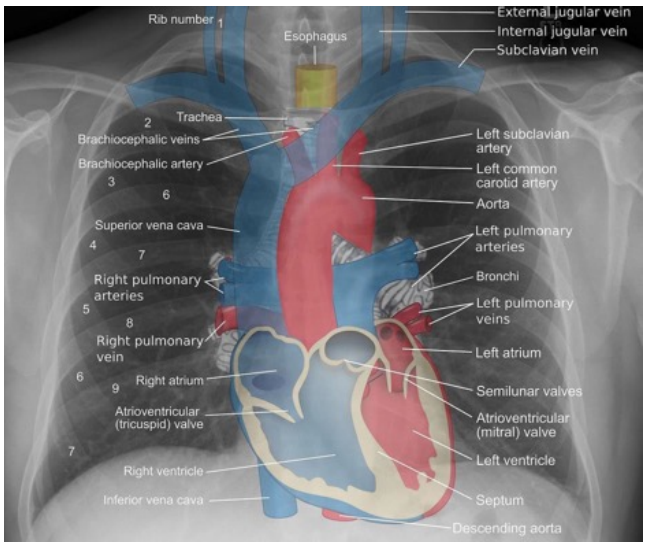

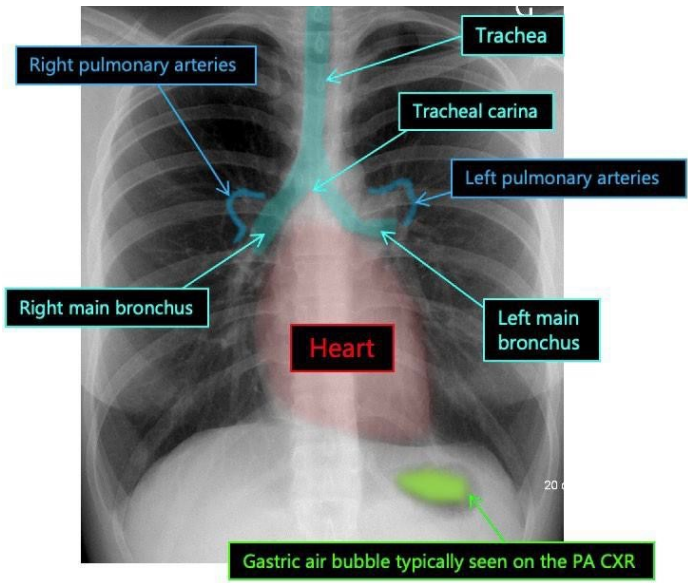

Image from: https://commons.wikimedia.org/wiki/File:Mediastinal_structures_on_chest_X-ray,_annotated.jpg

/ **Chest** Imaging

CHAPTER OUTLINE:

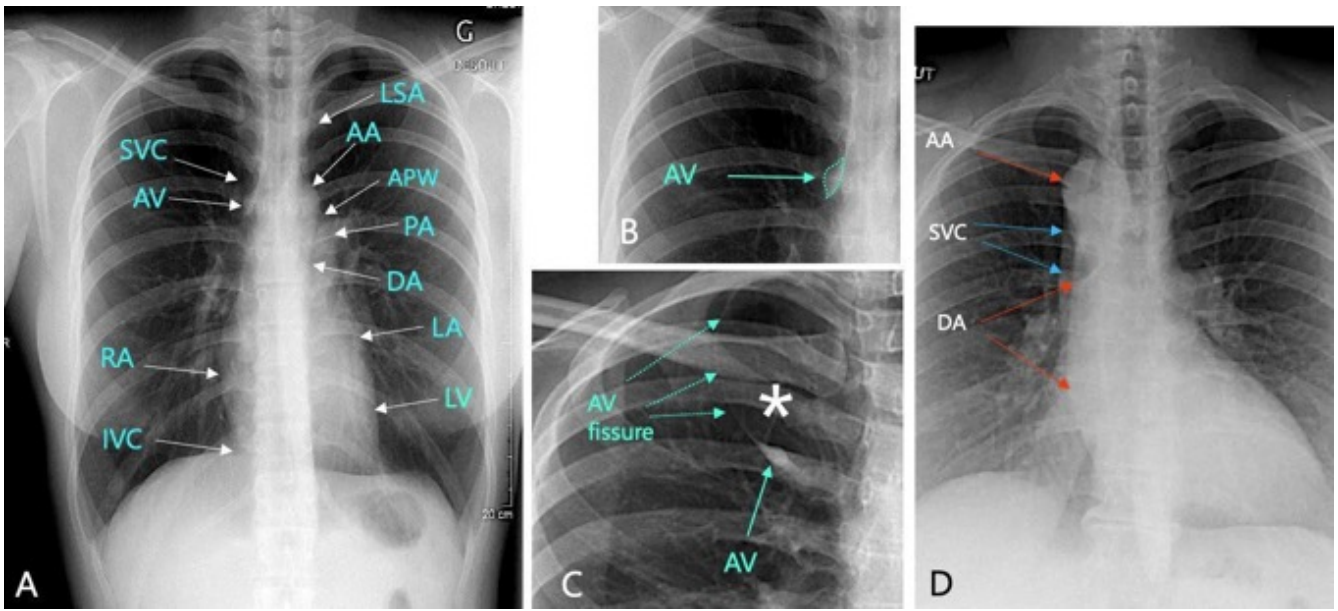

A. Normal mediastinal contours as seen on a CXR. Superior vena cava (SVC); Azygos vein (AV); Right atrium (RA); Inferior vena cava (IVC); Aortic arch (AA) also called aortic knuckle; Main pulmonary artery (PA); Aorto-pulmonary window (APW); Descending aorta (DA); Left atrial appendage (LA); Left ventricle (LV); Left subclavian artery (LSA). B. The AV is usually seen as a lenticular structure along the right mediastinal border. C. In about 1-2% of chest X-rays, the AV lies outside the mediastinum at the base of the azygos fissure, which is an accessory fissure. The azygos fissure separates the azygos lobe (*) from the upper lobe. D. A right-sided aortic arch (AA) can be an incidental finding or it can be associated with congenital heart disease or other vascular anomalies of the great vessels. The patient shown in D had no associated anomalies (right AA as a variant).

CHAPTER OUTLINE:

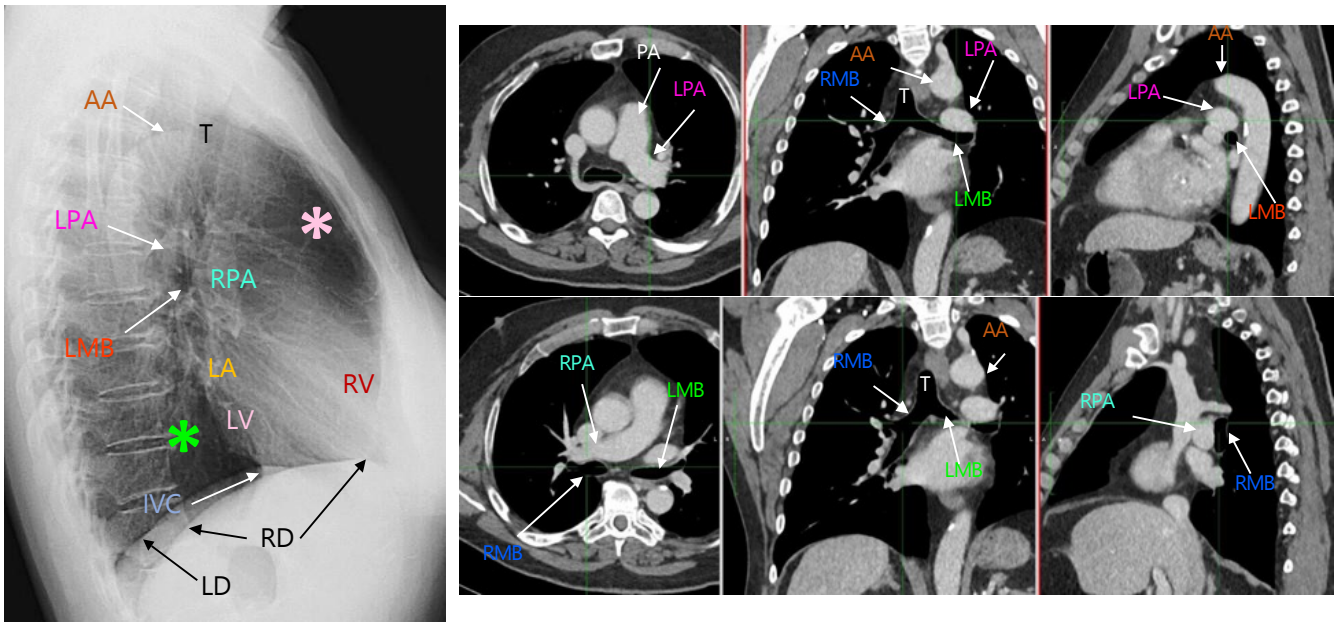

Normal anatomy on a lateral CXR and corresponding axial, coronal and sagittal contrast enhanced CT reformatted images. Trachea (**T**); Aortic arch (**AA**); Left pulmonary artery (**LPA**); Right pulmonary artery (**RPA**); Left atrium (**LA**); Left ventricle (**LV**); Right ventricle (**RV**); Inferior vena cava (**IVC**). The LPA is higher than the RPA as it passes over the left main bronchus (**LMB**), whereas the RPA passes in front of the right main bronchus (**RMB**). Right hemidiaphragm (**RD**); Left hemidiaphragm (**LD**). Note that the retrosternal area(pink asterisk) and the retrocardiac area (green asterisk) should not be obliterated, i.e., they have a low density as the lungs project over these areas.

Chest Imaging

CHAPTER OUTLINE:

/ Cardiothoracic Ratio (CTR)

The cardiothoracic ratio (CTR) is a simple method which helps to detect cardiac silhouette enlargement due to cardiomegaly. Nevertheless, pericardial effusion also results in cardiac silhouette enlargement on a CXR.

The CTR should always be measured on a PA CXR. It should not be measured on an AP CXR as the heart appears artificially enlarged on the AP projection (see explanation on page 18).

The CTR is a very approximative measurement for the estimation of cardiac pathology. For the evaluation of cardiac pathology in symptomatic patients, other imaging techniques are necessary

> see eBook chapter on Cardiac Imaging

<!> ATTENTION

Expiration and a prominent epicardial fat pad can result in a CTR > 0.50 – 0.55 despite absent cardiomegaly or absent pericardial effusion.

A CTR < 0.42 is often called small heart syndrome. It can be seen in cachectic states, adrenal insufficiency, heart transplant and other conditions.

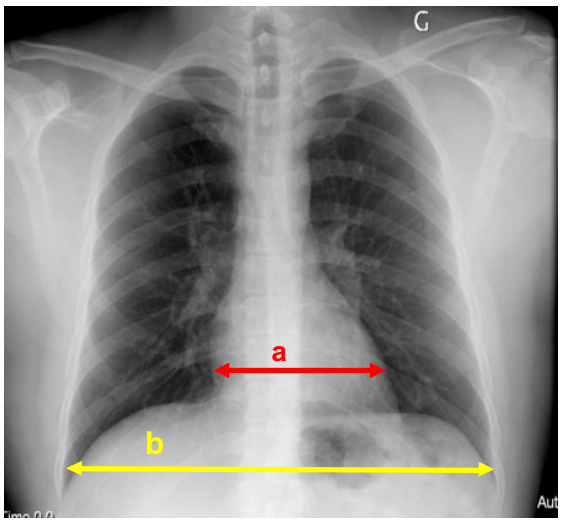

Maximum horizontal right-left cardiac silhouette diameter (a).
Maximum horizontal right-left thoracic diameter measured between the pleural edges (b).
Cardiothoracic ratio (CTR) = a/b < 0.50 – 0.55 and > 0.42

/ Compartments

<!> ATTENTION

The benefits of dividing the mediastinum into different compartments and using a standardised classification scheme include:

- / providing a relevant differential diagnosis for mediastinal masses identified at imaging, CT and MRI being the main imaging modalities for the evaluation and diagnosis of mediastinal pathology
- / facilitating discussions in multidisciplinary settings (i.e., "speaking the same language")
- / assistance in planning diagnostic interventional procedures and surgery

<∞> REFERENCES

Felson B. Chest roentgenology. Philadelphia, Pa: Saunders, 1973.
Goodman LR. Felson's principles of chest roentgenology, a programmed text. 5th edition. Elsevier 2020. ISBN-13 978-0323625678

Radiologists, surgeons and anatomists have used different mediastinal compartment classifications. For example, Felson's classification based on lateral CXRs has long been the most popular classification among radiologists, whereas the Shield classification based on intraoperative anatomic landmarks has long been most popular among surgeons.

The Felson classification is based on arbitrary landmarks. According to the Felson classification, the **anterior mediastinum (orange)** comprises everything from the posterior sternum surface to a line drawn from the anterior tracheal wall to the posterior inferior vena cava. The **middle mediastinum (blue)** extends from the posterior boundary of the anterior mediastinum to a line drawn 1 cm posterior to the anterior edge of the thoracic vertebrae. Finally, the **posterior mediastinum (purple)** lies behind the posterior boundary of the middle mediastinum.

A new classification was proposed by the International Thymic Malignancy Interest Group (ITMIG) based on anatomic landmarks seen at CT.

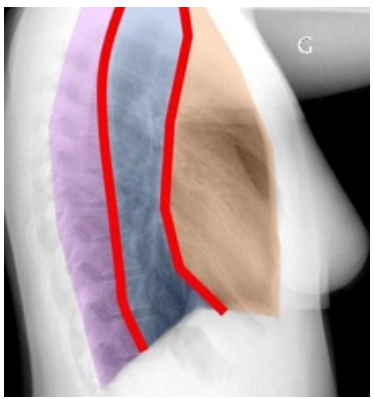

Mediastinal compartments according to Felson

The International Thymic Malignancy Interest Group (ITMIG) classification divides the mediastinum based on anatomic CT boundaries into the **prevascular (anterior) compartment (green)**, **visceral (middle) compartment (red)** and **paravertebral (posterior) compartment (blue)**.

The **prevascular (anterior) compartment** extends from the posterior sternum surface to the anterior aspect of the pericardium and from the thoracic inlet to the diaphragm. It contains the left brachiocephalic vein, the thymus, fat and lymph nodes. The prevascular compartment wraps around the pericardium/heart.

The **visceral (middle) compartment** extends from the posterior boundary of the anterior compartment to a vertical line connecting the points located 1 cm posterior to the anterior surface of the thoracic spine and – in the cranio- caudal direction – it extends from the thoracic inlet to the diaphragm. It contains vascular structures (heart, aorta, superior vena cava, intrapericardial pulmonary arteries and veins, thoracic duct), trachea, tracheal bifurcation, lymph nodes, vagal and phrenic nerves and the oesophagus.

The **paravertebral (posterior) compartment** extends from the posterior boundary of the middle mediastinum to a vertical line at the posterior margin of the chest wall at the lateral thoracic spine margin. It includes the thoracic spine and paravertebral soft tissues.

<!> ATTENTION

The ITMG classification is applicable only to cross-sectional imaging techniques. However, mediastinal masses are often detected on CXRs as CXRs are the most commonly performed examinations. On CXRs, mediastinal masses present as soft tissue densities on PA/AP and lateral projections leading to abnormal mediastinal contours, thickening of mediastinal stripes and lines and displacement of structures.

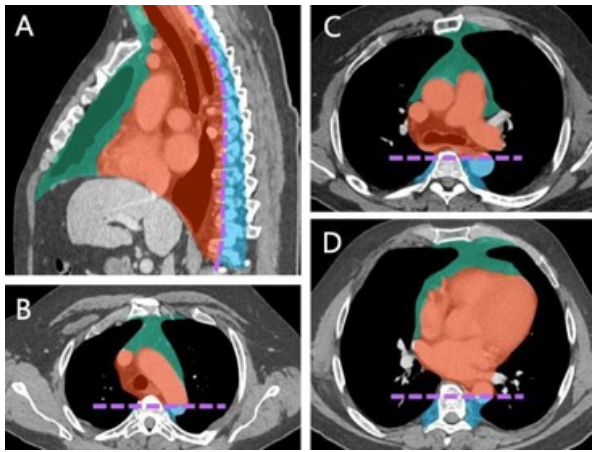

Mediastinal compartments according to the ITMIG classification. A. Sagittal reformatted CT image. Axial CT images at the level of the aortic arch (B), main pulmonary artery bifurcation (C) and left atrium (D). The dashed purple line is the boundary line between the visceral (middle) and paravertebral (posterior) mediastinal compartments.

<∞> REFERENCE

Carter BW, Benveniste MF, Madan R, et al. ITMIG Classification of Mediastinal Compartments and Multidisciplinary Approach to Mediastinal Masses. Radiographics. 2017 Mar-Apr;37(2):413-436. doi: 10.1148/rg.2017160095. Epub 2017 Jan 27. PMID: 28129068.

CHAPTER OUTLINE:

>|< COMPARE

Mediastinal compartments according to Felson

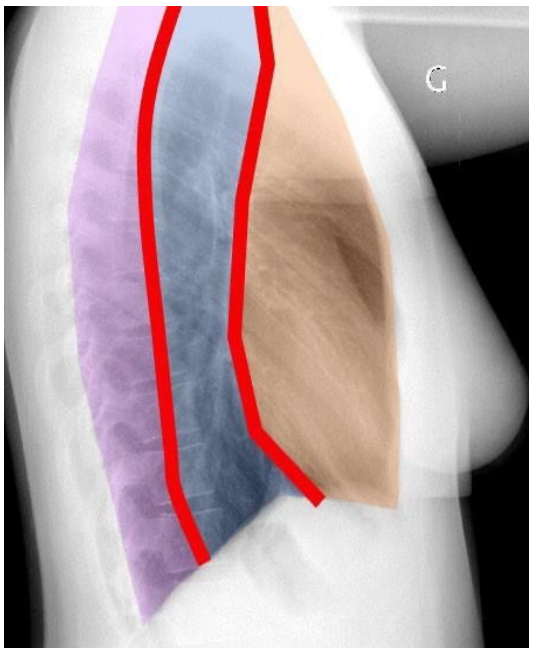

Mediastinal compartments according to the ITMIG classification

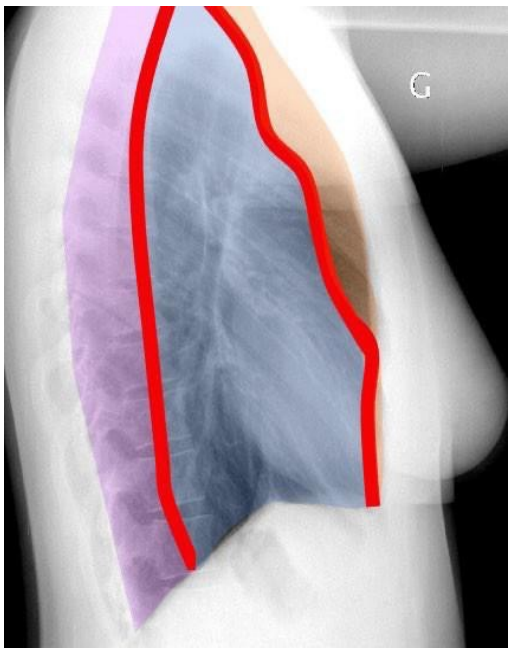

Although the ITMG classification is applicable only to cross-sectional imaging techniques, the lateral CXR shown above illustrates the mediastinal compartments according to this classification.

/ Mediastinal Lines, Stripes and Interfaces

<!> ATTENTION

Recognising normal and abnormal mediastinal lines and stripes on CXRs is very important to ensure that further CT examinations are judiciously prescribed.

Lines = thin tissue structures outlined on either side by air. Lines are mostly < 1 mm. They represent pleural-covered structures in the anterior and posterior mediastinum and include the **anterior junction line (green)** and the **posterior junction line (purple)**.

Stripes = thicker anatomic structures outlined by air. They include the **right paratracheal stripe (blue)** and the left **paratracheal stripe (light blue)**.

Interfaces = borders of solid structures with air. Some are often called "lines or stripes". Interfaces include: the **right paraspinal line (yellow)**, the **left paraspinal line (pink)**, the **azygo-oesophageal recess (red)**, the **aorto-pulmonary window reflection (blue arrow)**, the **aortic pulmonary stripe (light green)** and the **paraortic line (light pink)**.

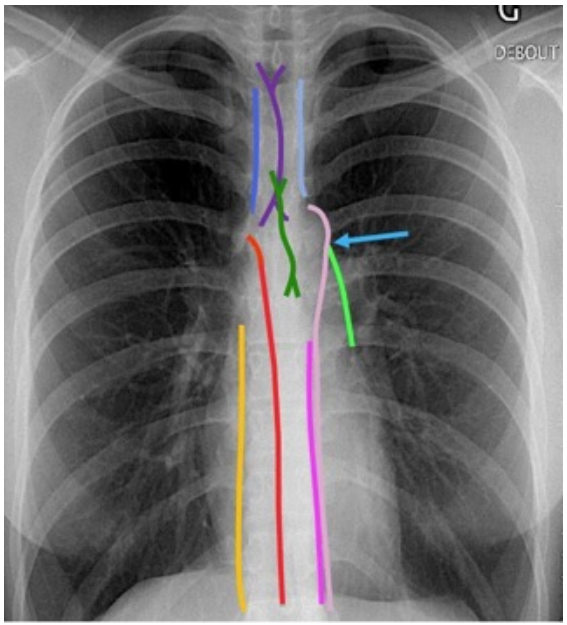

Mediastinal lines and stripes seen on CXRs

<∞> REFERENCE

Felson B. Chest roentgenology. Philadelphia, Pa: Saunders, 1973. Jiao A, Nadim B, Hammer M, Jhala K. 3D Visual Guide to Lines and Stripes in Chest Radiography. Radiographics. 2023 Sep;43(9):e230017. doi: 10.1148/rg.230017. PMID: 37590159.

/ Chest Imaging

CHAPTER OUTLINE:

The **anterior junction line (green)** is a normal anatomic landmark on CXRs. It is the point of contact of the left and right visceral and parietal pleurae meeting anteriorly at the midline. It is seen in about 25% - 57% of all CXRs in older children and adults; however, it is not seen in healthy infants.

The **posterior junction line (purple)** is a normal anatomic landmark on CXRs. It is seen as a vertical line projected through the tracheal air column and extending from the aortic arch superiorly above the clavicles. It is seen in about 40% of all CXRs in adults. It is formed by the apposition of the pleural surfaces of the posteromedial surfaces of the upper lung lobes posteriorly to the oesophagus but anterior to the thoracic spine.

Anterior junction line (green), posterior junction line (purple)

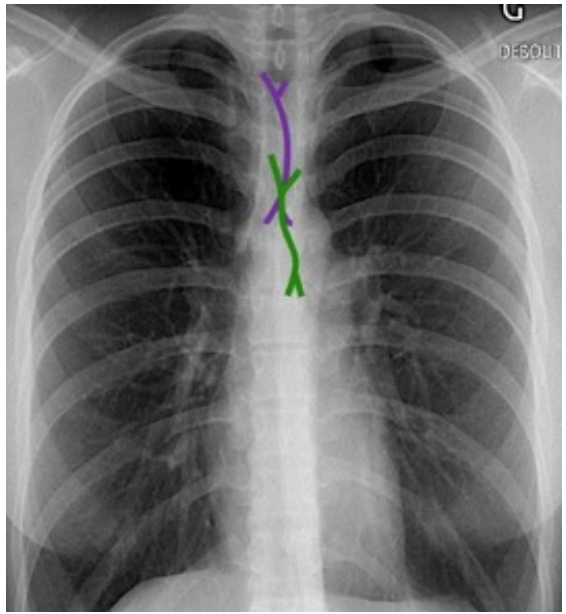

CHAPTER OUTLINE:

The **right paratracheal stripe (blue)** is a normal anatomic landmark on the PA/AP CXR. It is formed by the right tracheal wall, the adjacent pleural surfaces and the mediastinal fat between the pleural surfaces. It is visible because of the silhouette sign created by the tracheal air medially and air within the lung laterally. It is usually < 4 - 5 mm and it is seen in 65% - 97% of PA CXRs.

The **left paratracheal stripe (light blue)** is a normal anatomic landmark on the PA/AP CXR. It is formed by the left tracheal wall, the adjacent pleural surfaces of the left upper lobe and the mediastinal fat between the pleural surfaces.

It is seen in 21% - 31% of PA CXRs and it extends from the aortic arch to the subclavian artery. It has a variable thickness.

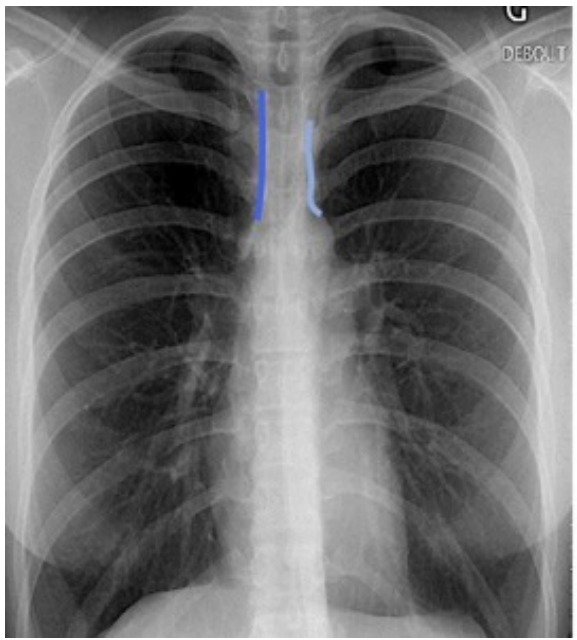

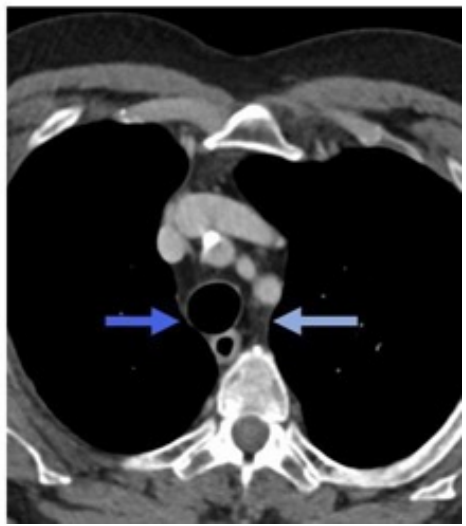

Right paratracheal stripe (< 4 - 5 mm, blue)
Left paratracheal stripe (variable thickness, light blue)

The **right paravertebral (paraspinal) line or stripe (yellow)** is an anatomic landmark seen on frontal CXRs. It is formed by the interface of the right lung pleura and the paraspinal soft tissues. The right paravertebral line is located medially from the **right heart border (blue)**.

The **left paravertebral (paraspinal) line or stripe (pink)** is formed by the interface of the left lung pleura and the paraspinal soft tissues.

The paraspinal lines extend below the diaphragm.

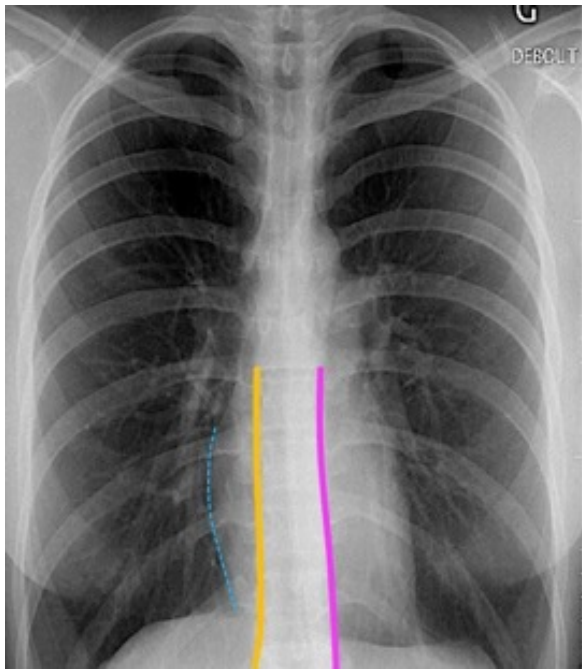

Visible on the right: 90%
Visible on the left: < 50%
Left paravertebral line (6 - 15 mm, yellow)
Right paravertebral line (2 - 4 mm, pink)
Right heart border (blue)

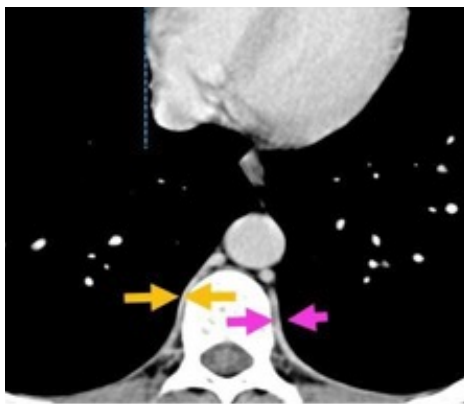

CHAPTER OUTLINE:

The **azygo-oesophageal recess** or **azygo-oesophageal line (red)** is the region inferior to the level of the azygos vein arch formed by the interface between the right lower lobe pleura, the azygos vein and the oesophagus. The recess is bordered anteriorly by the heart and posteriorly by the vertebral column.

In its upper third, the azygo- oesophageal line may deviate slightly towards the right while it is usually straight in its lower part.

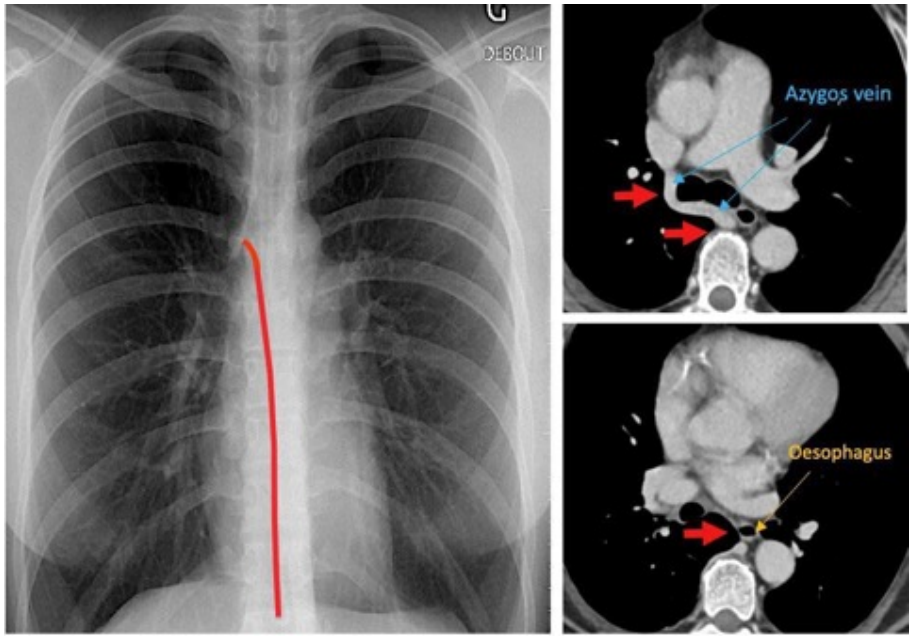

Azygo-oesophageal recess (red)

The **aorto-pulmonary window (APW, blue)** is a mediastinal space bordered superiorly by the aortic arch (AA), inferiorly by the pulmonary artery (PA), posteriorly by the descending aorta (DA), anteriorly by the ascending aorta (AscA), laterally by the left lung and medially by the trachea. It contains fat, lymph nodes, nerves (left recurrent laryngeal, left phrenic and left vagus nerve) and the ligamentum arteriosum.

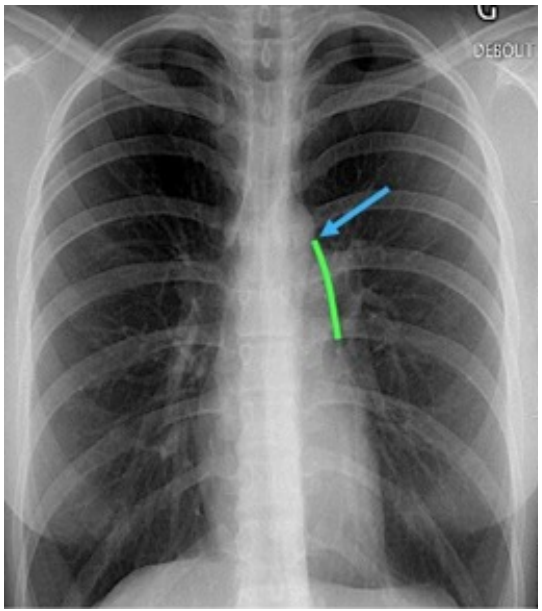

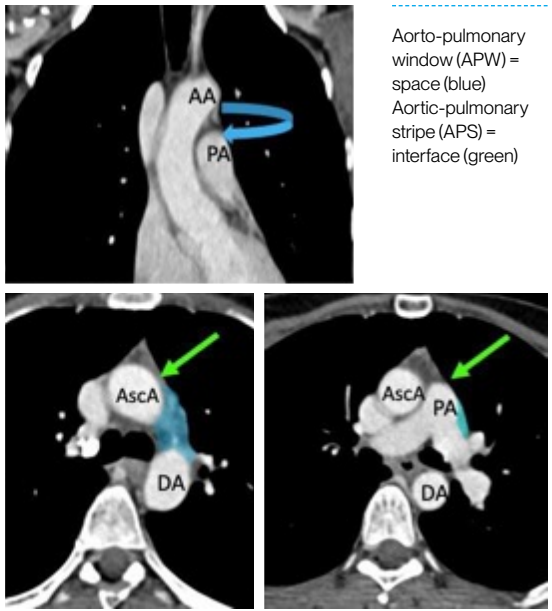

Aorto-pulmonary window (APW) = space (blue)
Aortic-pulmonary stripe (APS) = interface (green)

The **aortic-pulmonary stripe (APS, green)** is the interface between the left lung pleura and the mediastinal fat anterolateral to the aortic arch and pulmonary artery. It is rarely seen on CXRs.

<!> ATTENTION

The APW has a concave or a straight lateral border on the PA CXR and the APS appears as a straight line. A convex lateral APW border should be regarded as abnormal.

Chapter Imaging

CHAPTER OUTLINE:

The **para-aortic line (light pink)** is the interface between the pleura of the left lung and the mediastinal pleura located along the descending aorta.

This usually straight line is also seen below the diaphragm. It is located lateral to the **left paravertebral line (pink)**.

The para-aortic line is seen in at least 50% of CXRs.

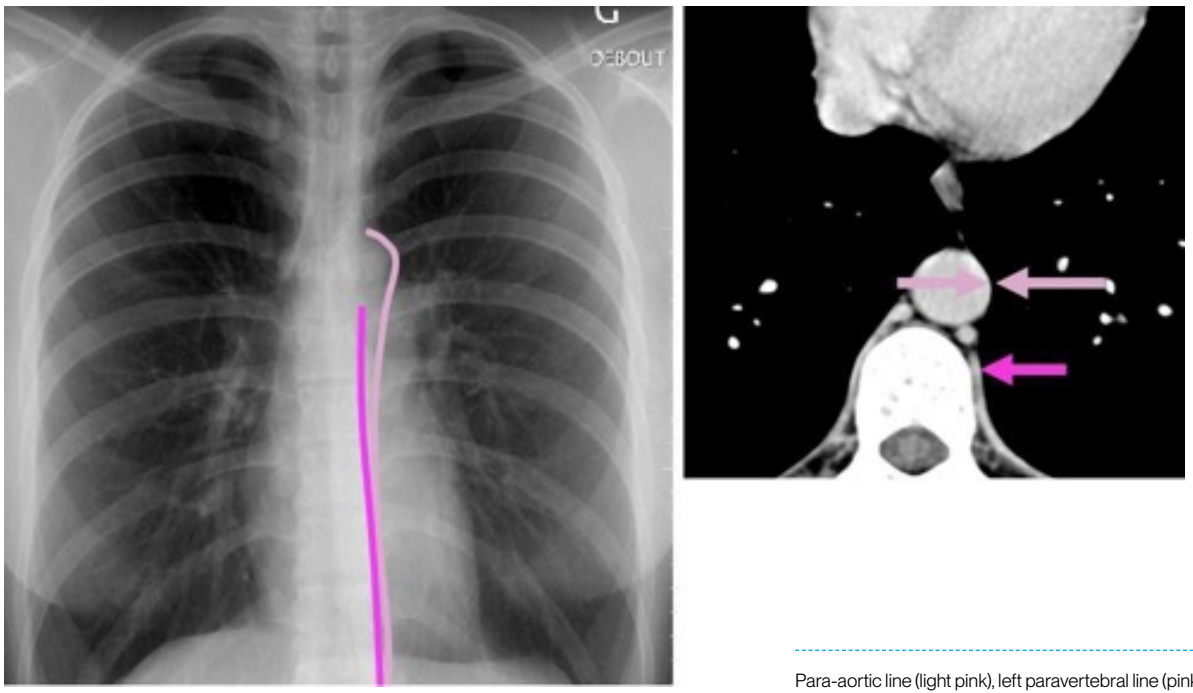

Para-aortic line (light pink), left paravertebral line (pink)

/ Hila

- The hila contain the major bronchi, the pulmonary vessels (99% of hilar volume) and lymph nodes.
- On normal CXRs, hilar nodes are not visible.
- The hila should have a similar size on CXR and a similar density.
- The hilar point (blue arrows) is the intersection point/angle of the upper and lower lobe lung vessels. It is a useful point of reference to determine the position of the hila.
- The left hilar point is 1 - 2 cm higher than the right hilar point on 96% of CXRs; in about 4% of CXRs, the hilar points are at the same level.

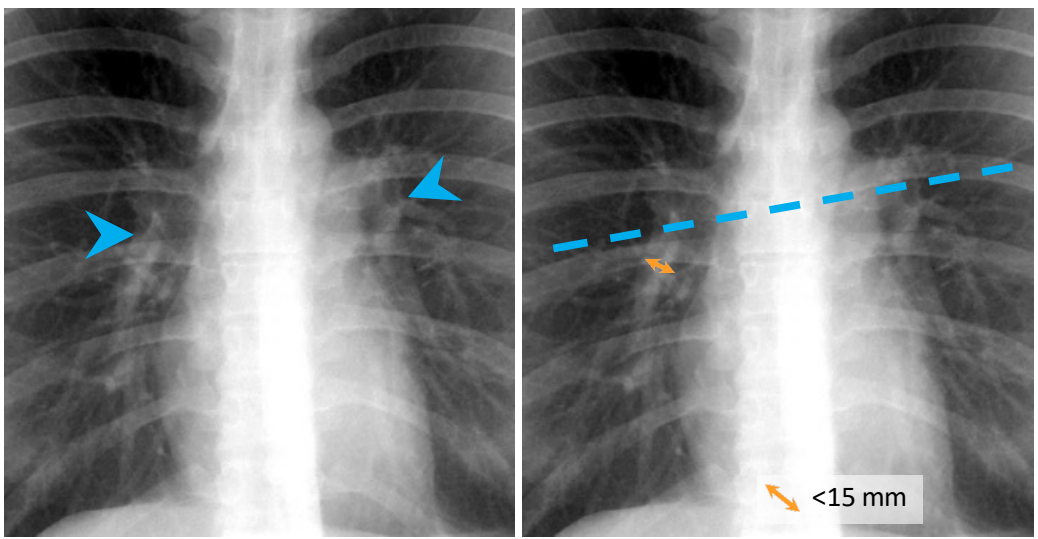

<!> ATTENTION

Enlarged hilar nodes can cause hilar enlargement.

Abnormally enlarged lymph nodes are the most common causes of pathological hilar enlargement!

/ Lung Lobes and Lung Segments

The right lung has three lobes (**upper [light blue]**, **middle [red]** and **lower [pink]**) while the left lung has two lobes (**upper [blue]** and **lower [light pink]**).

The **middle lobe** is separated from the **upper lobe** by the horizontal fissure and from the **lower lobe** by the oblique fissure. The middle lobe has 2 segments (medial and lateral). The medial segment of the middle lobe (**red asterisk**) is next to right heart border. The **right upper lobe** (above the horizontal fissure and anterior to the oblique fissure) has 3 segments (apical, posterior and anterior). The **right lower lobe** has 5 segments (superior, medial, anterior, lateral and posterior).

The **left upper lobe** is located anteriorly and superiorly to the left oblique fissure. It has 4 segments (apicoposterior, anterior, superior lingular and inferior lingular). The ligula (**blue asterisk**) abuts the left heart border. The **left lower lobe** has 4 segments (superior, antero-medial, lateral and posterior).

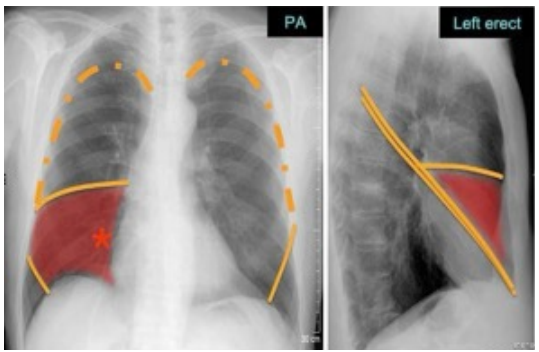

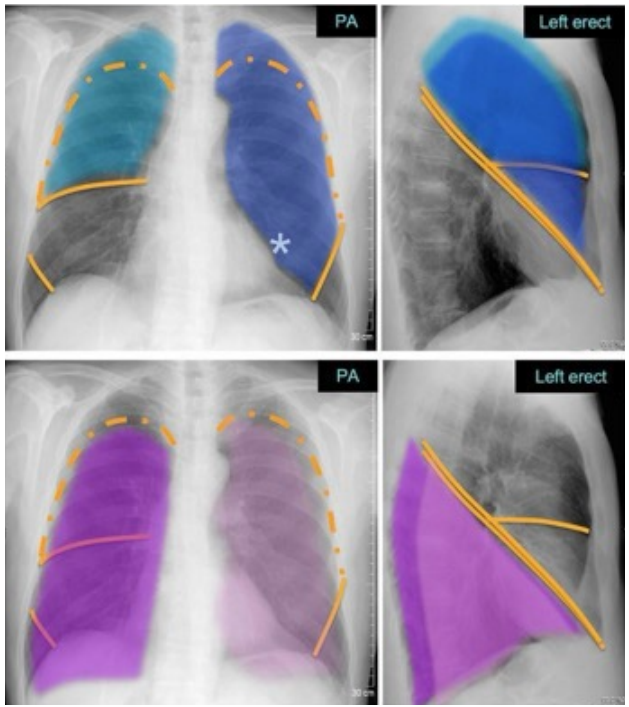

/ **Chest** Imaging

CHAPTER OUTLINE:

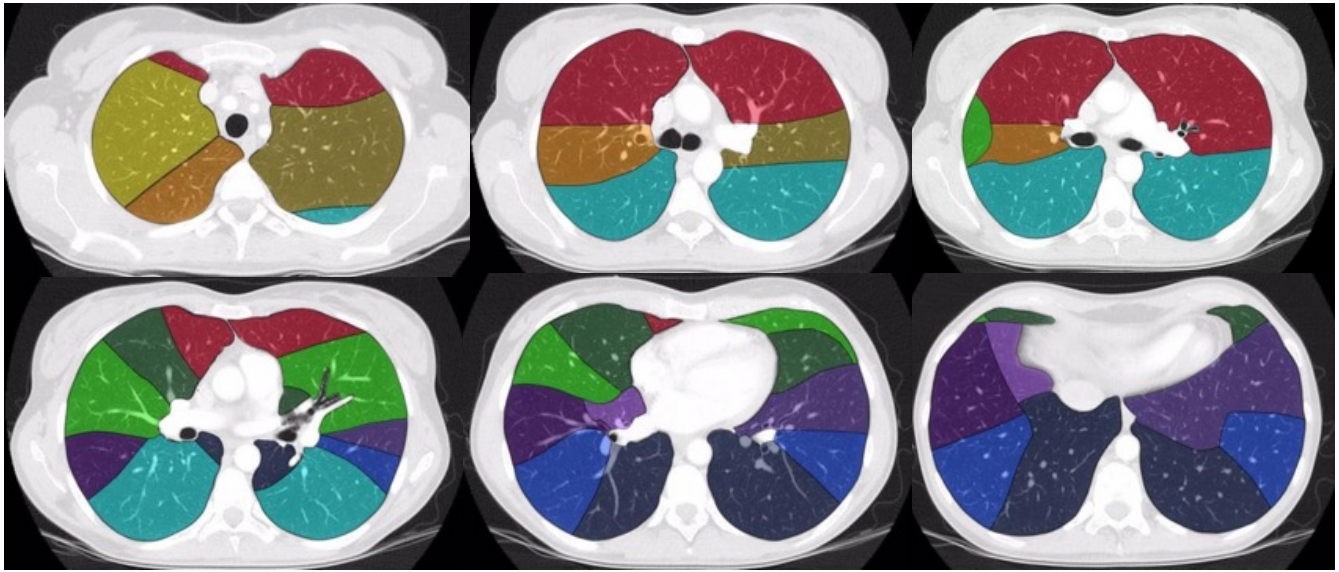

Selected axial CT slices of the chest illustrating the anatomic position of the lung segments. Images reproduced from : https://radiopaedia.org/play/59737/entry/1093 616/case/54511/studies/60738?lang=us (playlist contributed by Dirk Sehr)

CHAPTER OUTLINE:

/ Lung Zones and Lung Vasculature

The lung zones serve only the purpose of radiologic description and assessment of parenchymal abnormality by comparing each zone with the opposite side. The **upper (blue)**, **middle (red)** and **lower (yellow)** lung zones, which occupy each one third of the cranio-caudal lung size do not correspond to lung lobes. If the density of lungs in corresponding lung zones (e.g., left and right middle zones) is asymmetrical and if technical factors, e.g., rotation have been excluded, lung pathology is very likely on a CXR.

The upper zone vessels are smaller than the lower zone vessels on a PA CXR because in an erect position there is an increasing gradient of perfusion per lung volume unit from apex to base (effects of gravity superimposed on the low pressure, low resistance vascular bed).

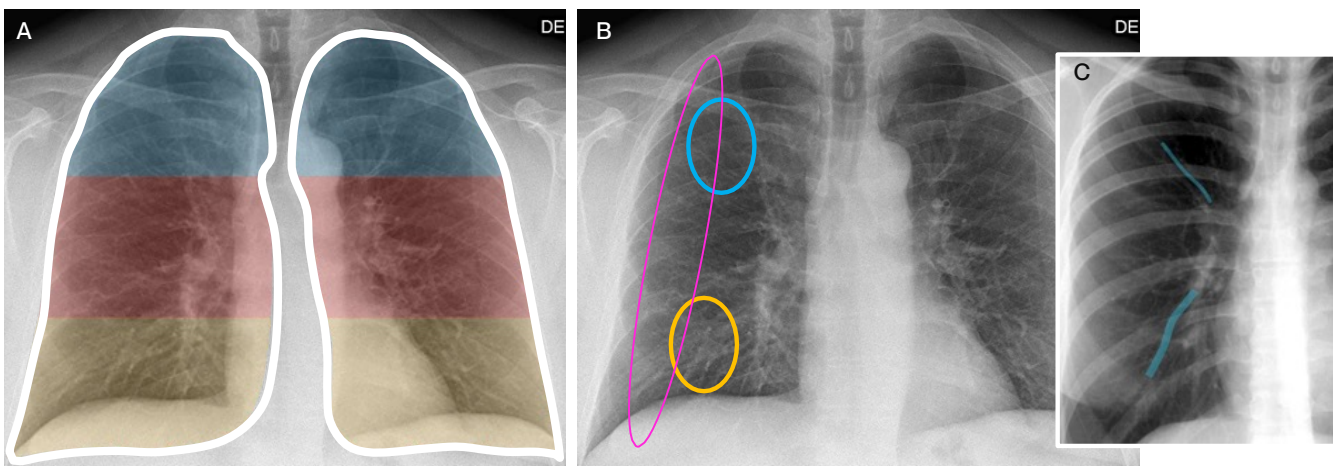

A. Lung zones: Upper lung zones (blue); Middle lung zones (red); Lower lung zones (yellow). B and C. In the erect position, the veins in the upper lung zones (i.e., the veins that branch superiorly from the hilum) are about 1/3 the size of those in the lower zones. Also, vessels in the upper lung zones are fewer than those in the lower zones. In the outer 1/3 of the lung zones (pink), lung vessels are fewer and smaller than in the inner third.

The Silhouette Sign

CHAPTER OUTLINE:

/ The Silhouette Sign

<!> ATTENTION

Definition: The loss of the normal silhouette of a structure on the CXR is called the silhouette sign.

Two opacities of similar density seen on a CXR

- **are next to each other if their borders (silhouettes) cannot be made out (silhouette sign is present)**
- **are not next to each other if their borders (silhouettes) are well seen (silhouette sign is absent).**

This sign is very useful in localising lung opacities as the borders of the cardiac silhouette are in contact with specific lung portions.

- the right cardiac silhouette is next to the medial segment of the right middle lobe
- the left cardiac silhouette is next to the lingula

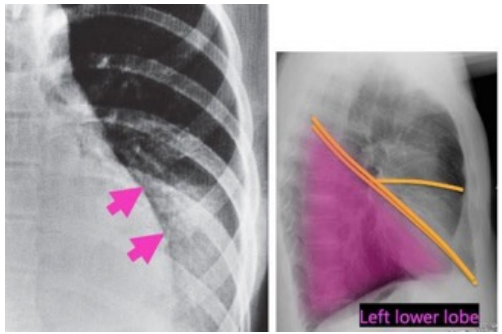

Consolidation (in this case pneumonia) has a similar density as the heart. If the consolidation is in the left lower lobe, which is located more posteriorly in the chest than the heart, the silhouette sign is absent (i.e., the normal silhouette of the left ventricle is seen).

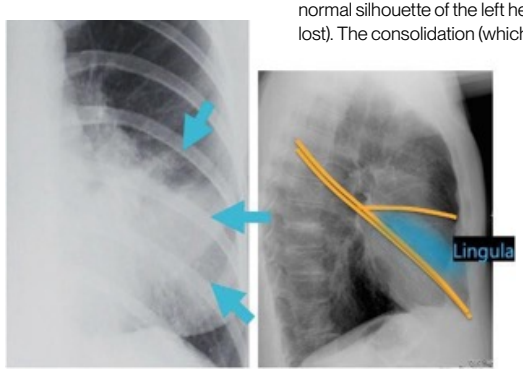

The silhouette sign is present (i.e., the normal silhouette of the left heart border is lost). The consolidation (which has a similar density as the heart) is in the lingula, which abuts the left ventricle.

CHAPTER OUTLINE:

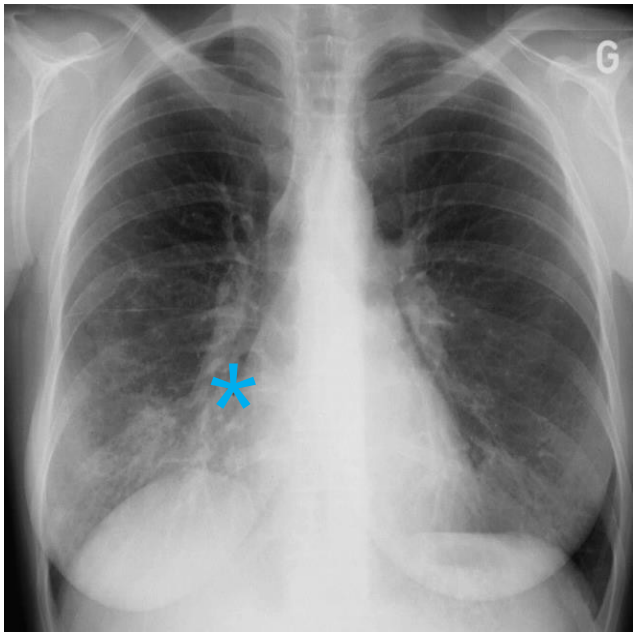

Consolidation (in this case pneumonia, blue) is in the middle lobe. The silhouette sign is present (i.e., the normal silhouette of the right atrium is not clearly seen).

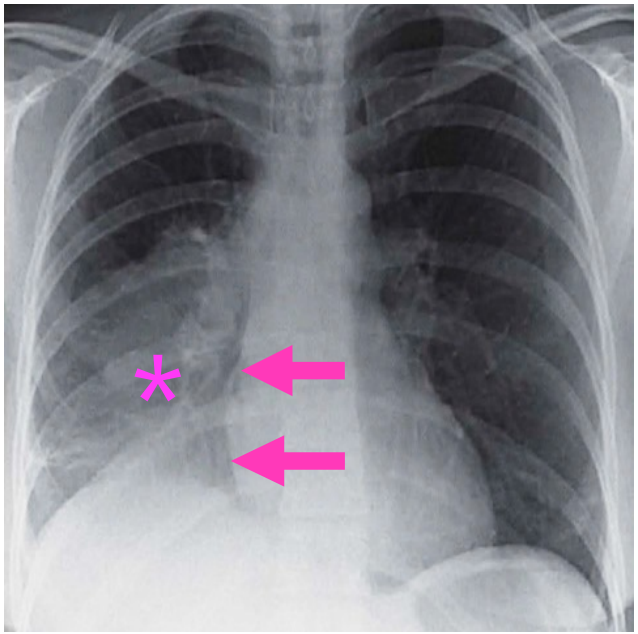

Consolidation (in this case pneumonia, pink) is in the right lower lobe, which is located more posteriorly in the chest than the heart, the silhouette sign is absent (i.e., the normal silhouette of the right atrium is seen).

CHAPTER OUTLINE:

Chest Imaging

This silhouette sign can also be used for lesion localisation on lateral CXRs.

It also explains why the **left diaphragm (green line)** can be seen only to a point where it borders the heart (**green arrow**) while the **right diaphragm (red line)** is seen all the way to the anterior chest wall (**red arrow**).

The heart, the left diaphragm abutting the heart and the structures below the left diaphragm all have the same density and they are next to each other (the silhouette sign is present). The right diaphragm is seen as the interface between the air in the right lung and the abdominal soft tissues, which have a different density.

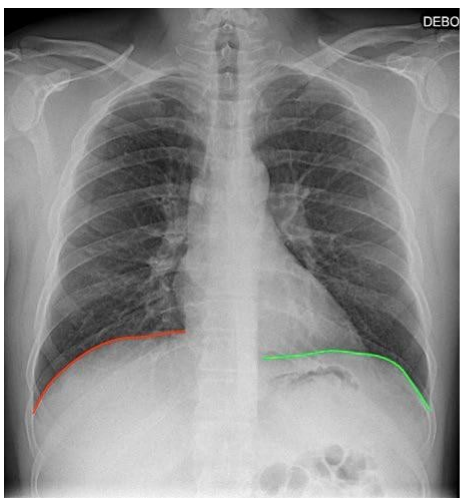

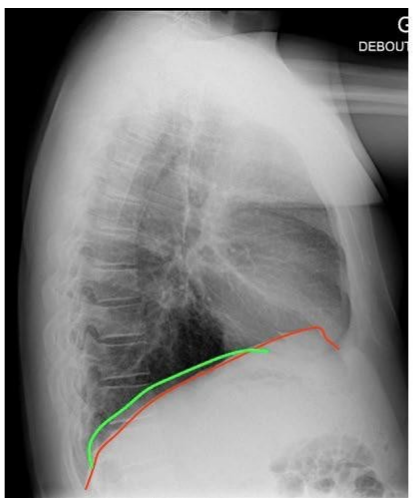

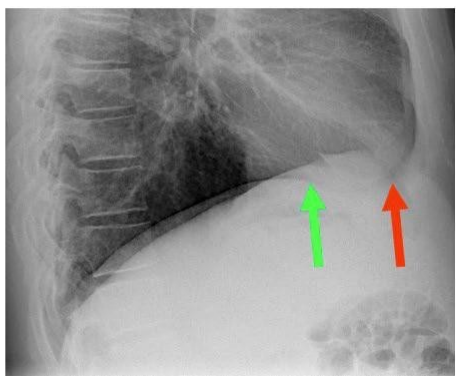

Soft Tissue Asymmetry on CXRs

CHAPTER OUTLINE:

/ Soft Tissue Asymmetry on CXRs

An asymmetrically decreased soft tissue density can be seen in patients with mastectomy or subcutaneous emphysema (air in the soft tissues following trauma, pleural drain placement or infection with anaerobes).

An asymmetrically increased soft tissue density can be seen in the presence of a large soft tissue mass, hematoma or asymmetric breast tissue.

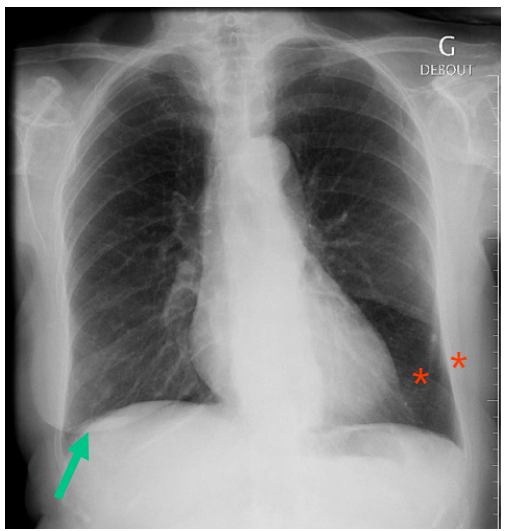

Decreased soft tissue density on the left **(red asterisk)** and breast asymmetry because of **left mastectomy.** Normal **right breast contour (green arrow)**.

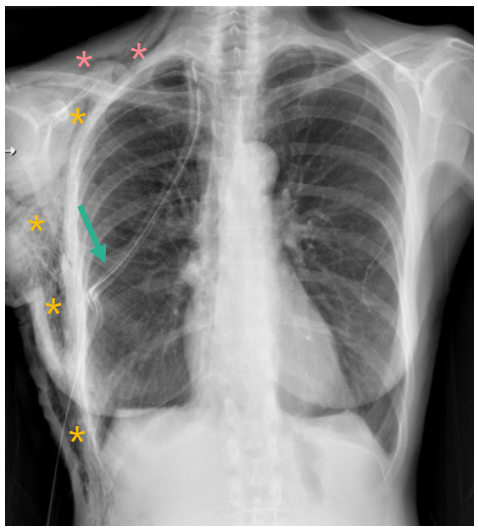

Irregular **hyperlucent (very low-density) areas** (yellow asterisks) along the right chest wall extending into the **supraclavicular region (pink asterisks)** because of soft tissue emphysema (air in the soft tissues) after thoracostomy tube **(green arrow)** placement to drain pneumothorax (see pages 60-63).

CHAPTER OUTLINE:

Medical Devices and Other Foreign Bodies on CXRs

CHAPTER OUTLINE:

/ Medical Devices and Other Foreign Bodies on CXRs

Medical devices are often seen on CXRs. They can be located inside the body (e.g., pacemakers, sternal wires, cardiac valve devices or replacements, nasogastric tubes, endotracheal tubes, pleural drainage tubes, dialysis catheters, osteosynthesis material) or outside the body but projecting on the CXR (e.g., oxygen tubes, electrodes for ECG, clamps).

Objects non-related to treatment can be also be seen on CXRs, e.g., buttons from hospital gowns, hair pins, hair braids, etc. These different types of medical devices and non-related foreign bodies are easily recognisable on CXRs.

To correctly locate a foreign body or a medical device, both a PA and a lateral CXR are necessary.

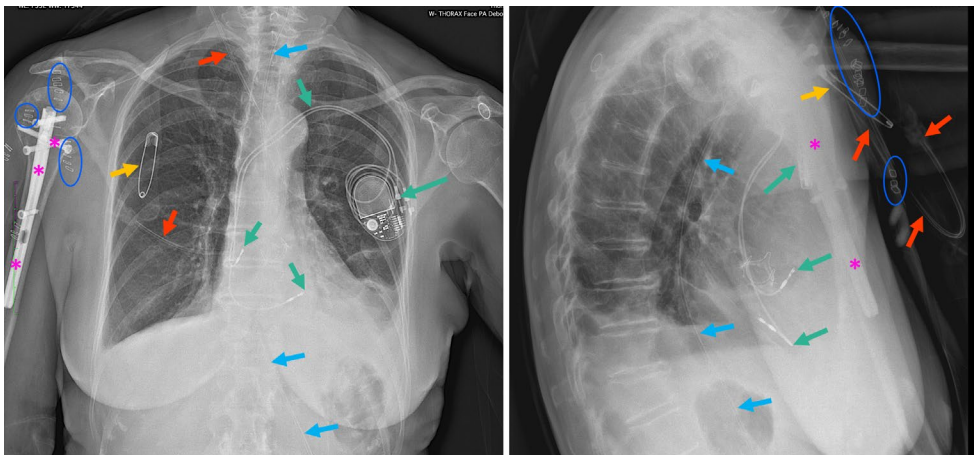

Patient with multiple medical devices seen on the CXR: Pacemaker with electrodes (green arrows), nasogastric tube (blue arrows), internal fixation hardware of the humerus (pink asterisks), Redon drain (red arrows), safety pin (yellow arrows), surgical staples (dark blue areas).

Bone Pathology on CXRs

CHAPTER OUTLINE:

/ Bone Pathology on CXRs

Bone abnormalities include fractures, degenerative bone changes, metastatic bone disease or direct bone invasion by adjacent tumours.

Rib fractures are common in blunt chest trauma. They can be isolated or multiple and they can be associated with life-threatening complications including pneumothorax and haemothorax, lung contusion and laceration, brachial plexus and large vessel injury.

Isolated rib fractures are often hardly visible on CXRs, whereas multiple fractures are more easily recognised. Multiple rib fractures (yellow circles) typically involve ribs 4 – 10.

Fractures of ribs 1-3 indicate high velocity trauma.

Segmental fractures of > 3 ribs produce paradoxical chest wall movement with respiration. This is called flail thoracic segment or flail chest.

Older rib fractures are recognised on CXRs because of callus formation

> see eBook chapter on Musculoskeletal Imaging

Rib fractures can also occur because of metastatic disease (pathologic fractures).

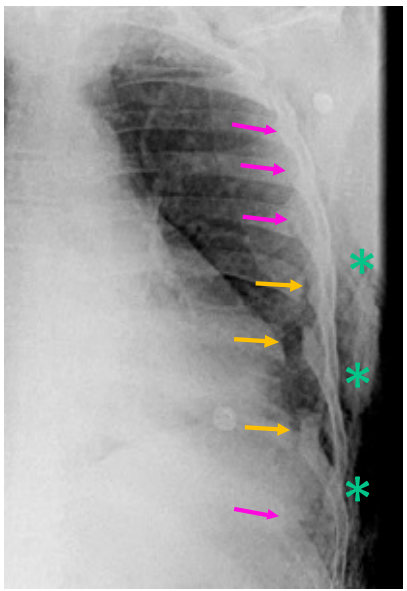

Patient with multiple rib fractures following a motor vehicle accident. Fractures are well seen whenever the rib ends are displaced (yellow arrows). Fractures are less conspicuous whenever the rib ends are not displaced (pink arrows). Associated soft tissue emphysema (green asterisks), see page 56.

<!> ATTENTION

Bone abnormalities may be easily overlooked on CXRs and, therefore, must be looked for very carefully.

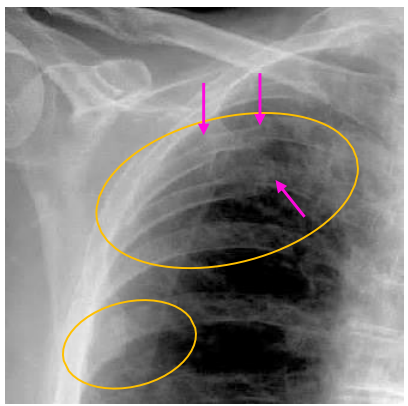

Detail of a PA CXR of a patient with multiple rib fractures (yellow ellipses) following a motor vehicle accident 8 weeks earlier. Fracture lines (pink arrows) are poorly seen and calcified callus is visible. The fractures are almost healed (complete healing usually occurs by 12 weeks).

Chest Imaging

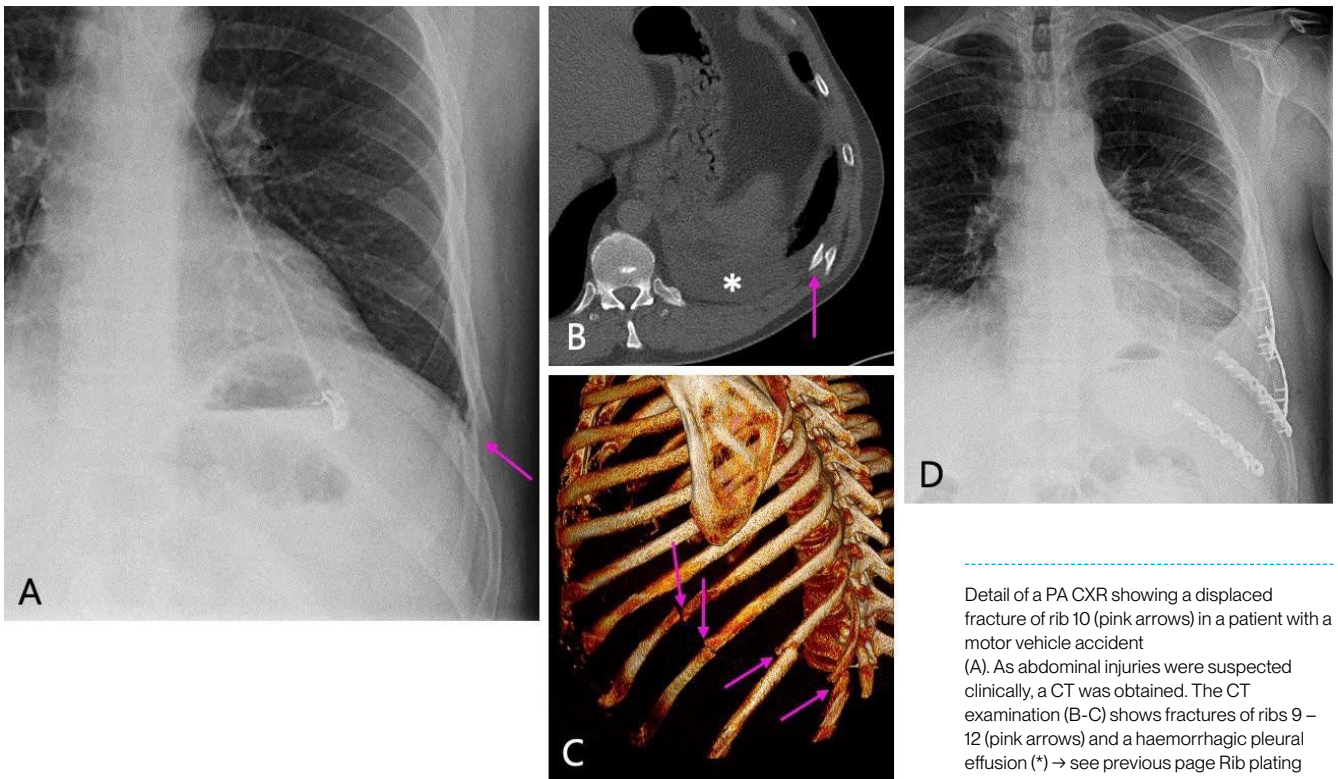

Detail of a PA CXR showing a displaced fracture of rib 10 (pink arrows) in a patient with a motor vehicle accident (A). As abdominal injuries were suspected clinically, a CT was obtained. The CT examination (B-C) shows fractures of ribs 9 – 12 (pink arrows) and a haemorrhagic pleural effusion (*) → see previous page Rib plating was carried out for flail chest. D. PA CXR obtained after rib plating.

CHAPTER OUTLINE:

Bone is the third most common site of metastasis behind lung and liver. Bone metastases are classified as osteolytic, osteoblastic or mixed. Osteolytic metastases are characterised by destruction of bone; they are most often seen in multiple myeloma, lung cancer and non-Hodgkin lymphoma.

Osteoblastic (osteosclerotic) metastases are characterised by new bone deposition. This deposition pattern is typically seen in prostate cancer, small cell lung cancer and Hodgkin lymphoma. The mixed pattern corresponds to both osteolytic and osteoblastic bone lesions or to lesions with both components.

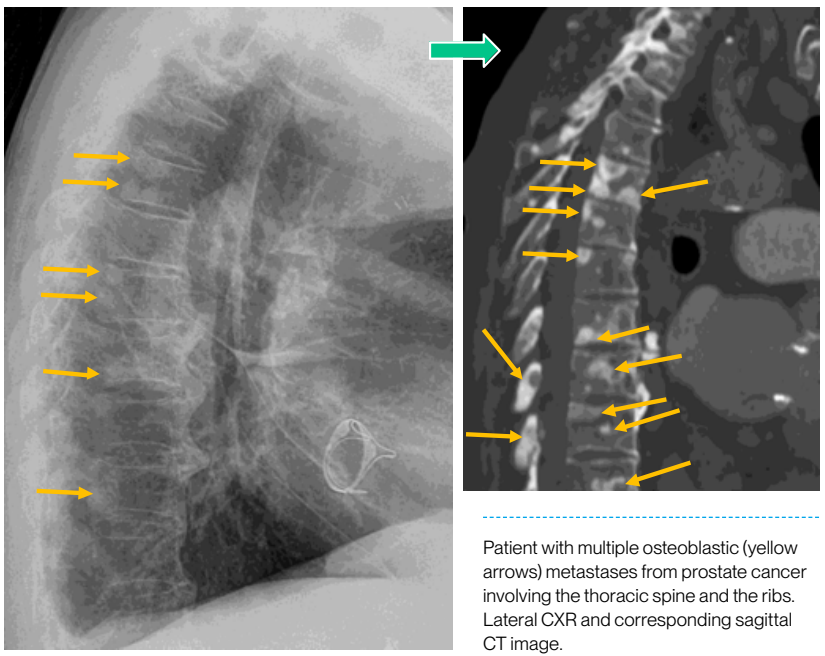

Patient with multiple osteoblastic (yellow arrows) metastases from prostate cancer involving the thoracic spine and the ribs. Lateral CXR and corresponding sagittal CT image.

Osteolysis of ribs and vertebral bodies can also occur by direct bone invasion from lung or pleural tumours.

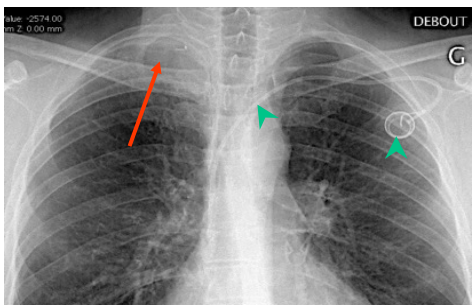

Patient with a Pancoast tumour (= apical lung tumour, most often a primary squamous cell carcinoma of the lung at histology). Note absent visualisation of the 3rd right rib due to osteolysis (red arrow) by the tumour. On this PA CXR, the tumour appears as a soft tissue opacity at the lung apex. Compare with the normal left lung apex. Port-a-cath (green arrowheads) for chemotherapy.

Chest Imaging

CHAPTER OUTLINE:

Pathology of the Pleura and Pleural Cavity

CHAPTER OUTLINE:

/ Pleural Effusion

Pleural disorders include effusion, pneumothorax, pleural soft tissue thickening and plaque formation.

Pleural effusion = abnormal fluid accumulation in the pleural cavity.

Normally, the pleural cavities contain about 15 ml of serous fluid. A physiologic imbalance between fluid production and absorption results in a pleural effusion.

Pleural effusions can be divided into transudates and exudates, which differ in terms of protein and lactate dehydrogenase concentration and specific gravity (all three are lower in transudates).

Transudates are mainly seen in cardiac failure, nephrotic syndrome and cirrhosis. They are caused by increasing hydrostatic pressure or by decreasing oncotic capillary pressure.

Exudates are a consequence of changes in microcirculation or lymphatic pleural drainage. Exudates occur in chest neoplasms including metastases, infection and autoimmune diseases.

Pleural effusions result in passive atelectasis of the adjacent lung portions > see page 127.

<!> ATTENTION

- PA and AP erect CXRs are insensitive to small pleural effusions.
- Pleural effusions < 300 ml can be undetectable on an erect CXR.
- Lateral CXRs detect effusions earlier than PA and AP erect projections. Effusions > 100 ml are detectable on the lateral CXR. They are seen in the posterior costophrenic angle.
- Supine CXRs may miss large amounts of pleural effusion as the fluid collects posteriorly, thus resulting in hardly visible density changes.
- Ultrasound (US) can detect very small effusions.
- CXRs and US cannot distinguish between transudate, exudate, pus, blood or chylous contents based on their radiologic aspect alone.

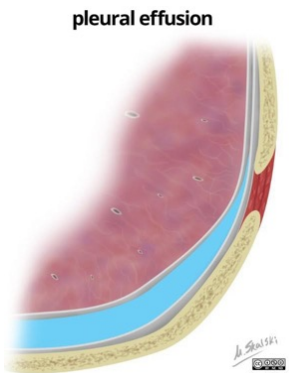

Illustration courtesy of Matt Skalski, https://radiopaedia.org/?lang=us Radiopaedia.org. From the case https://radiopaedia.org/cases/53333?lang=us rID: 53333

CHAPTER OUTLINE:

<!> ATTENTION

Radiologic features of pleural effusions include blunting of the costophrenic angles, meniscus sign (in large effusions), fluid accumulation in the lung fissures and mediastinal shift away from the effusion (in very large effusions).

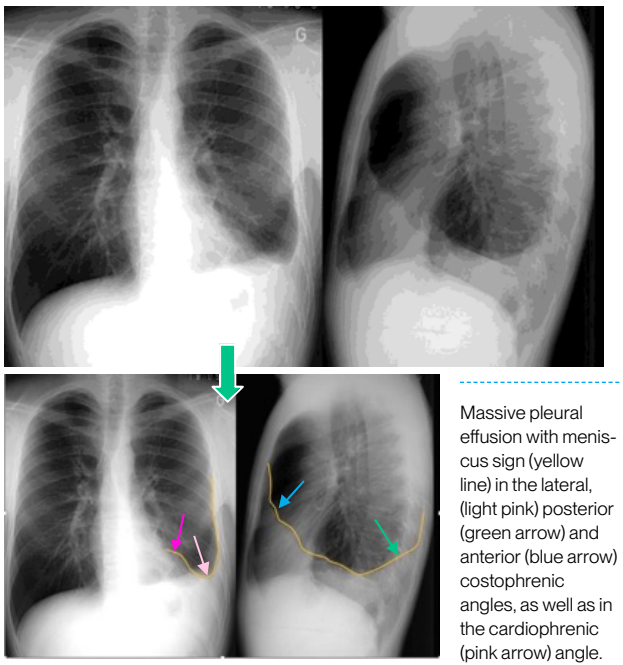

Massive pleural effusion with meniscus sign (yellow line) in the lateral, (light pink) posterior (green arrow) and anterior (blue arrow) costophrenic angles, as well as in the cardiophrenic (pink arrow) angle.

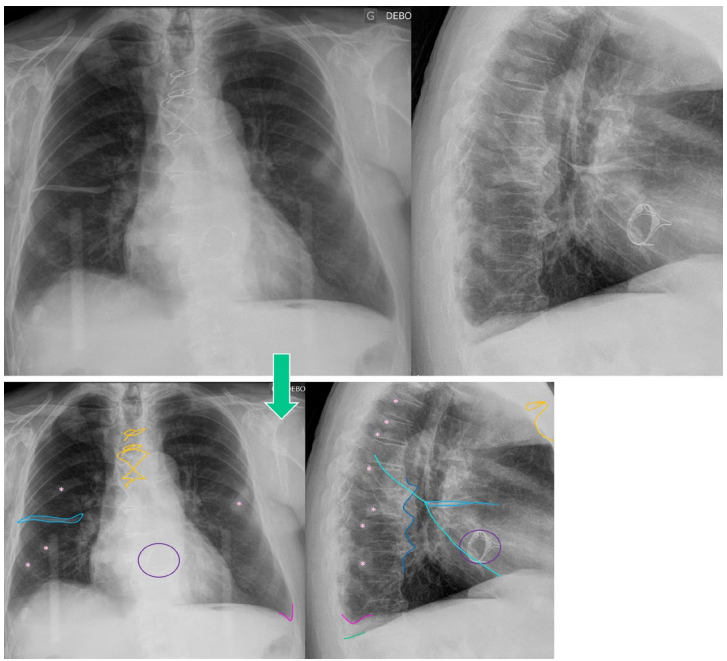

Pleural effusion with meniscus sign (pink lines) on the left, blunting of the posterior right (green line) costophrenic angle and fluid in the horizontal fissure (light blue line) and in the rightoblique fissure (turquoise line). Mitral valve replacement (purple circle). Cerclage wires (yellow lines) after median sternotomy. Note that the patient has multiple osteoblastic metastases light pink asterisks). Osteophytes (dark line).

Interlobar fluid accumulation is most frequently seen in patients with congestive cardiac failure. It is either a transudate due to heart failure or it is the end result of an inflammatory process (less often).

Some interlobar fluid accumulations are walled off by pleural scarring while other fluid accumulations enter the fissures as an extension from the free pleural space.

During heart failure pleural reactions are very frequent.

Upon resorption, scars or thickened pleura remain.

<!> ATTENTION

- Loculated pleural effusion (= trapped pleural fluid does not layer out in dependent position) can mimic pleural masses.
- Causes of pleural fluid loculation include pleural scarring, thick fluid with pus (empyema) or lung distortion, e.g., following surgery.

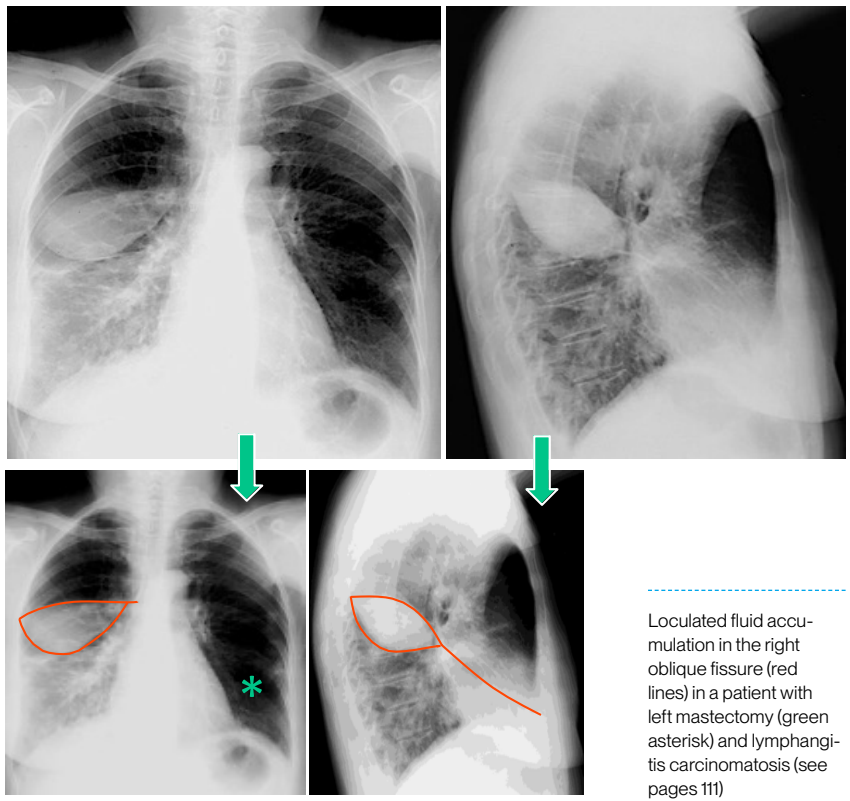

Loculated fluid accumulation in the right oblique fissure (red lines) in a patient with left mastectomy (green asterisk) and lymphangitis carcinomatosis (see pages 111)

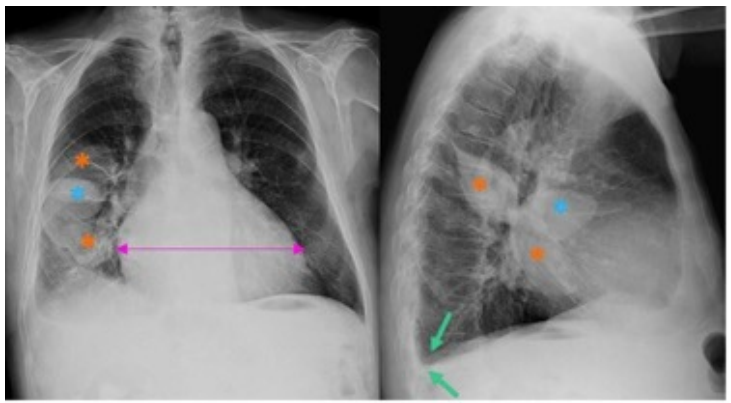

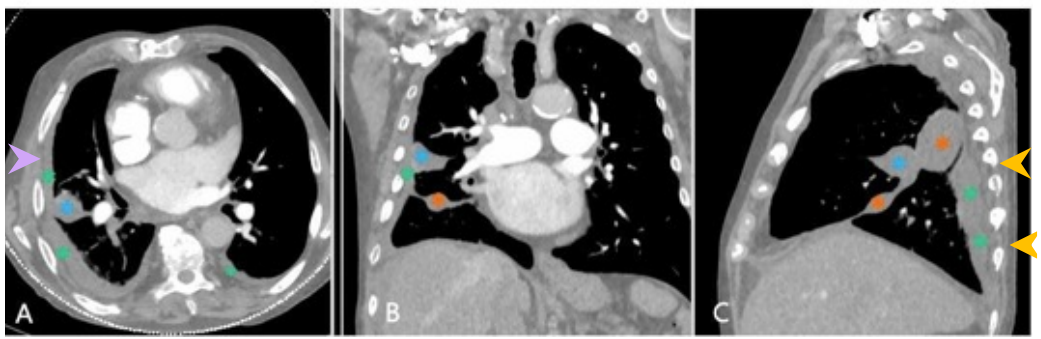

Loculated fluid accumulations in the right oblique fissure (orange asterisks) and in the horizontal fissure (blue asterisks) in a patient with congestive cardiac failure. Note cardiomegaly (pink arrow) and blunted left and right posterior costophrenic angles (green arrows) due to bilateral pleural effusions. Corresponding CT images with axial (A), coronal (B) and sagittal (C) reconstructions of the same patient show pleural effusions trapped in the right oblique (orange asterisks) and horizontal (blue asterisks) fissures and free pleural fluid bilaterally (green asterisks). As the patient is lying on his back, the free pleural fluid extends posteriorly (yellow arrowheads) and laterally (purple arrowhead) along the pleural cavity.

<!> ATTENTION

The typical aspect of loculated pleural fluid accumulations on CXRs includes an elongated opacity along the direction of the fissures and with tapering ends.

CT is usually not needed to make the diagnosis unless the opacities fail to resolve after congestive cardiac failure treatment.

/ Pneumothorax

Pneumothorax = accumulation of air in the pleural space

Causes include:

- / trauma (with rib fractures) and percutaneous lung biopsy
- / malignant tumours (typically osteosarcoma metastases)
- / emphysema, honeycomb lung (pulmonary fibrosis = destroyed and fibrotic lung tissue with cystic airspaces and fibrous walls and loss of acinar architecture)
- / spontaneous pneumothorax (typically in thin and tall adolescents and in smokers)

<!> ATTENTION

Signs of a pneumothorax on CXRs include:

- / the lung "edge" (= visceral pleura) is outlined by air in the pleural cavity
- / usually, a pneumothorax is well seen on a PA CXR in inspiration – however, a small pneumothorax is better seen on a PA CXR done in expiration (because of reduced lung volume in expiration, the pneumothorax appears larger)

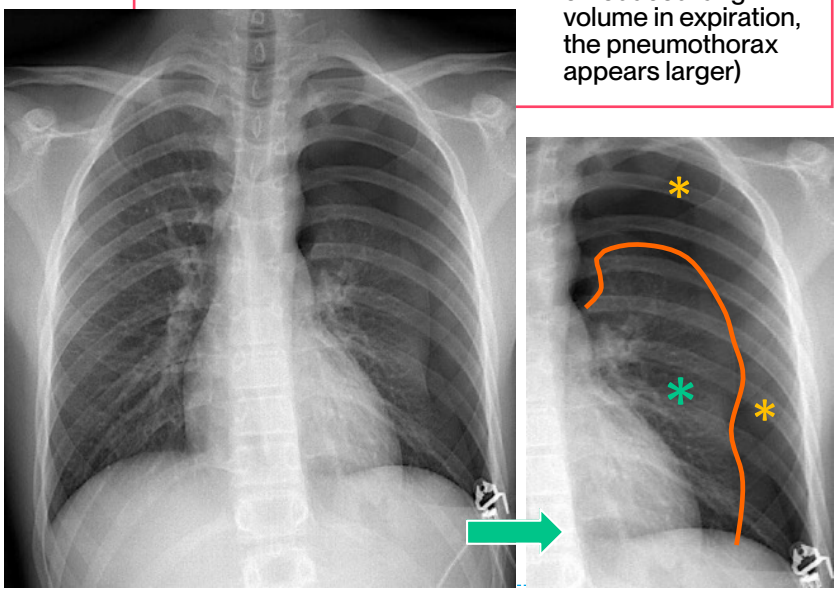

Spontaneous left pneumothorax (yellow asterisks). The left visceral pleura (orange line) is seen as a thin line outlining the collapsed left lung (green asterisk).

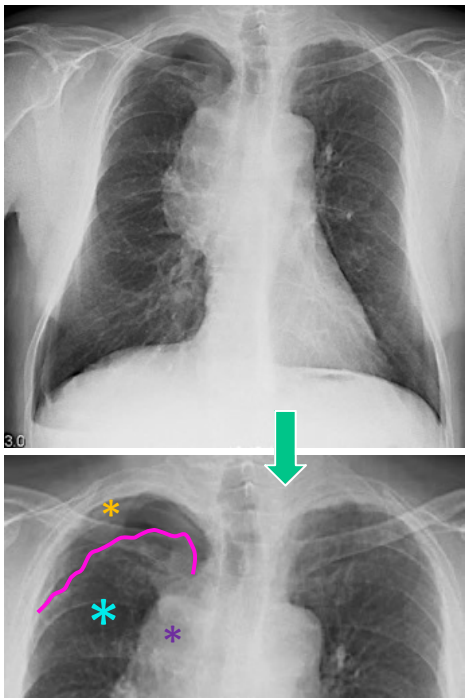

On erect CXRs, a small pneumothorax is typically seen at the lung apices. The figure above shows a small right pneumothorax (yellow asterisk) after CT-guided biopsy of a large mediastinal mass (purple asterisk). The right visceral pleura (pink line) is seen as a thin line outlining the partially collapsed left lung (turquoise asterisk).

On supine CXRs, the only sign of a pneumothorax (yellow asterisk) may be an abnormally deepened costo-phrenic angle, known as the "deep-sulcus sign" (orange line). It is due to collection of air basally within the non-dependent regions of the lung in the supine position.

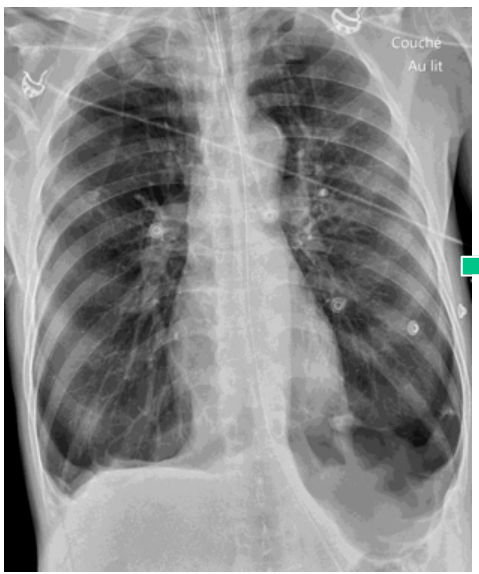

Deep sulcus sign (orange line) on the left. Visceral pleura (pink line) of the partly collapsed left lung. Left pneumothorax (yellow asterisk). Normal lateral right costophrenic angle (green line).

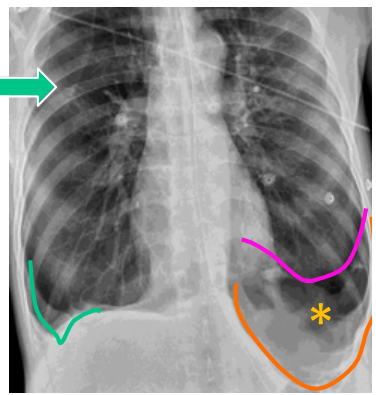

/ Chest Imaging

CHAPTER OUTLINE:

Tension pneumothorax occurs when air continues to penetrate the pleural cavity. This leads to further progressive lung compression and an increased volume of the affected hemithorax.

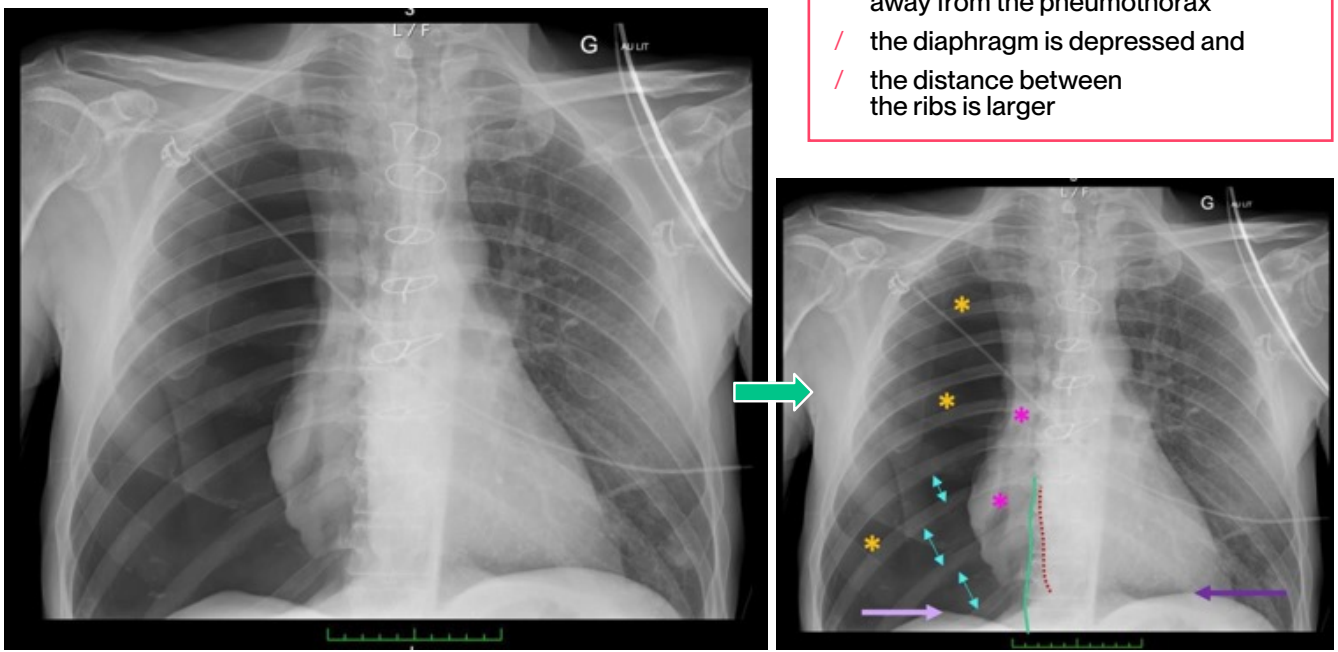

Tension pneumothorax (yellow asterisks) after cardiac surgery. The right lung (pink asterisks) is entirely collapsed. Shift of the mediastinum to the left (note that the right cardiac border (dark red line) projects medially of the right paraspinal line (green line)). Expansion of the right hemithorax and increased distance between the ribs (turquoise arrows) of the right hemithorax. Inferior displacement of the right hemidiaphragm (light purple arrow) in comparison to the left hemidiaphragm (purple arrow).

<!> ATTENTION

Signs of a tension pneumothorax on CXRs include:

- the mediastinum is displaced away from the pneumothorax
- the diaphragm is depressed and
- the distance between the ribs is larger

/ Pleural Thickening and Plaques

Pleural thickening = descriptive term, which corresponds to thickening of the visceral or parietal pleura. It can occur because of infection (e.g., tuberculosis, pleural empyema) and trauma (delayed complication of haemothorax) or it can be a manifestation of pleural plaques or of pleural tumours. Pleural plaques are the most common manifestation of asbestos exposure. Neoplastic conditions causing pleural thickening include pleural mesothelioma, pleural metastases and tumours with secondary pleural invasion.

Calcification of pleural plaques is common especially in patients with asbestos exposure, which tends to involve the diaphragmatic pleura. Calcified pleural plaques are also seen in tuberculosis, after empyema and haemothorax. The plaques, which originate from the parietal pleura, most often involve the lower chest pleura.

<!> ATTENTION

Signs of pleural plaques on CXRs include:

- pleural-based convex soft tissue opacities when these are perpendicular to the film/detector and poorly defined opacities when these are parallel to the film/detector
- holy leaf aspect (= irregular and thickened plaque edges)
- calcifications
- blunted costophrenic angles (the differential diagnosis includes pleural effusion). However most often the costophrenic angles and the apical pleura are spared by pleural plaques

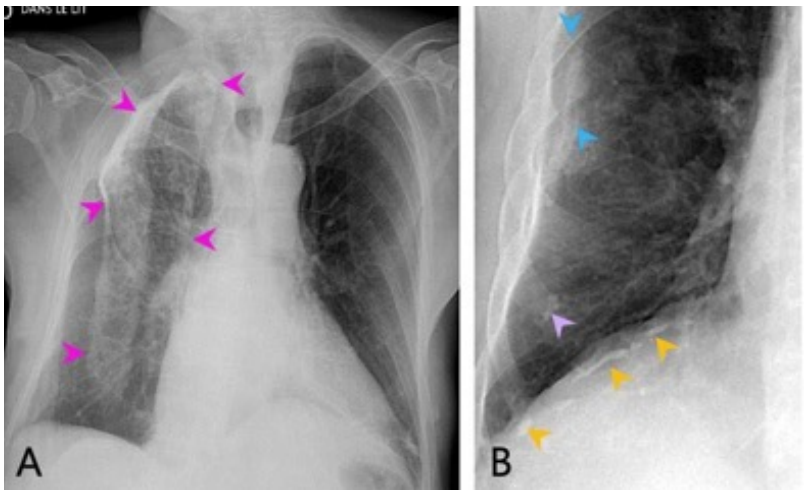

Two different patients with calcified pleural plaques. A. Large calcified plaque (pink arrowsheads) in a patient with a previous history of tuberculosis. B. Patient with asbestos exposure and calcified plaques along the diaphragm (yellow arrowheads), anterior/posterior pleura (purple arrowhead) and lateral pleura (blue arrowheads). The left lateral plaque shows soft tissue thickening and calcifications.

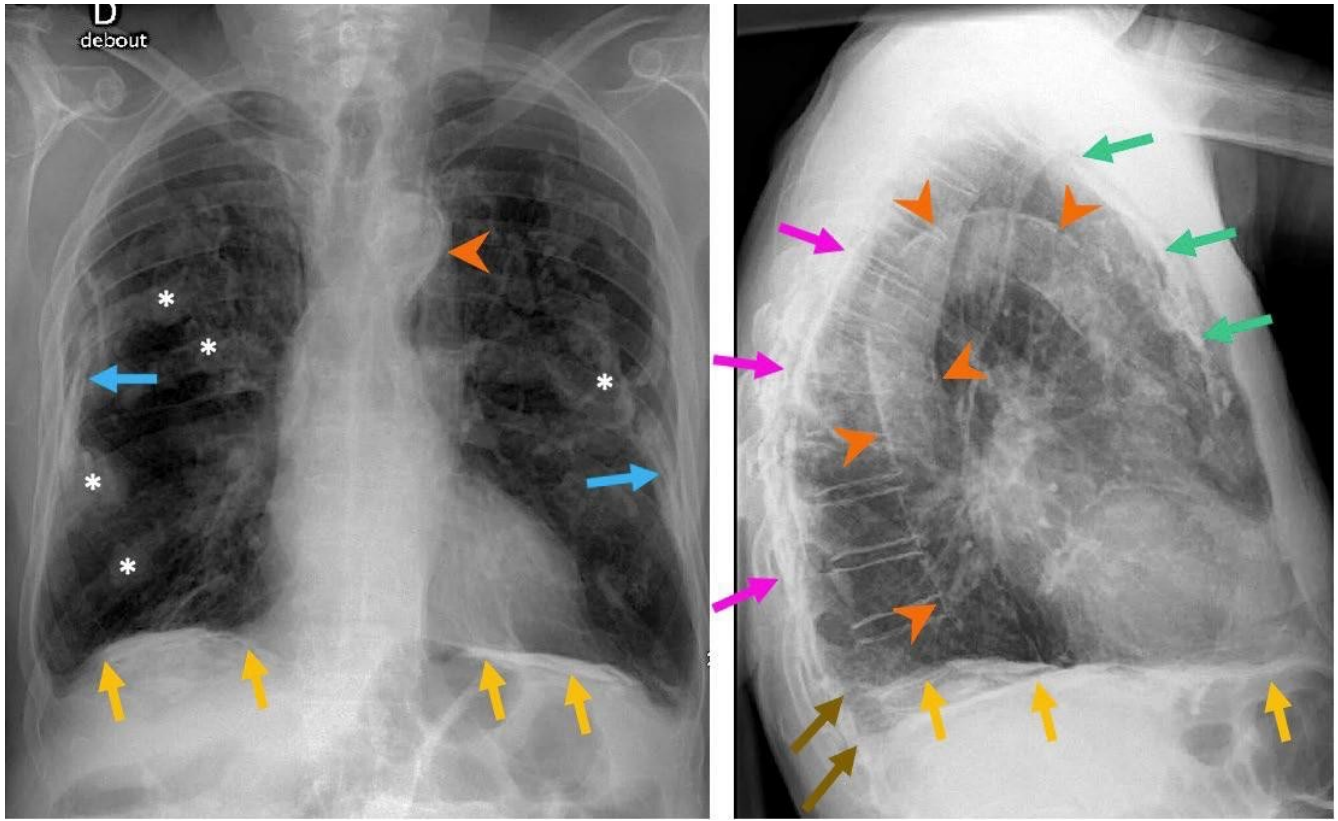

Patient with asbestos exposure and calcified pleural plaques along the diaphragm (yellow arrows), anterior pleura (green arrows), posterior pleura (pink arrows) and lateral pleura (blue arrows). Note that the anterior (green arrows) and posterior (pink arrows) plaques (*) show typical calcifications and a holy leaf aspect (*). Blunting of the costophrenic angles (brown arrows). Extensive aortic calcifications (orange arrowheads) due to atherosclerosis.

CHAPTER OUTLINE:

Pleural plaques are most often asymptomatic. They are found incidentally on a CXR. Most pleural plaques are benign and they do not require follow-up or aggressive treatment.

<!> ATTENTION

CT is the imaging modality of choice to identify pleural plaques due to its high sensitivity and specificity compared to CXR. On CT, pleural plaques appear as quadrangular soft tissue thickenings ± calcifications.

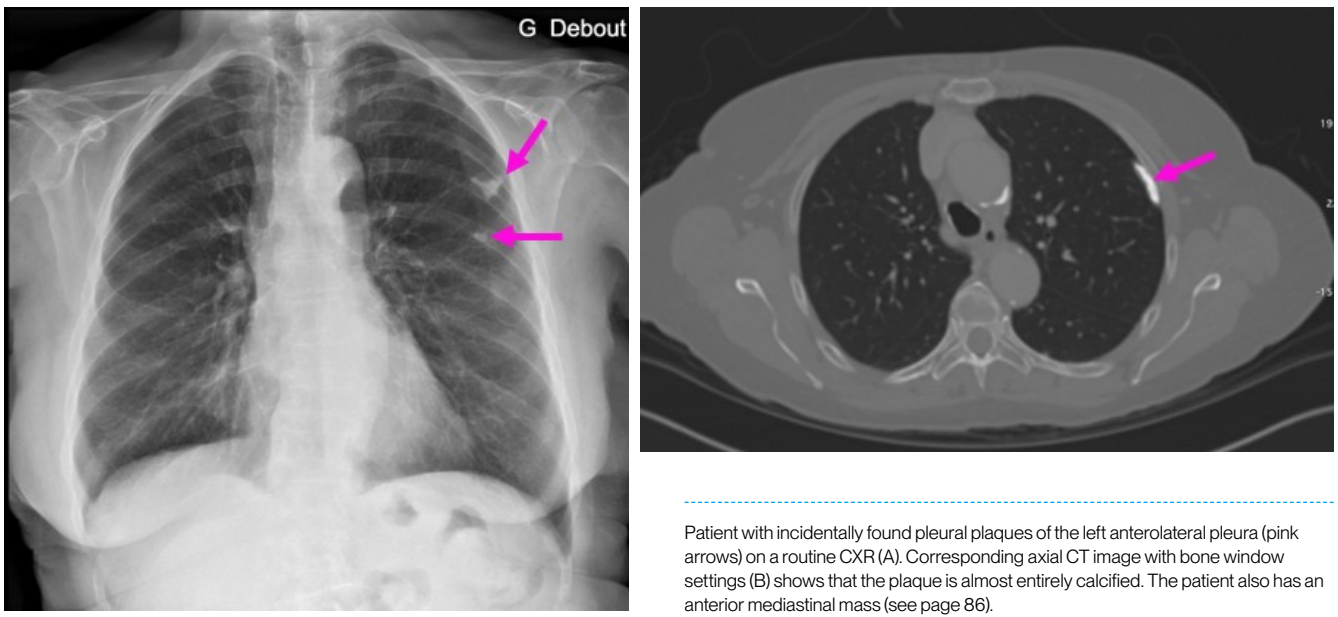

Patient with incidentally found pleural plaques of the left anterolateral pleura (pink arrows) on a routine CXR (A). Corresponding axial CT image with bone window settings (B) shows that the plaque is almost entirely calcified. The patient also has an anterior mediastinal mass (see page 86).

Most pleural malignant lesions are metastases from lung cancer, breast cancer, ovarian cancer or lymphoma. Pleural metastases are more common than pleural mesothelioma. The first manifestation of pleural metastases is pleural effusion due to impaired lymphatic drainage or increased capillary permeability.

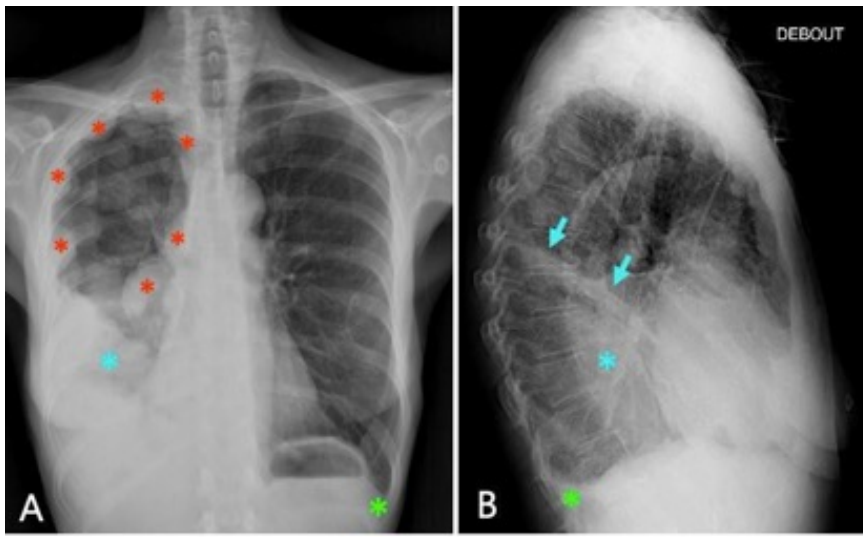

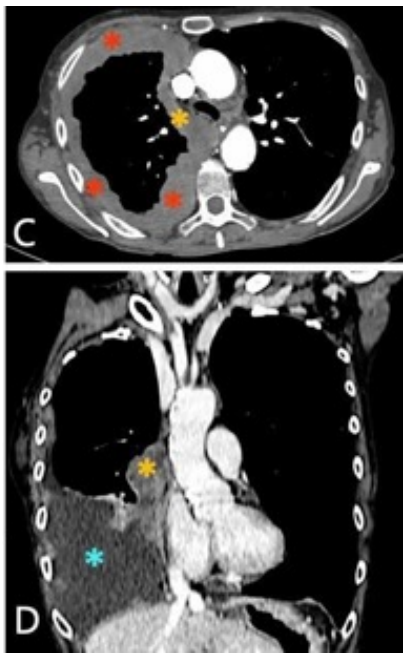

Patient with histologically proven right pleural metastases from head and neck squamous cell carcinoma. Nodular pleural thickening (orange asterisks) on PA CXR (A) and lateral CXR (B), large right pleural effusion (turquoise) and small left pleural effusion (green asterisks). Corresponding axial (C) and coronal (D) CT images show extensive nodular thickening of the right pleura (orange asterisks) including the mediastinal pleura (yellow asterisks) corresponding to tumour dissemination and an associated right pleural effusion (turquoise asterisk). There was equally a small pleural effusion on the left (not shown).

<!> ATTENTION

Characteristic imaging features of malignant pleural lesions include pleural effusion and nodular pleural thickening.

The Abnormal Mediastinum

CHAPTER OUTLINE:

/ Pneumomediastinum

Pneumomediastinum = extraluminal gas in the mediastinum

Causes comprise chest trauma, vigorous exercise, post-surgical situations, tracheobronchial and oesophageal perforation (caused by endoscopy, foreign bodies or malignant tumours) and certain types of infection. As with pneumothorax, spontaneous pneumomediastinum and tension pneumomediastinum can also occur. Except for tension pneumomediastinum, which can be rapidly fatal, pneumomediastinum usually requires no drainage.

Radiologic signs include curvilinear lucencies that contour the mediastinal structures. In children, the thymus may appear elevated and outlined by air (angel wing sign)

> see eBook chapter on Paediatric Radiology.

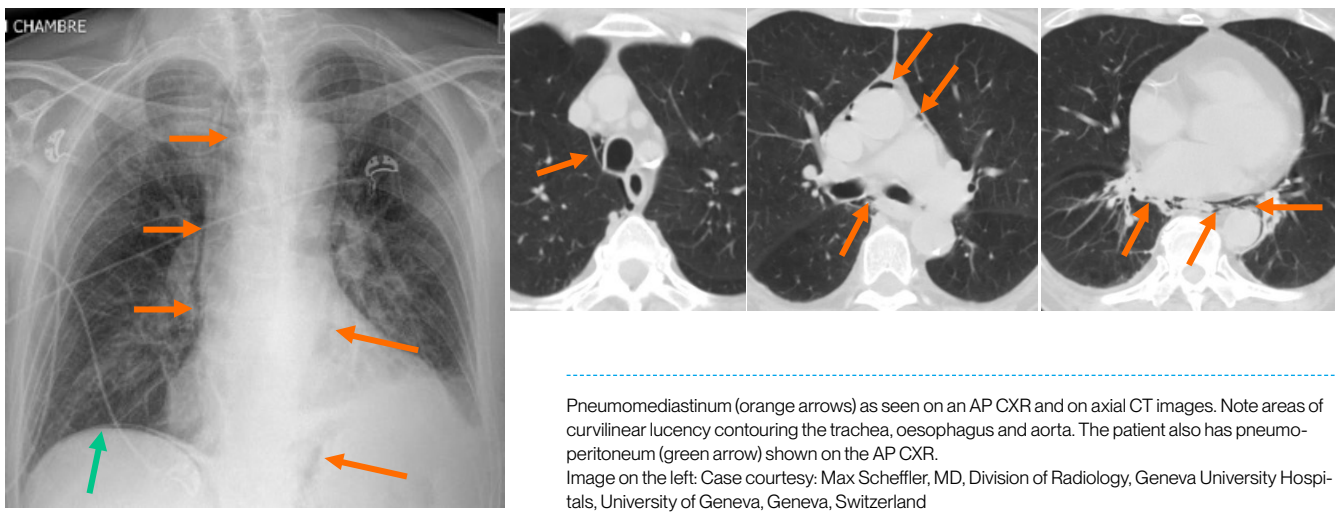

Pneumomediastinum (orange arrows) as seen on an AP CXR and on axial CT images. Note areas of curvilinear lucency contouring the trachea, oesophagus and aorta. The patient also has pneumoperitoneum (green arrow) shown on the AP CXR.
Image on the left: Case courtesy: Max Scheffler, MD, Division of Radiology, Geneva University Hospitals, University of Geneva, Geneva, Switzerland

/ Mediastinal Widening

On CXRs, the mediastinum is considered as widened when it is larger than 6cm on the PA projection or larger than 8 cm on the AP projection. Widening of the mediastinum has many different causes including neoplastic, infectious, traumatic and congenital. Some of the most important life-threatening concerns with a widened mediastinum include acute aortic dissection, acute aortic rupture and cardiac tamponade.

<!> ATTENTION

A widened mediastinum can also be caused by a poor CXR technique, e.g., due to inappropriate distance between the X-ray source and the detector plate or due to patient rotation. Therefore, assessing the quality of the CXR technique is very important before making the diagnosis of a widened mediastinum.

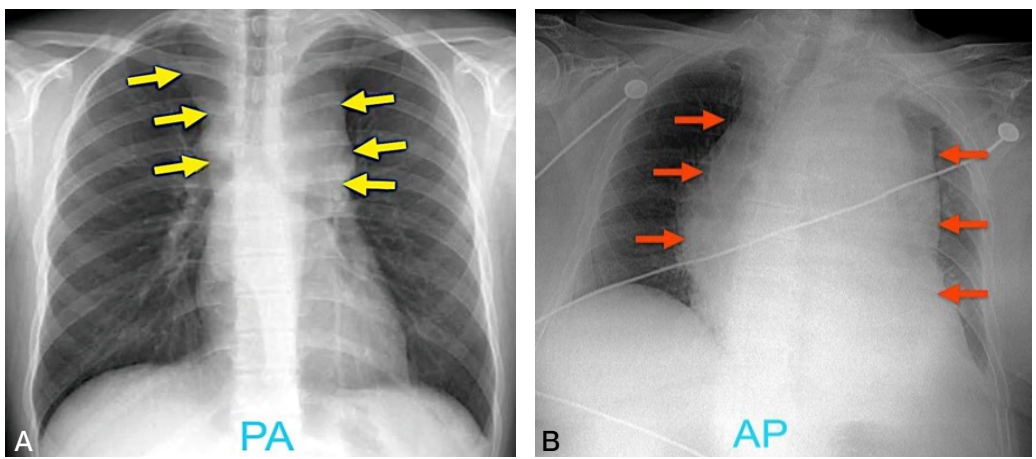

Two different patients with a widened mediastinum on the PA and on the AP projection, respectively. The patient in A had a lymphoma. The patient in B had traumatic aortic rupture with mediastinal haematoma.

/ Mediastinal Masses (MMs)

Slightly > 50% of mediastinal masses (MMs) are in the prevascular (anterior) mediastinal compartment. About 25% are in the visceral (middle) compartment and about 25% of MMs are in the paravertebral (posterior) compartment.

In many cases, contrast-enhanced CT (CE CT) in combination with clinical presentation ± MRI ± FDG PET CT are sufficient to make the diagnosis. However, image-guided or surgical histologic sampling can be necessary for a precise histologic tumour diagnosis and to guide further management.

If a large MM involves several compartments, to enable correct identification of the compartment from which a mass lesion originated, the "centre method" and the "structure displacement method" are used to interpret CT images.

- the "centre method" states that the largest size of a mass lesion seen on axial CT images corresponds to the compartment from which the mass originated
- the "structure displacement method" states that a large MM tends to displace structures from abutting compartments, e.g., an anterior MM may displace posteriorly structures from the middle mediastinum

To diagnose MMs on CXRs several criteria are applied: the angle border sign and the silhouette sign.

- the angle border sign allows distinguishing between a mediastinal and a pulmonary mass located next to the mediastinum > the sign is explained on the next page
- the silhouette sign refers to the loss of normal borders of intrathoracic structures: for example, a mass in the right anterior mediastinum may obscure the SVC and the right heart border a mass in the posterior mediastinum may result in loss of the paraspinal stripes. The hilum overlay sign is a useful sign to localize mediastinal abnormalities, see next pages

/ How to Distinguish a Mediastinal Mass (MM) from a Pulmonary Mass (PM)

>|< COMPARE

Mediastinal Mass

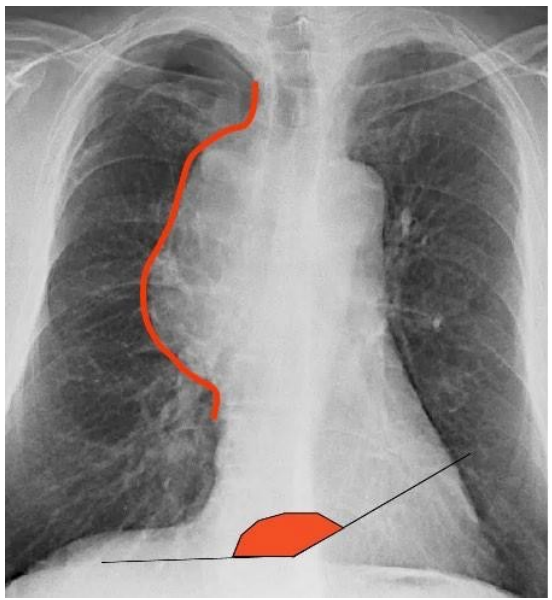

/ Obtuse angle with the lung → angle border sign

/ Mediastinal lines interrupted (silhouette sign)

Pulmonary Mass

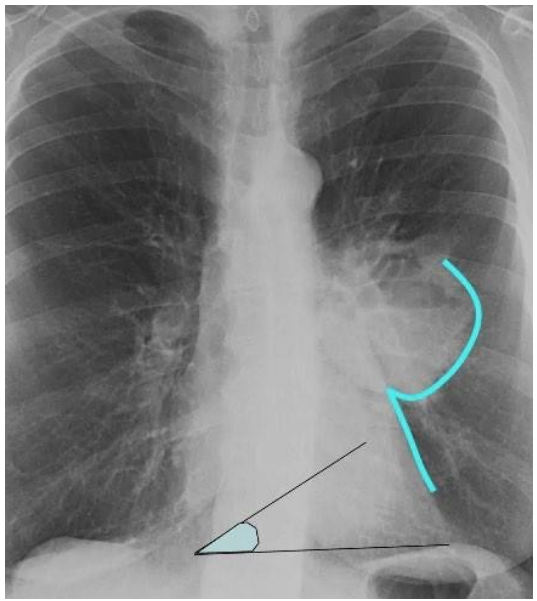

/ Acute angle with the lung → angle border sign

/ Mediastinal lines are not interrupted (no silhouette sign)

/ The Hilum Overlay Sign

The hilum overlay sign is used to localise an opacity, which projects in the hilar region on a frontal CXR (and if no lateral projection is available). If the silhouette of the hilar vessels is seen “through the mass”, then the mass is either located anteriorly or posteriorly. In other words, the mass is not located in the middle mediastinum. If the mass arises from the middle mediastinum or from the hilum, the silhouette of the hilar vessels is not visible anymore.

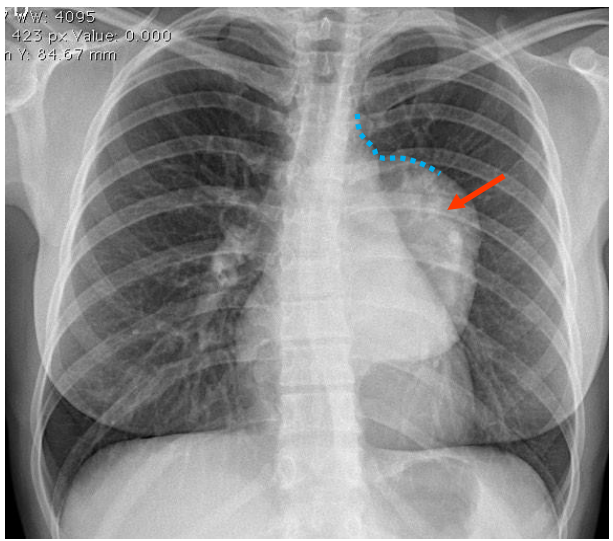

The mass is in the mediastinum (obtuse angle, blue line). The silhouette of the right hilum vessels (red arrow) is not obliterated by the mass. The mass is, therefore, either in the anterior or in the posterior mediastinum.

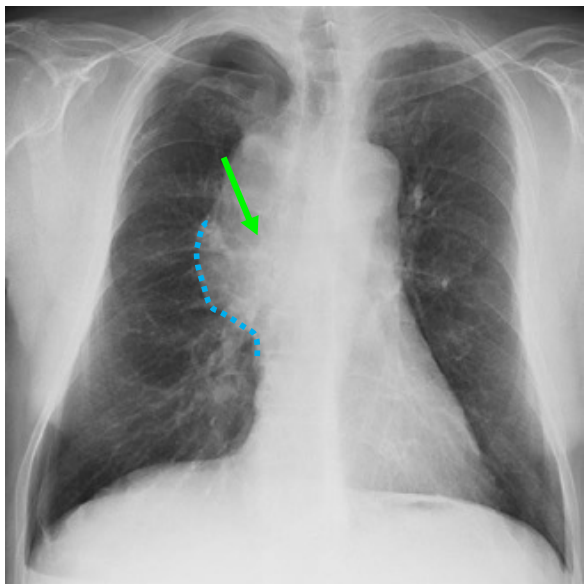

The mass is in the mediastinum (obtuse angle, blue line). The silhouette of the left hilum vessels (green arrow) is obliterated by the mass. The mass is, therefore, in the middle mediastinum.

/ CT for Characterisation of MMs

<!> ATTENTION

CT is used for the following purposes in MMs:

- / accurate localisation of a MM
- / precise assessment of the contents of a MM: fat, calcifications, teeth, air, fluid, solid tissue
- / assessment of invasion, compression or displacement of mediastinal structures (e.g., trachea, superior vena cava, heart, vertebral column)
- / biopsy under CT guidance

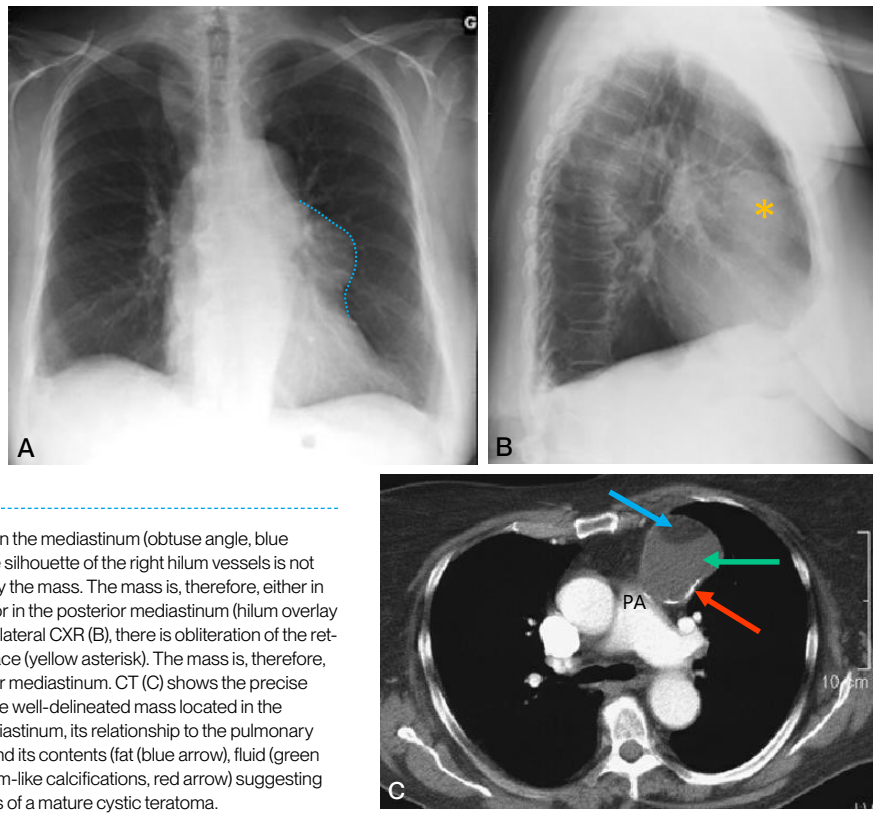

The mass is in the mediastinum (obtuse angle, blue line in A). The silhouette of the right hilum vessels is not obliterated by the mass. The mass is, therefore, either in the anterior or in the posterior mediastinum (hilum overlay sign). On the lateral CXR (B), there is obliteration of the retrosternal space (yellow asterisk). The mass is, therefore, in the anterior mediastinum. CT (C) shows the precise position of the well-delineated mass located in the anterior mediastinum, its relationship to the pulmonary artery (PA) and its contents (fat (blue arrow), fluid (green arrow) and rim-like calcifications, red arrow) suggesting the diagnosis of a mature cystic teratoma.

/ Anterior Mediastinal Masses (AMMs)

/ Differential Diagnosis (DD) and Radiologic Signs

Anterior (prevascular) MMs are located anteriorly to the pericardium and below the clavicle (ITMIG classification). The differential diagnosis of anterior MMs includes lesions arising in the thymus (e.g., thymoma, thymic carcinoma, thymic cyst), thyroid masses (e.g., goitre, thyroid cancer), masses arising in lymph nodes and germ cell tumours (e.g., teratoma, seminoma). The most common masses in the anterior mediastinum are of lymph node or of thymic origin.

<!> ATTENTION

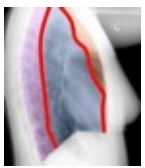

MNEMONIC for anterior MMs (the "4 Ts")

- T > thymus
- T > thyroid
- T > "terrible" lymphoma
- T > teratoma (> germ cell tumours)

<!> ATTENTION

Signs of anterior MMs on CXRs:

- displaced anterior junction line
- retrosternal space obliteration
- cardio-phrenic angle obliteration
- hilum overlay sign

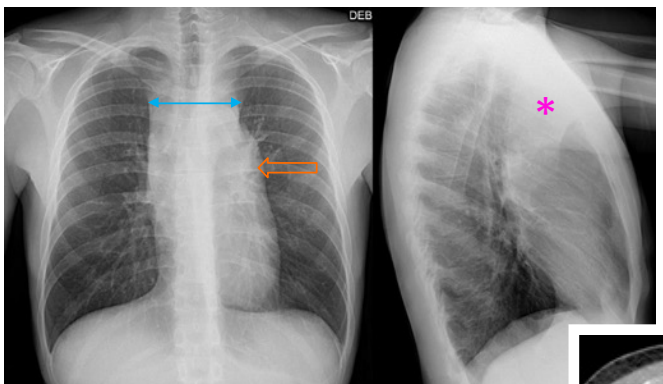

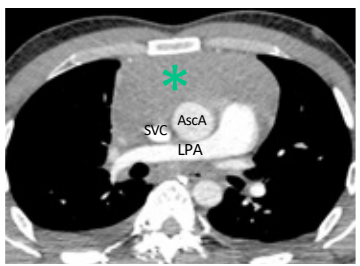

Mediastinal enlargement (blue arrow) on the PA CXR. Obliteration of the retrosternal space (pink asterisk) on the lateral CXR. Hilum overlay sign (orange arrow) on the PA CXR. Axial CT image obtained prior to biopsy confirms anterior mediastinal origin. Note posterior displacement of middle compartment structures by the tumour (green asterisk). Ascending Aorta (AscA), left pulmonary artery (LPA), superior vena cava (SVC). Biopsy revealed non-Hodgkin lymphoma.

<!> ATTENTION

CT is the mainstay for diagnosis!

In most cases, CXR does not allow distinction between the different types of MMs.

/ Thymic Epithelial Tumours

Thymic epithelial tumours, though rare, are the most common primary neoplasms of the thymus and anterosuperior mediastinum.

The WHO classification of thymic tumours divides them according to histological appearance (which reflects the likelihood of invasiveness) into:

- thymoma (types A, AB, B1, B2, B3 and other types)
- thymic carcinoma (e.g., squamous cell carcinoma, salivary gland-like carcinoma, thymic carcinoma not otherwise specified and other carcinoma types)
- thymic neuroendocrine neoplasms (e.g., carcinoid)

Thymomas are associated with over 30 conditions, notably myasthenia gravis (10% - 20% of cases), pure red cell aplasia (50% of cases), systemic lupus erythematosus, rheumatoid arthritis, Graves' disease and Cushing syndrome. Most thymomas are located in the anterior mediastinum, while 4% arise in ectopic sites.

<∞> REFERENCE

WHO Classification of Tumours Editorial Board. WHO Classification of Thoracic Tumours. (2021) ISBN: 9789283245063

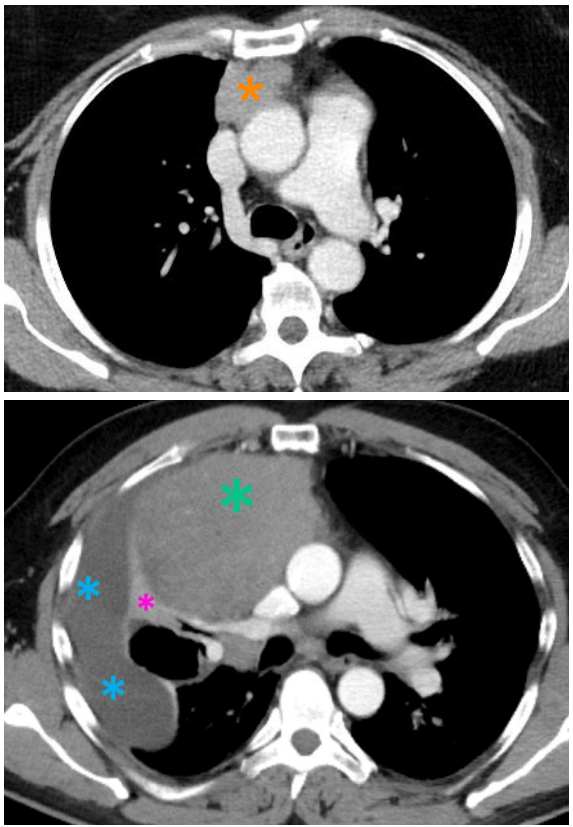

59-year-old woman who presented with myasthenia gravis. Axial CT image shows a well-defined lobulated homogeneous mass (orange asterisk) in the prevascular (anterior) mediastinum. Histology revealed thymoma type B3 ("atypical thymoma": epithelial cell sheets with mild to moderate atypia and scant lymphocytes). The clinical behaviour of this tumour type is more similar to thymoma than carcinoma.

52-year-old man with previous history of asthma presented with increasing respiratory complaints. Axial CT shows a large, relatively well-defined, slightly heterogeneous mass (green asterisk) in the prevascular (anterior) mediastinum. Associated pleural fluid (blue asterisks) and compression atelectasis (pink asterisk). Histology revealed thymoma type B1 (tumour with large areas indistinguishable from normal thymic cortex and areas resembling thymic medulla). This tumour type has a non-aggressive behaviour even in advanced stages.

/ Chest Imaging

CHAPTER OUTLINE:

/ Germ Cell Tumours (Seminoma)

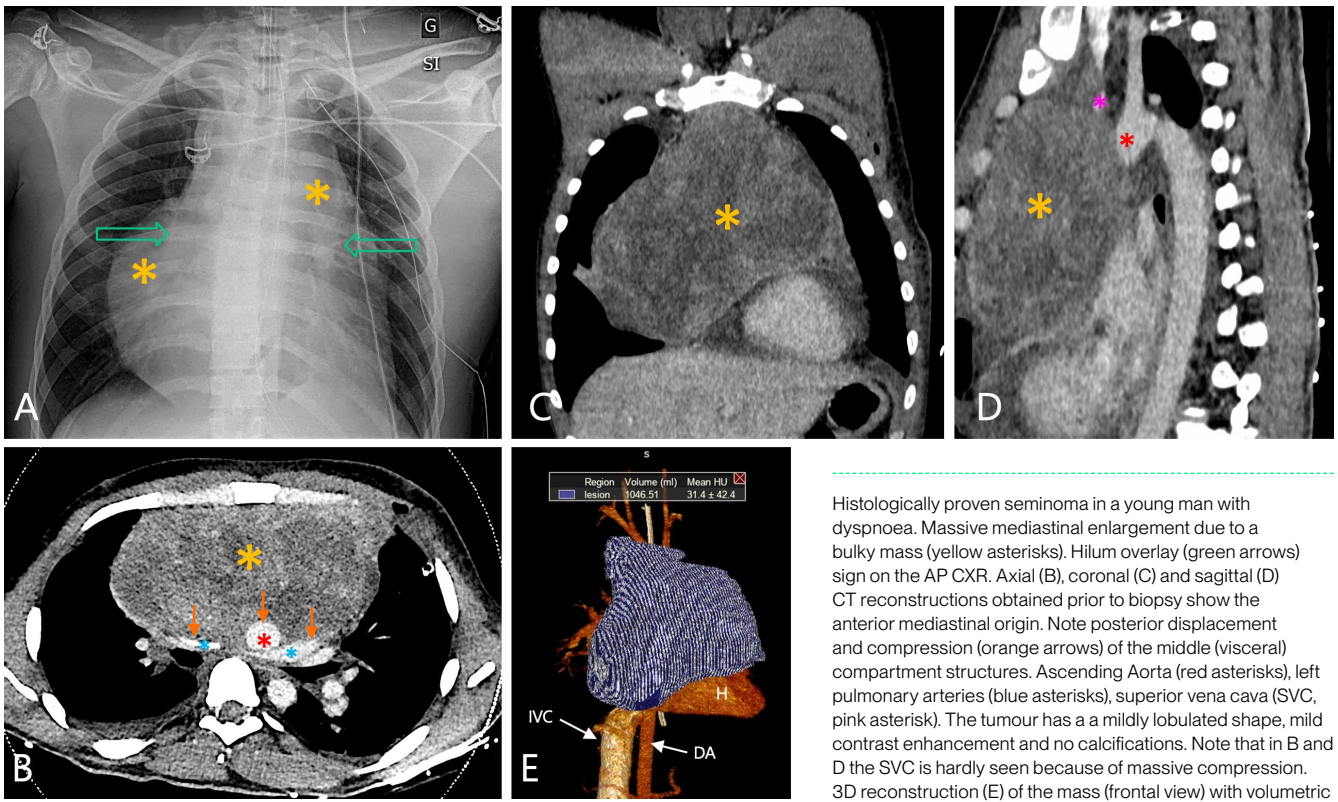

Histologically proven seminoma in a young man with dyspnoea. Massive mediastinal enlargement due to a bulky mass (yellow asterisks). Hilum overlay (green arrows) sign on the AP CXR. Axial (B), coronal (C) and sagittal (D) CT reconstructions obtained prior to biopsy show the anterior mediastinal origin. Note posterior displacement and compression (orange arrows) of the middle (visceral) compartment structures. Ascending Aorta (red asterisks), left pulmonary arteries (blue asterisks), superior vena cava (SVC, pink asterisk). The tumour has a a mildly lobulated shape, mild contrast enhancement and no calcifications. Note that in B and D the SVC is hardly seen because of massive compression. 3D reconstruction (E) of the mass (frontal view) with volumetric measurement (Vol = 1046 ml). Descending aorta (DA). Inferior vena cava (IVC).

<!> ATTENTION

Although CT does not always allow distinction between different MMs, the correct histologic diagnosis is possible whenever specific features are identified on CT scans, e.g., in teratoma, dermoid, cysts or vascular malformations.

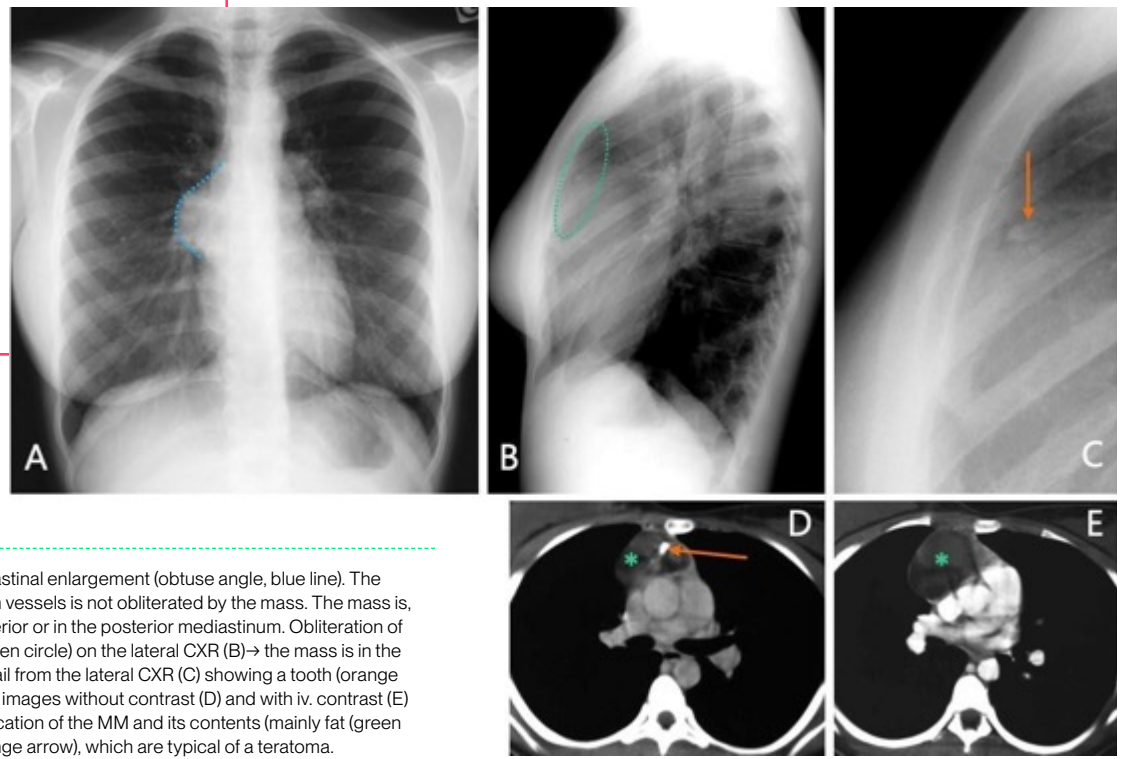

PA CXR (A) showing mediastinal enlargement (obtuse angle, blue line). The silhouette of the right hilum vessels is not obliterated by the mass. The mass is, therefore, either in the anterior or in the posterior mediastinum. Obliteration of the retrosternal space (green circle) on the lateral CXR (B)→ the mass is in the anterior mediastinum. Detail from the lateral CXR (C) showing a tooth (orange arrow) within the mass. CT images without contrast (D) and with iv. contrast (E) show the precise lesion location of the MM and its contents (mainly fat (green asterisks) and a tooth, orange arrow), which are typical of a teratoma.

CHAPTER OUTLINE:

/ Lymphoma

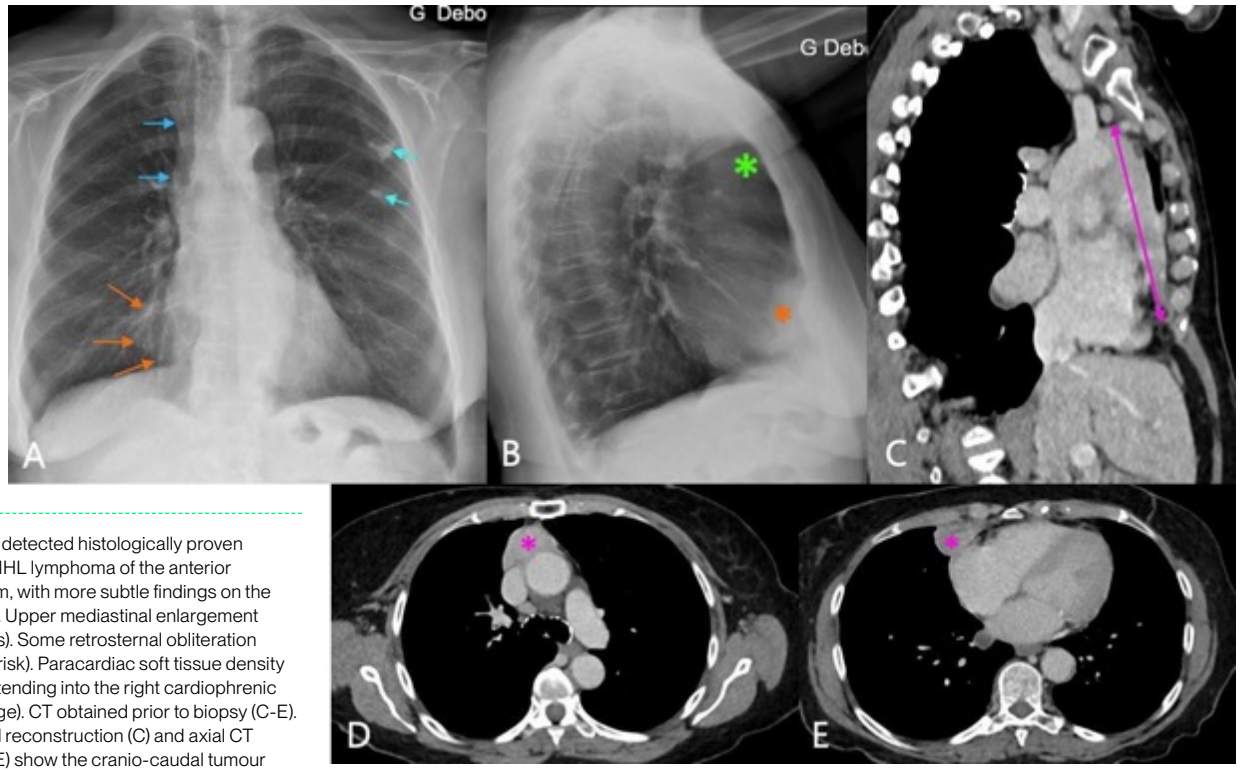

Incidentally detected histologically proven low grade NHL lymphoma of the anterior mediastinum, with more subtle findings on the CXRs (A, B). Upper mediastinal enlargement (blue arrows). Some retrosternal obliteration (green asterisk). Paracardiac soft tissue density (orange) extending into the right cardiophrenic angle (orange). CT obtained prior to biopsy (C-E). Parasagittal reconstruction (C) and axial CT images (D, E) show the cranio-caudal tumour extent (pink). The calcified pleural plaques (turquoise arrows) seen on the PA CXR were also seen on the CT scans (see page 73).

/ Chest Imaging

CHAPTER OUTLINE:

/ Middle Mediastinal Masses (MMMs)

/ Differential Diagnosis (DD) and Radiologic Signs

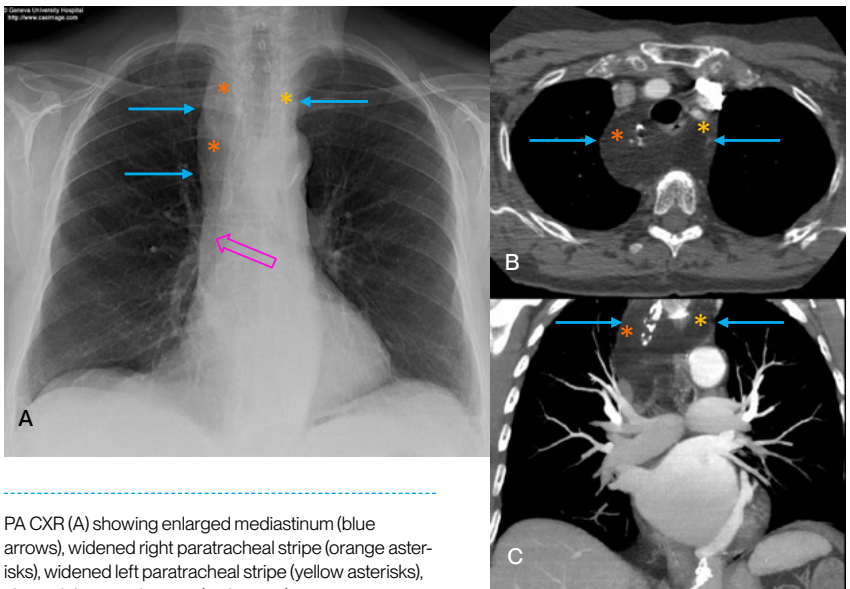

PA CXR (A) showing enlarged mediastinum (blue arrows), widened right paratracheal stripe (orange asterisks), widened left paratracheal stripe (yellow asterisks), absent hilum overlay sign (pink arrow) suggesting a middle mediastinal mass. Contrast-enhanced axial CT image (B) and coronal MIP (C) reconstruction confirm the presence of a middle MM. The mass contains fatty tissue and was a lipoma at surgery.

<!> ATTENTION

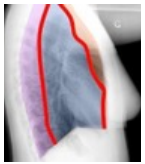

Middle (visceral compartment) MMs include

- / lymphadenopathy
- / vascular masses, e.g., aneurysms arising from the aorta or pulmonary arteries
- / tumours of the trachea and main bronchi, heart, pericardium, vagal and phrenic nerves or oesophagus
- / congenital cysts (bronchial, oesophageal, pericardial)
- / hiatus hernia

<!> ATTENTION

Signs of middle MMs on CXRs:

- / no hilum overlay sign
- / widened paratracheal stripes
- / widened right azygo-oesophageal recess
- / convex aorto-pulmonary window (APW)
- / mass anterior to the spine on lateral CXR
- / doughnut sign with the left or right bronchus on a lateral CXR

CHAPTER OUTLINE:

Convex APW (blue arrow) on PA CXR

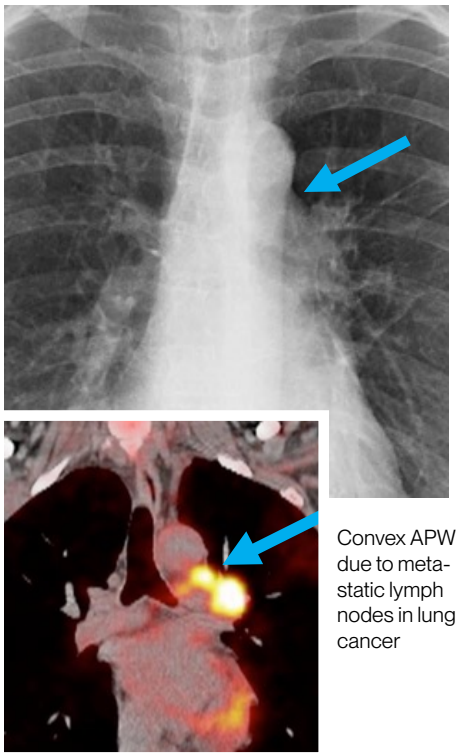

Convex APW due to metastatic lymph nodes in lung cancer

MM anterior to the spine (orange asterisk) on lateral CXR

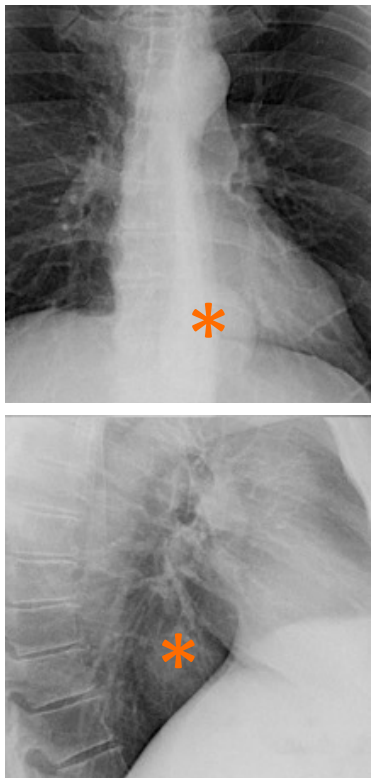

Hiatus hernia

Doughnut sign (pink circles) on lateral CXR

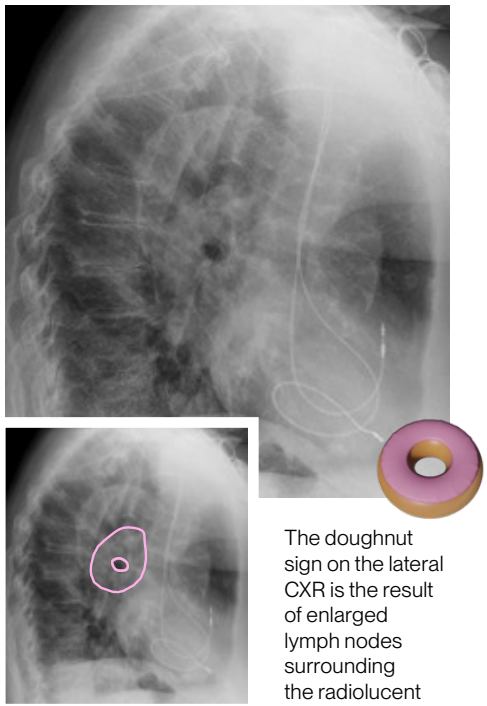

The doughnut sign on the lateral CXR is the result of enlarged lymph nodes surrounding the radiolucent trachea and upper lobe bronchi.

Lateral CXR image from: https://commons.wikimedia.org/wiki/File:Doughnut_sign_im_seitlich en_Roentgenbild_der_Lunge_94W_-_CR_seitlich_-_001.jpg

CHAPTER OUTLINE:

/ Small Cell Lung Cancer (SCLC)

About 20% of lung cancers are small cell lung cancers (SCLCs). SCLC is a neuroendocrine subtype of lung cancer associated with cigarette smoking. It has "small cells" at histology and unique clinical and imaging features, as well as distinguishing management implications. More than 90% of SCLCs are located centrally as the tumours typically arise from the mucosa of the mainstem or lobar bronchi. Therefore, they can manifest as MMs on CXRs. SCLC is often necrotic and haemorrhagic and it infiltrates mediastinal structures.

SCLC is the most common cause of superior vena cava (SVC) obstruction, which manifests with facial, neck and upper extremity swelling, dyspnoea or headache. SCLC is often also associated with paraneoplastic syndromes. Lymph nodes and distant metastases are common. Prognosis is rather poor. Staging of SCLC is done in the same way as the staging of non-SCLC (NSCLC) > see page 90.

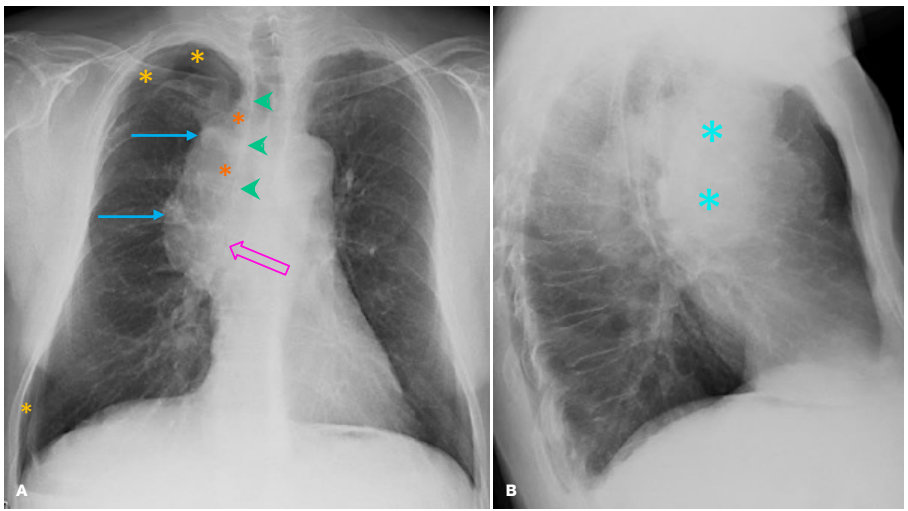

PA CXR (A) showing mediastinal enlargement on the right (blue arrows), widened right paratracheal stripe (orange asterisks), absent hilum overlay sign (pink arrows) and displaced trachea to the left (green arrows) suggesting a middle mediastinal mass. The lateral CXR (B) confirms that the MM (turquoise asterisks) is in the visceral compartment. As the CXR was performed after image guided biopsy, a small pneumothorax (yellow asterisks) caused by the biopsy is seen. Histology revealed SCLC. FDG PET CT (C) performed for staging purposes shows that the infiltrative middle MM (turquoise asterisk) has a high glucose metabolism. There were no distant metastases.

<!> ATTENTION

SCLC presents only rarely as a solitary lung nodule.

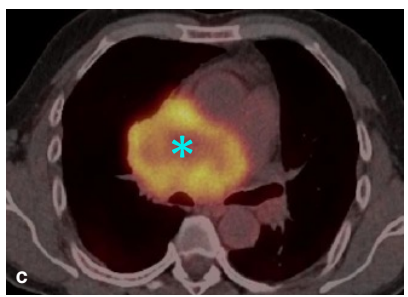

/ Chest Imaging

CHAPTER OUTLINE:

/ Non-Small Cell Lung Cancer (NSCLC)

Non-small cell lung cancer (NSCLC) can also manifest as an MMM. NSCLC does not have "small cells" at histology. NSCLC includes many different histologic tumour types, e.g., squamous cell carcinoma (SCC), adenocarcinoma (AC), large cell carcinoma, carcinoid and many more. AC is the most common histologic type of lung cancer followed by SCC. SCC is the most common type of Pancoast tumour (> see page 62).

SCC of the lung typically arises centrally. Regional lymph node metastases and distant metastases to the adrenal glands, liver, brain and bone are common.

Central tumour location results in enlargement of the mediastinum and hilum on CXRs due to tumour and lymph node involvement. Bronchus obstruction can lead to lobar collapse or pneumonitis. Cavitation in SCC represents a more aggressive tumour subtype.

Staging of NSCLC is done according to the TNM classification system. Survival depends on stage, histological and immunohistochemical characteristics. In general, for the same stage, survival in SCC is better than in AC.

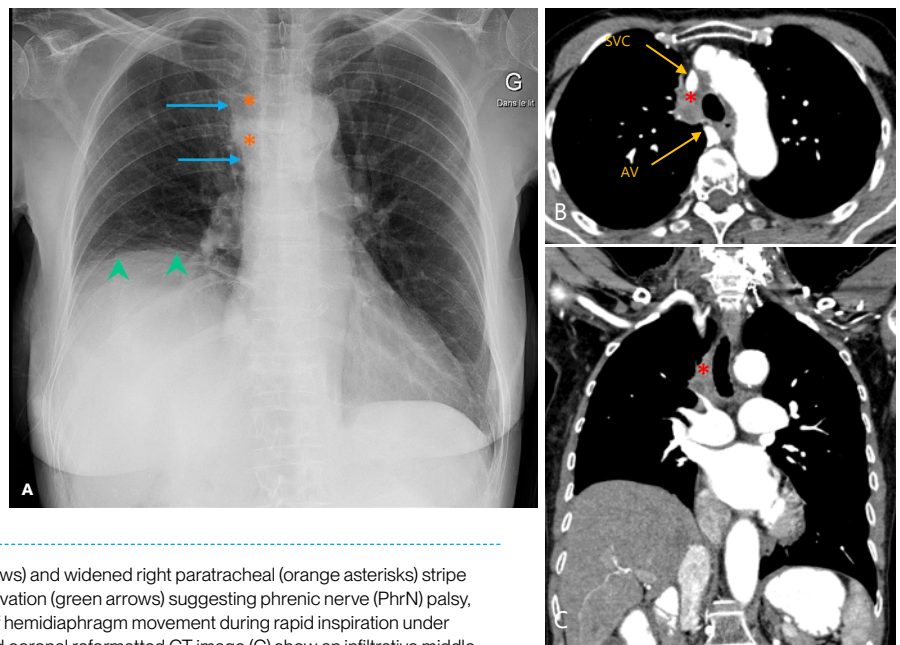

PA CXR (A) showing mediastinal enlargement (blue arrows) and widened right paratracheal (orange asterisks) stripe suggesting a middle MM. Note right hemidiaphragm elevation (green arrows) suggesting phrenic nerve (PhrN) palsy, which was confirmed by the "sniff test" (= observation of hemidiaphragm movement during rapid inspiration under fluoroscopy). Axial contrast-enhanced CT image (B) and coronal reformatted CT image (C) show an infiltrative middle MM (red asterisks) with encasement of the superior vena cava (SVC) and dilatation of the azygos vein (AV). The MM is located along the right PhrN, which descends lateral to the SVC and right atrium in the mediastinum.

/ Hiatus Hernia (HH)

Hiatus hernia (HH) is the result of herniation of abdominal contents (most often of the stomach) through the diaphragmatic oesophageal hiatus into the chest cavity. Sliding HH is the most common type (>90%) while rolling (para-oesophageal) HH and mixed (rolling and sliding) hernias are uncommon. If the gastric fundus is above the diaphragm, the HH presents as a retrocardiac middle MM.

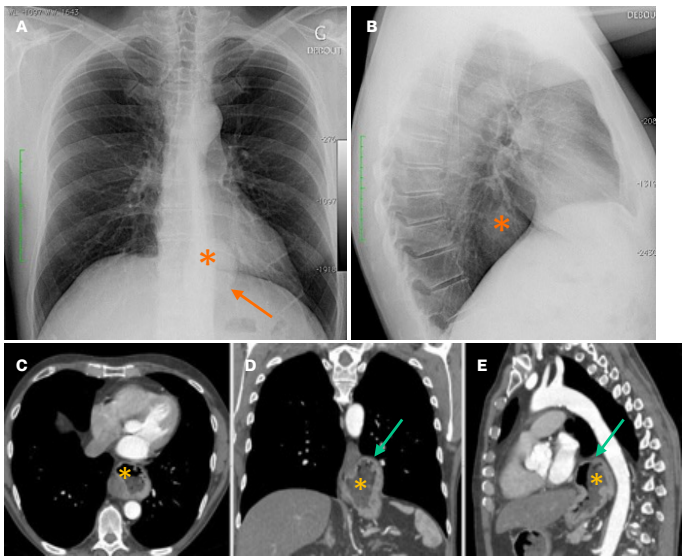

PA CXR (A) and lateral CXR (B) showing a retrocardiac middle MM (orange asterisks) partly projecting below the diaphragm (orange arrow). Axial contrast-enhanced CT (C), coronal (D) and sagittal (E) reformatted images show a sliding HH (yellow asterisks) with the gastric fundus (green arrows) extending well above the diaphragm.

<!> ATTENTION

- / Patients with HH can be entirely asymptomatic, in which case HH is an incidental finding.
- / In minimally symptomatic and in older patients watchful waiting is recommended.
- / Symptomatic HH, especially the rolling, the mixed types and HHs containing other viscera than the stomach are usually managed surgically.

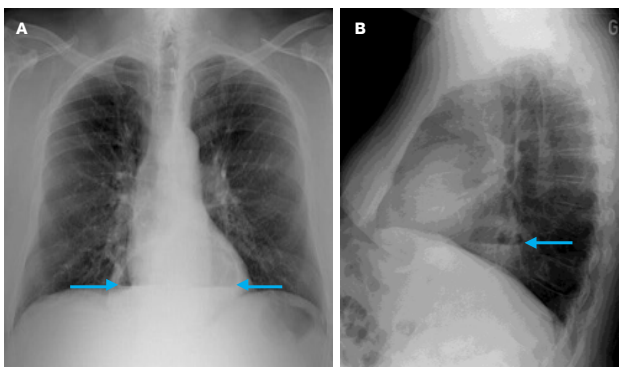

PA CXR (A) and lateral CXR (B) showing a retrocardiac middle MM with a gas-fluid level (blue arrows) typical of the diagnosis of a HH.

/ **Chest** Imaging

CHAPTER OUTLINE:

/ Posterior Mediastinal Masses (PMMs)

/ Differential Diagnosis (DD) and Radiologic Signs

<!> ATTENTION

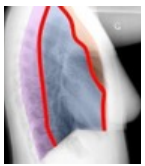

Posterior (paravertebral compartment) MMs include

- / neurogenic tumours, e.g., schwannoma, neurofibroma, malignant peripheral nerve sheath tumour, paraganglioma, pheochromocytoma, neuroblastoma
- / non-neurogenic tumours, e.g., chordoma, lymphoma, metastases
- / vascular lesions, e.g., descending thoracic aortic aneurysm
- / infection, e.g., abscess (from spinal infection)
- / meningoceles (in neurofibromatosis)
- / neurenteric cysts (with vertebral anomalies)

<!> ATTENTION

Signs of posterior MMs on CXRs

- / hilum overlay sign
- / cardiac border clearly seen
- / widened paraspinal and para-aortic lines
- / mass projecting on the spine on lateral CXR

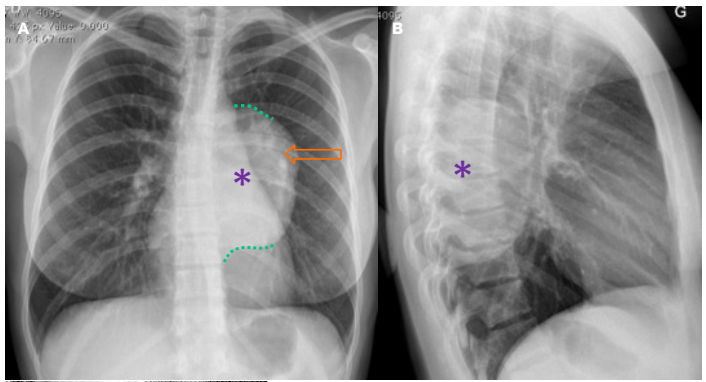

For paraganglioma
> See also eBook chapter on Endocrine System

The mass is in the mediastinum (obtuse angle (green line) in A). The silhouette of the left hilum vessels is not obliterated. The mass is, therefore, either in the anterior or in the posterior mediastinum (hilum overlay sign, orange arrow). The cardiac border is clearly seen > this is a posterior MM (purple asterisks). Lateral CXR (B) confirms the posterior mediastinal position. MRI (C) shows a well-delineated posterior MM, its relationship to the descending aorta (DA) and thoracic vertebral bodies (VB) and multiple flow voids (= low signal in enlarged and tortuous vessels with vigorously flowing blood, green arrows) suggesting a paraganglioma. Surgery confirmed the diagnosis.

/ Aneurysm of the Descending Aorta

Thoracic aneurysms are often identified incidentally on CXRs. Their shape and size can be very variable. If the axial diameter of the ascending aorta is > 5 cm and and the axial diameter of the descending aorta is > 4 cm, the term aneurysm is used. Although aneurysms are usually obvious on PA and lateral CXRs, due to magnification effects, the size of the aneurysm cannot be reliably assessed.

CT angiography and MR angiography are the modalities of choice to image aortic aneurysms.

<∞> REFERENCE

> See also eBook chapter on Vascular Imaging

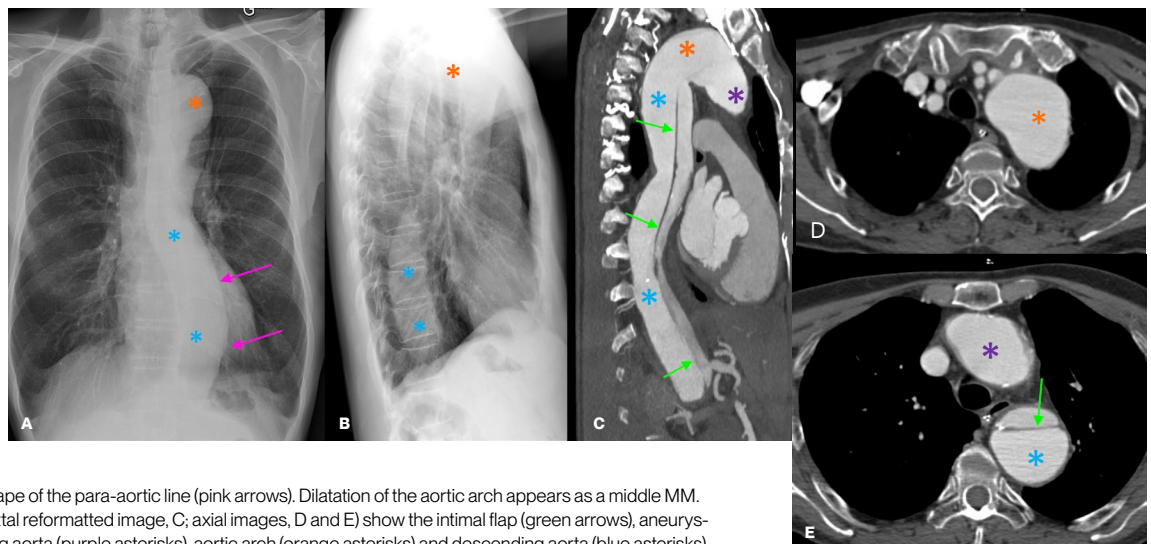

Patient with known aortic dissection Stanford type B (> see eBook chapter on Vascular Imaging) and aneurysmal dilatation of the ascending aorta, aortic arch and descending aorta. PA CXR (A) and lateral CXR(B) showing aortic arch dilatation (orange asterisks) and dilatation of the descending aorta (blue asterisks). Dilatation of the descending aorta appears as a tubular posterior MM. Note displacement and curved shape of the para-aortic line (pink arrows). Dilatation of the aortic arch appears as a middle MM. Contrast-enhanced CT (sagittal reformatted image, C; axial images, D and E) show the intimal flap (green arrows), aneurysmal dilatation of the ascending aorta (purple asterisks), aortic arch (orange asterisks) and descending aorta (blue asterisks).

CHAPTER OUTLINE:

Pathology of the Hilum

CHAPTER OUTLINE:

/ Differential Diagnosis and Radiologic Signs

The hila contain the proximal pulmonary arteries, bronchi, pulmonary veins and lymph nodes. Normal sized lymph nodes do not cause hilar enlargement. Hilar enlargement can be unilateral or bilateral. It is caused by enlarged lymph nodes, enlarged pulmonary arteries or bronchial masses. Most often, a significant degree of hilar enlargement needs to be present to be detected on CXRs. In addition to CT and PET CT, bronchoscopy, endobronchial ultrasound and mediastinoscopy may be needed for the diagnosis.

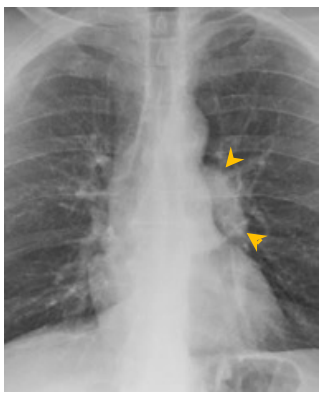

Case courtesy of Alborz Jahangiri, Radiopaedia.org, rID: 47026

<!> ATTENTION

Differential diagnosis of unilateral hilar enlargement

- bronchogenic carcinoma*
- lymphadenopathy
  - lymphoma (more often bilateral)
  - metastases from lung cancer and non-lung primary neoplasms*
  - infection (tuberculosis*, mycoplasma)
- enlarged pulmonary artery
  - unilateral pulmonary massive embolus
  - aneurysm of the pulmonary artery
  - pulmonary stenosis with post-stenotic left dilatation

* Most common causes of unilateral enlargement

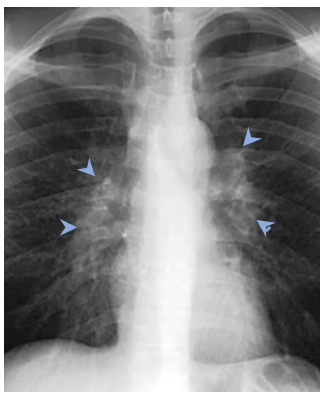

<!> ATTENTION

Differential diagnosis of bilateral hilar enlargement

- bronchogenic carcinoma
- lymphadenopathy
  - lymphoma (often bilateral and asymmetric)
  - metastases from lung cancer and non-lung primary neoplasms
  - sarcoidosis*
  - infection (tuberculosis, mycoplasma)
  - silicosis
- enlarged pulmonary arteries
  - pulmonary arterial hypertension*

* Most common causes of bilateral enlargement

/ Bilateral Hilar Enlargement

/ Sarcoidosis

Sarcoidosis is a non-caseating granulomatous disease of unknown aetiology with pulmonary, mediastinal, cardiac, central nervous system, head and neck and skin manifestations. It typically affects adults in their 2nd – 4th decades of life. The incidence is highest in African-Americans followed by northern European Caucasians.

More than 90% of patients with sarcoidosis have lung and mediastinal involvement although about 50% of patients are asymptomatic. Skin involvement, salivary gland, lacrimal gland and ocular involvement is common.

Pulmonary involvement is the major cause of morbidity and mortality. Pulmonary sarcoid granulomas typically occur along the bronchovascular lymphatics and along the interlobular septa. On CT scans, the following pulmonary changes are seen: nodules/micronodules with a perilymphatic distribution, alveolar opacities and centrally predominant pulmonary fibrosis (see description of the different pulmonary opacities later in this chapter.

<!> ATTENTION

PA CXRs are used to stage pulmonary sarcoidosis based on the presence and pattern of nodal and parenchymal involvement, whereas high resolution CT (HRCT) and FDG PET CT are usually employed to guide therapeutic decisions. Nevertheless, CT is more sensitive than CXRs for assessing sarcoidosis.

>=< FURTHER KNOWLEDGE

The stage of sarcoidosis as assessed by CXRs does not correlate with the level of clinical severity. Stage 0

> normal CXR, no granulomas

Stage 1 > hilar or mediastinal nodal enlargement due to granulomas
Stage 2 > both lymphadenopathy and pulmonary changes due to granulomas
Stage 3 > only pulmonary granulomas
Stage 4 > pulmonary fibrosis

The likelihood of spontaneous resolution decreases continuously from stage 1 (up to 90% spontaneous resolution) to stage 5 (0% spontaneous resolution).

CXRs typically reveal bilateral symmetric and massive hilar enlargement (due to so-called "potato nodes" (orange arrows) because of bulky and irregular morphology) and an enlarged right paratracheal stripe (light purple arrow) due to right paratracheal enlarged nodes (blue arrows) on CT. The enlarged right paratracheal nodes are more easily identified on PA CXRs than the left paratracheal nodes (green arrow) on CT, aortopulmonary nodes and subcarinal nodes (pink asterisks) on CT.

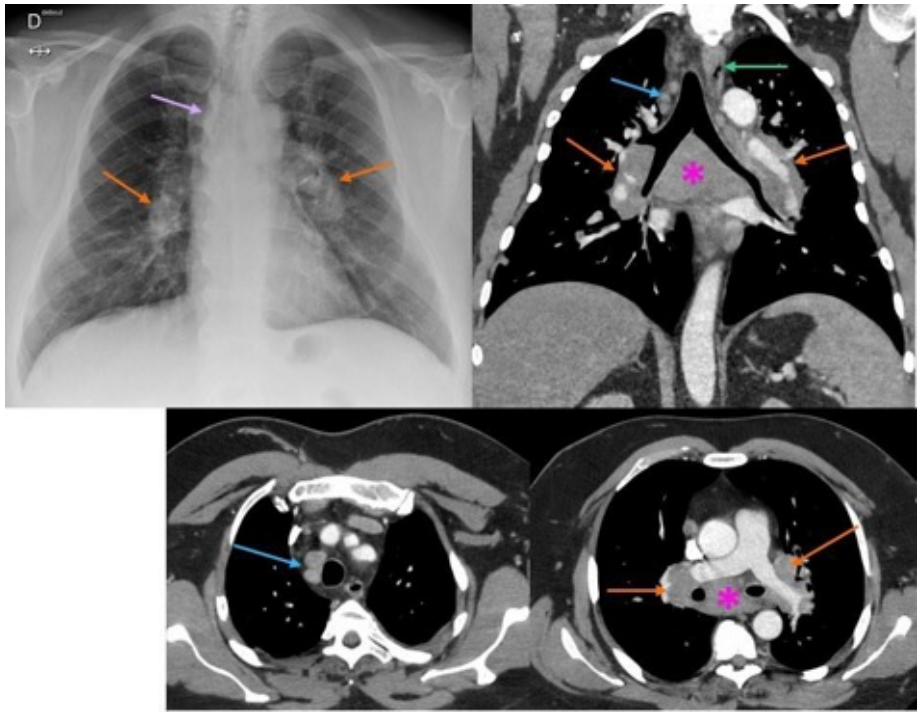

While hilar nodes are nearly always involved in sarcoidosis, isolated mediastinal lymphadenopathy is rare.

Lymphadenopathy in long-standing sarcoidosis can display punctate or eggshell calcifications.

>=< FURTHER KNOWLEDGE

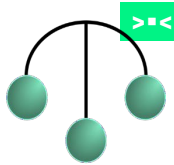

The combination of right paratracheal nodes, right and left hilar nodes is also known as the pawnbroker's sign or the 1-2-3 sign.

CHAPTER OUTLINE:

/ Lymphoma

Lymphoma can be limited to lymph nodes or it can arise in any organ (extra-nodal disease).

Hodgkin lymphoma (HL) is less common than Non-Hodgkin lymphoma (NHL) although both tumour types are quite rare.

HL typically begins in lymph nodes of the neck, mediastinum, hila and armpits, whereas NHL can arise in lymph nodes anywhere in the body.

Extra-nodal disease is much more common in NHL than in HL. In HL, involvement of lung parenchyma is rare at initial presentation and it is most often due to contiguous spread of disease from mediastinal and/or hilar lymphadenopathy. However, in recurrent HL, involvement of lung parenchyma can occur without hilar/mediastinal involvement.

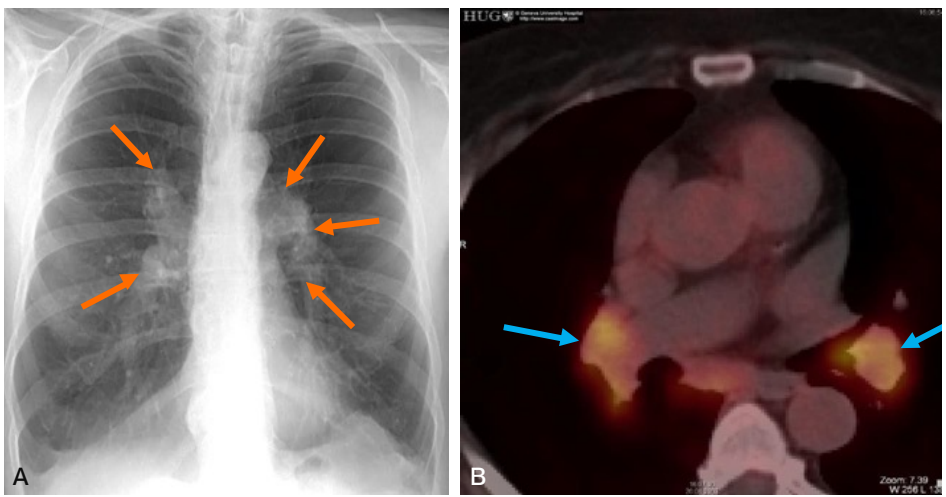

PA CXR (**A**) shows bilateral enlargement of the hila (orange arrows). Axial FDG PET CT image (**B**) at the level of the hila shows strongly FDG avid enlarged lymph nodes (blue arrows). Histology revealed HL.

<!> ATTENTION

Bilateral hilar involvement is more common in HL than in NHL at initial presentation.

/ Unilateral Hilar Enlargement

/ Nodal Metastases from Lung Cancer

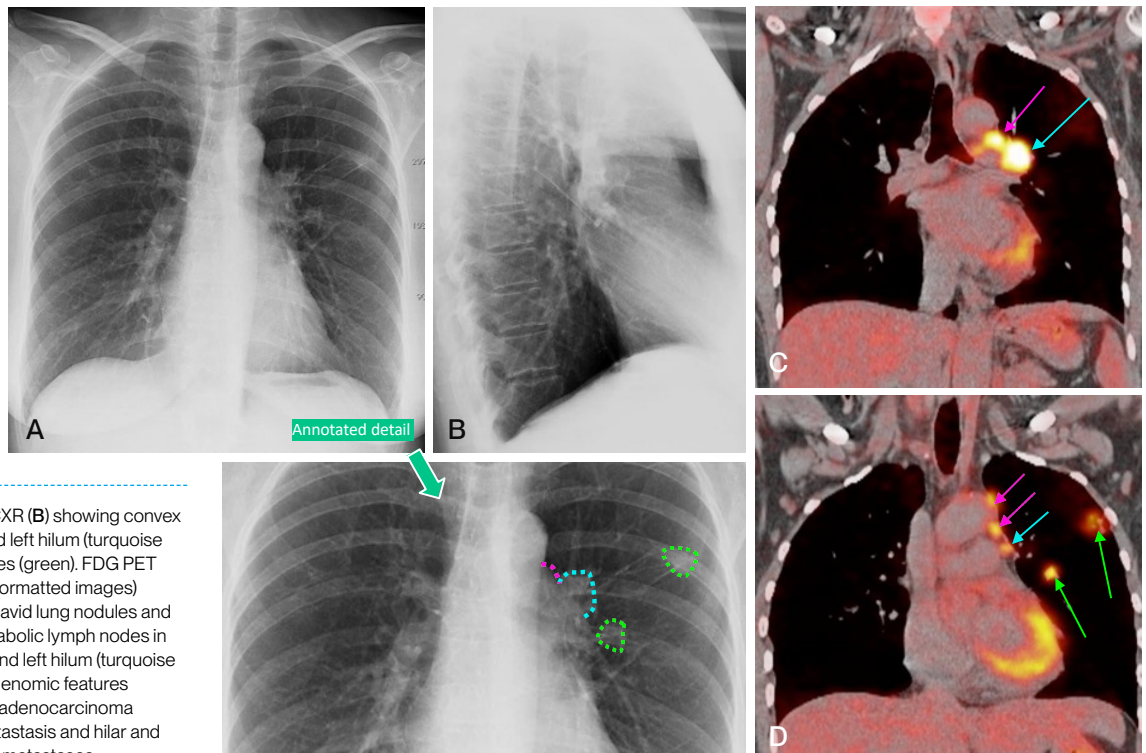

PA CXR (**A**) and lateral CXR (**B**) showing convex APW (pink line), enlarged left hilum (turquoise line) and two lung nodules (green). FDG PET CT (**C** and **D**, coronal reformatted images) show two strongly FDG avid lung nodules and enlarged and hypermetabolic lymph nodes in the APW (pink arrows) and left hilum (turquoise arrows). Histology and genomic features confirmed primary lung adenocarcinoma with intrapulmonary metastasis and hilar and mediastinal lymph node metastases.

/ Lymphoma

PA CXR (**A**) shows enlargement of the left hilum (orange arrows) and a pulmonary mass (green) located along the left mediastinal border (acute angle with the left heart border, green). This mass extends from the hilum into the left lower lobe (absent silhouette sign, therefore it is posterior to the heart). Note a second pulmonary mass located just above the left diaphragm (blue). FDG PET CT images (**B - E**) show that all mass lesions are strongly FDG avid. Histology revealed diffuse large B-cell lymphoma with hilar and left lower lobe involvement.

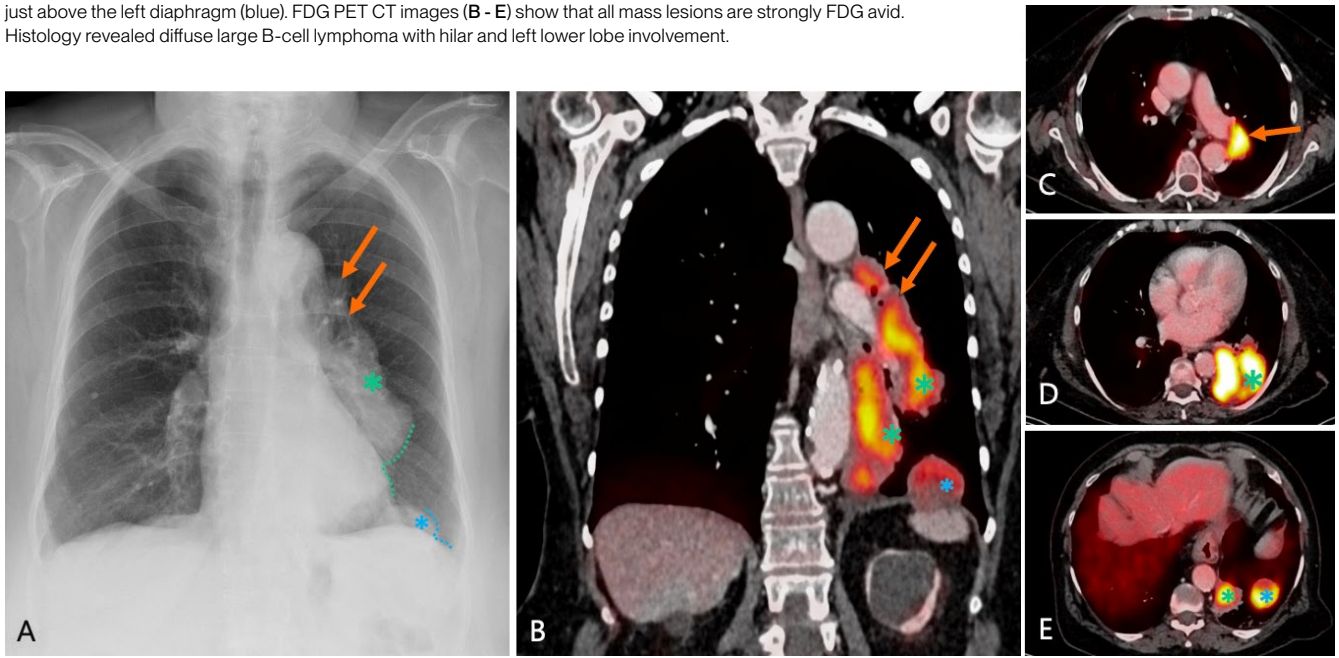

Abnormal Lung Parenchyma

CHAPTER OUTLINE:

/ Pulmonary Acinus and Pulmonary Lobule

The lungs comprise the airspaces (alveoli) and the interstitium. The interstitium contains supporting connective tissue, branching bronchi and bronchioles, arteries, veins and lymphatics. The distal bronchioles divide into terminal bronchioles (the most distal segment of the conducting zone), which in turn give rise to respiratory bronchioles (start of the respiratory zone). Respiratory bronchioles divide into alveolar ducts which give rise to alveolar sacs and alveoli.

The pulmonary acinus is supplied by a first order respiratory bronchiole. It comprises 2000 - 4000 alveoli. The secondary pulmonary lobule also called pulmonary lobule contains about 30 acini. It is supplied by a distal pulmonary artery and a terminal bronchiole. The pulmonary lobules are separated by incomplete interlobular septa which contain the distal pulmonary veins and lymphatics. The size of the pulmonary lobules varies (a peripheral lobule is larger than a central lobule). The interlobular septa are in continuity with the peribronchovascular and subpleural interstitium.

<!> ATTENTION

Pulmonary pathology may involve the alveoli, the interstitium or both.

Distinction between alveolar and interstitial abnormalities on CXR and HRCT are one of the most important factors to narrow down the differential diagnosis.

>|< COMPARE

Pulmonary acinus

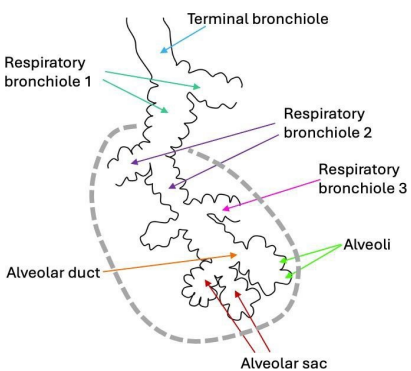

Secondary pulmonary lobule

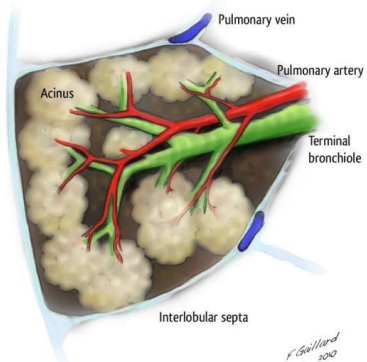

Image from: Gaillard F, Secondary pulmonary lobule (illustration). Case study, Radiopaedia.org https://doi.org/10.53347/rID-8760

/ Pulmonary Opacification Patterns

Pulmonary opacification is a nonspecific term that corresponds to a decreased ratio of gas to soft tissue (and therefore an increased attenuation on CXR and CT).

Pulmonary opacification can be divided into different patterns:

- alveolar opacification (consolidation)
- interstitial opacification
- nodular opacification
- atelectatic opacification (some authors use the term “atelectasis* as a synonym of collapse while others use it only for partial collapse; in this chapter, both terms will be used as synonyms)

Alveolar opacification

Interstitial opacification

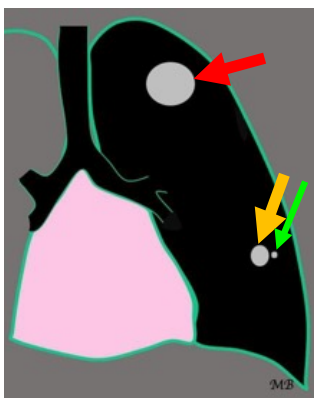

Nodules and masses

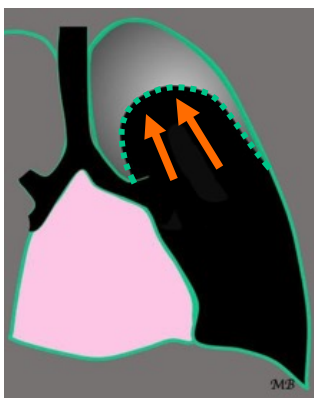

Atelectatic opacification

/ Alveolar Opacification (Consolidation)

Alveolar opacification (consolidation or airway opacification) seen on CXRs means that "something other than air" fills the alveoli.

Causes include transudate (lung oedema secondary to congestive heart failure, nephrotic syndrome, cirrhosis, hypoproteinaemia), exudate (inflammatory fluid/pus due to infection), haemorrhage, aspiration of gastric contents or of water (drowning) and cells (either due to lepidic tumour growth = tumour growth along the alveolar lining or caused by organising pneumonia). Correlation with clinical findings and patient history is a must as the observed attenuation on CXRs is nonspecific.

<!> ATTENTION

Features of alveolar opacification are:

- ill-defined, patchy, coalescent areas of opacification
- no loss of volume in the affected lung parts
- air bronchogram > the air-filled bronchi (dark) are outlined by the opacified (whitish/grey) alveoli. If the bronchi contain fluid, there is no air bronchogram.
- extension to a fissure without crossing it.

Alveolar opacification can display the following distribution patterns:

- segmental or lobar
- multiple opacities
- bat wing (see pages 107 and 135)
- reversed bat wing (see page 107)

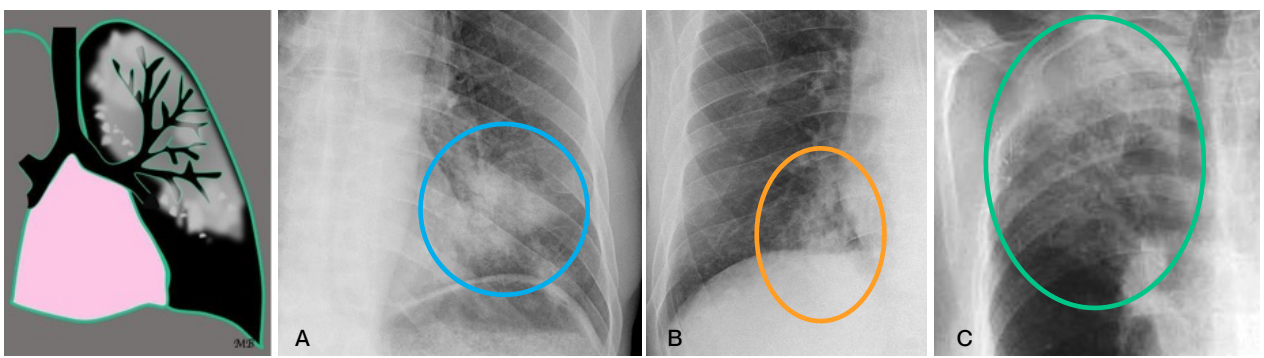

Three different patients (**A-C**) with alveolar opacification on PA CXRs involving the lingula (**A**, silhouette sign), the right lower lobe (**B**, no silhouette sign) and the right upper lobe (**C**), respectively. Note ill-defined areas of patchy opacification and air-bronchogram especially well visible in **C**.

/ Pneumonia

Pneumonia = infection of the lung by a pathogenic organism (as opposed to pneumonitis, which is a non-infective inflammation)

Pneumonia can be classified into many ways, e.g., according to:

- patterns of spread → lobar pneumonia (usually confined to a lobe) versus bronchopneumonia, i.e., initial peribronchiolar involvement → then spread to different lung segments and different lobes (multifocal involvement), which can progress to diffuse consolidation
- infection setting → community acquired pneumonia versus hospital acquired versus ventilator associated pneumonia

<!> ATTENTION

- Pneumonia is one of the major death causes related to infection.
- The most common bacterial pathogens include Streptococcus pneumoniae, Staphylococcus aureus, Klebsiella pneumoniae and Haemophilus influenzae.
- Viral pathogens include COVID-19 and varicella.
- Fungal pneumonia (Pneumocystis pneumonia) is virtually never seen in immunocompetent patients.

<!> ATTENTION

Lobar consolidation is the most common consolidation type.

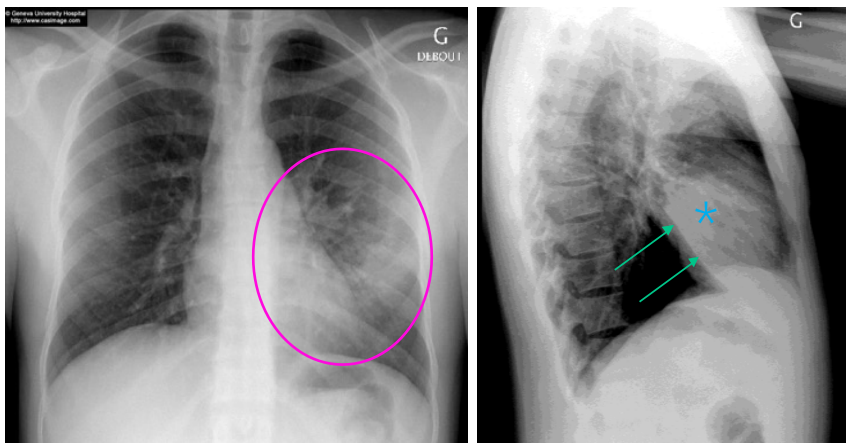

Lobar consolidation involving the left upper lobe mainly the lingula (pink circle). Note air bronchogram and no volume loss. Sharply defined opacification (blue asterisk) by the left oblique fissure (green arrows) on the lateral CXR.

/ Multifocal Distribution Pattern vs. Lobar Pattern

- Pneumonia is the most common cause of lobar (see previous page) and multi-focal consolidation.
- Lobar consolidation is also seen in patients with lung contusion and infarction, certain neoplasms (e.g., adenocarcinoma in situ formerly called bronchoalveolar carcinoma), as well as in some inflammatory conditions, e.g., sarcoidosis.
- Besides bronchopneumonia, multifocal consolidation can also be a manifestation of neoplasms and septic emboli.

<!> ATTENTION

The clinical history is essential for the differential diagnosis, in particular distinction between acute and chronic consolidation. The most common causes of acute consolidation are pulmonary oedema due to heart failure, pneumonia and aspiration, whereas neoplasms and sarcoidosis are the most common causes of chronic consolidation.

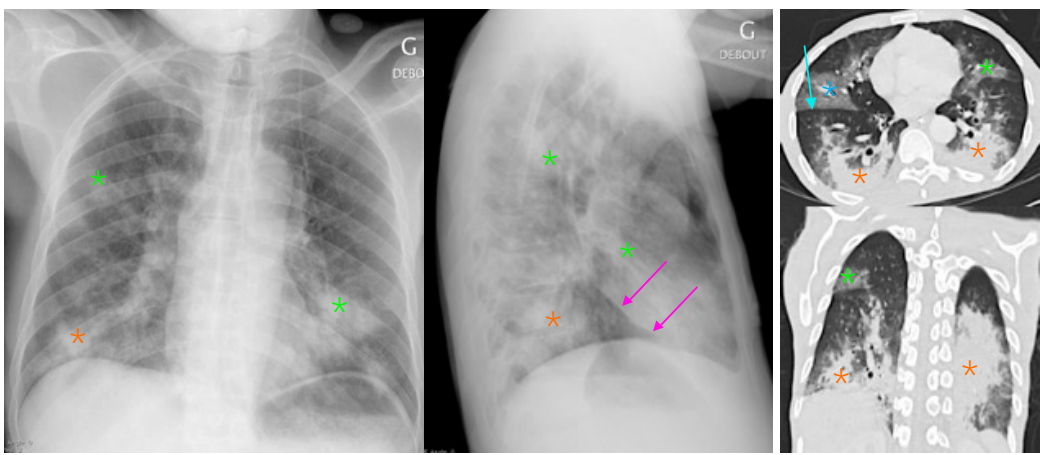

Multifocal alveolar opacification in bronchopneumonia (Staphylococcus aureus). Involvement of both lower lobes (orange asterisks), middle lobe (blue asterisk) and upper lobes (green asterisks)including the lingula. Note sharp delineation of the left oblique fissure (pink arrows) by upper lobe consolidation on the lateral CXR and sharp delineation of the horizontal fissure (turquoise arrow) on CT. On CT, vascular contours are not seen in the consolidated areas → see page 108 for distinguishing consolidation from ground glass opacity (GGO)..

/ Bat Wing and Reversed Bat Wing Distribution Pattern

>|< COMPARE

Bat wing opacities or butterfly opacities → bilateral perihilar alveolar opacities (see below). The pattern is seen on frontal CXRs and on CT. The most common cause is cardiogenic lung oedema (see page 137).

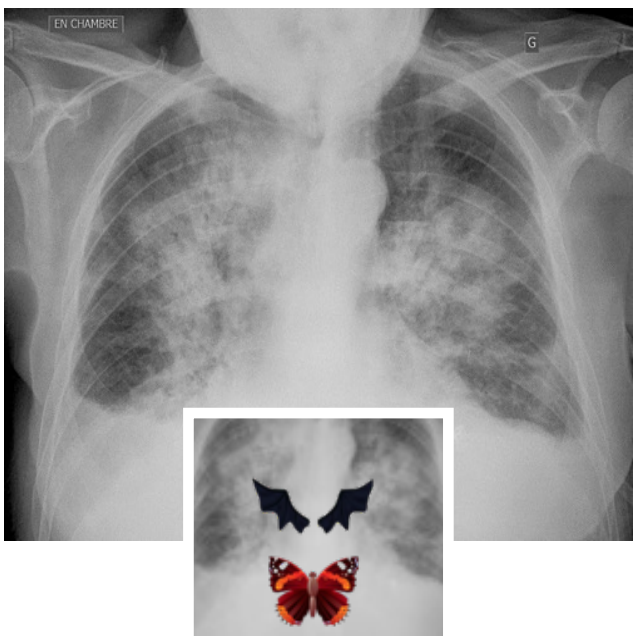

Reversed bat wing opacities → bilateral peripheral alveolar opacities sparing the perihilar regions (see below). The most common cause is chronic eosinophilic pneumonia (rare idiopathic

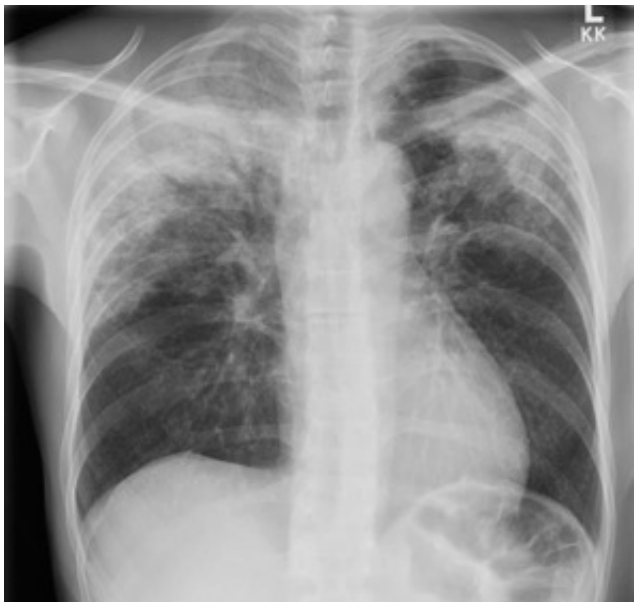

Case courtesy: Elswood T, Eosinophilic pneumonia. Case study, Radiopaedia.org https://doi.org/10.53347/rID-74170

/ Chest Imaging

CHAPTER OUTLINE:

/ Alveolar opacification (consolidation) versus ground glass opacity (GGO)

Ground glass opacity (GGO) = radiologic descriptive term that corresponds to a hazy increase in lung attenuation (opacity) on CT. GGO does not obscure lung vasculature on CT and bronchial markings are preserved.

<!> ATTENTION Although the term should only be used with CT, some radiologists also use it with CXRs.

Causes of GGO include:

- / normal expiration
- / partial alveolar filling with transudate, exudate, blood or lepidic tumour growth
- / mild interstitial thickening due to inflammation or fibrosis beyond the resolution of current CT scanners
- / partial alveolar collapse

GGO can predominantly affect the upper, middle or lower lung zones. On axial CT images, the distribution can be centrilobular, peribronchovascular, peripheral, subpleural or diffuse.

The distribution pattern plays an important role for the differential diagnosis, e.g., diffuse and bilateral GGO is typically seen in pneumocystis and other viral pneumonias or in heart failure.

<!> ATTENTION Not all GGOs are pathological, e.g., if CT is obtained during expiration or in bed-ridden patients due to prolonged supine position.

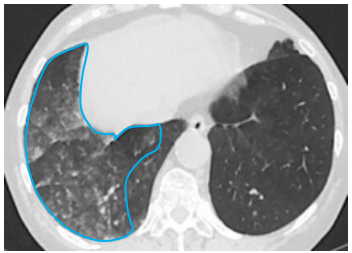

Partially nodular GGO in a patient with mucinous invasive lung adenocarcinoma (blue line).

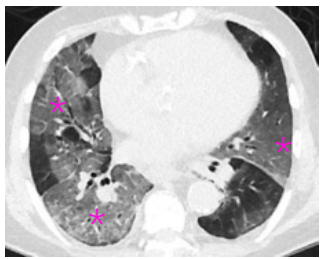

Large areas of GGO (*) in Covid-19 pneumonia (pink asterisks).

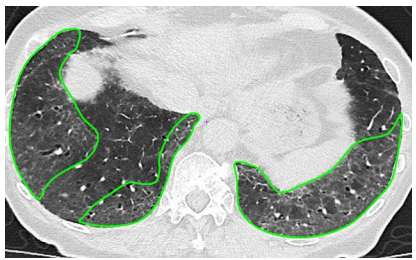

Sub-pleural/peribronchovascular GGO in connectivitis-related interstitial lung disease (green lines).

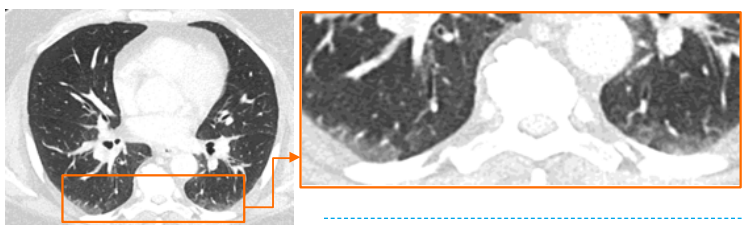

GGO in the dependant lung zones in the supine position.

/ Chest Imaging

CHAPTER OUTLINE:

/ Interstitial Opacification

/ Pattern Types and Differential Diagnosis

Interstitial opacification means that the pathology is within or next to the lung interstitium (which includes alveolar epithelium, pulmonary capillary endothelium, basement membrane, perivascular and perilymphatic spaces).

Causes of acute interstitial opacification include interstitial oedema (see page 136) and viral pneumonia. Subacute interstitial opacification is seen in lymphangitis carcinomatosis whereas chronic interstitial opacification is mostly seen in cystic fibrosis, connective tissue disorders, sarcoidosis, silicosis and tuberculosis.

Several patterns of interstitial opacification can be distinguished: reticular/linear, nodular, reticulonodular, cystic, honeycombing and GGO.

<!> ATTENTION

- / It is often difficult to detect interstitial opacification on CXRs.
- / CT is the modality of choice to detect and assess the distribution of interstitial opacification and to distinguish between the different patterns. The combination of pattern types, distribution and associated chest findings plays an essential role for the differential diagnosis.

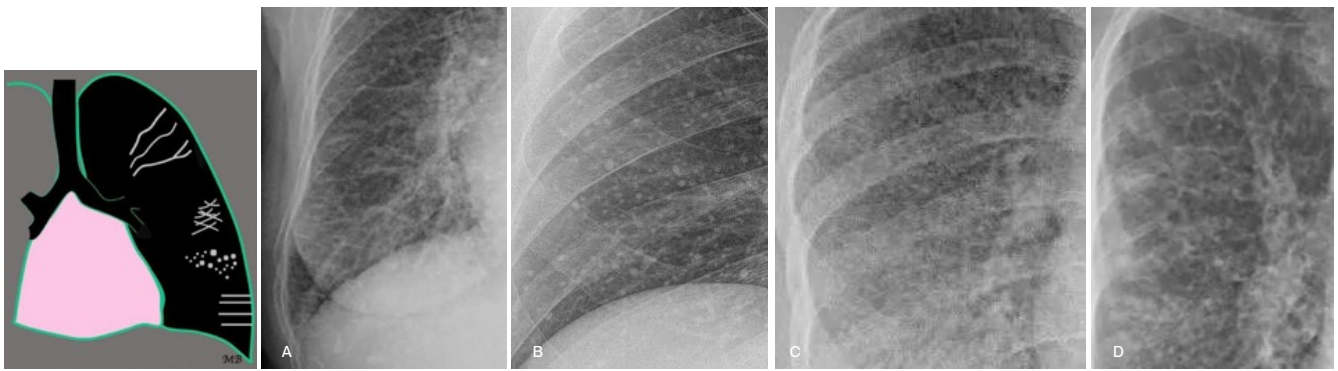

A. Linear pattern (Kerley lines) = network of fine lines caused by thickened connective tissue septa in a patient with cardiac failure. B. Nodular pattern in a patient with healed varicella pneumonia. C. Reticulonodular pattern (nodules and lines) in a patient with lymphangitis carcinomatosis. D. Coarse reticulations and honeycombing, which represent the end stage of many interstitial pathologies.

CHAPTER OUTLINE:

/ Micronodular Pattern on CXR

Micronodular interstitial opacification is characterised by 1 - 5 mm nodules, which are well defined and are not associated with air bronchograms. Nodules tend to be very numerous; when they are distributed randomly throughout the lungs, the term ”miliary nodules” is used.

In febrile patients, tuberculosis, viral and fungal infections are the most common causes.

In afebrile patients, miliary tuberculosis, healed varicella pneumonia, sarcoidosis and miliary metastases (thyroid cancer, melanoma, breast cancer) are the top differential diagnoses.

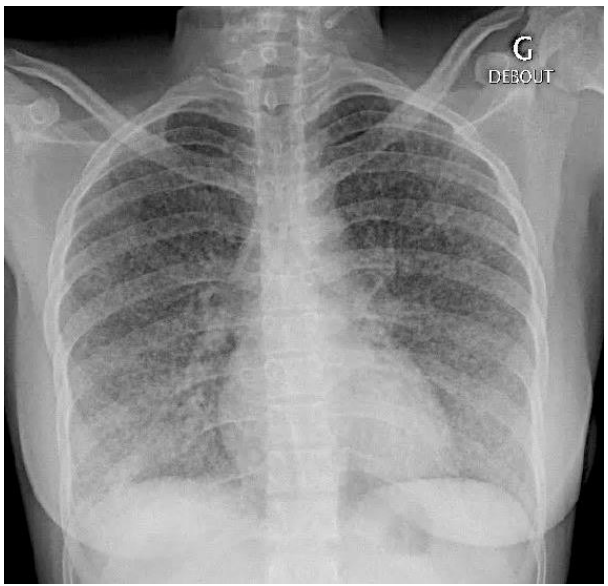

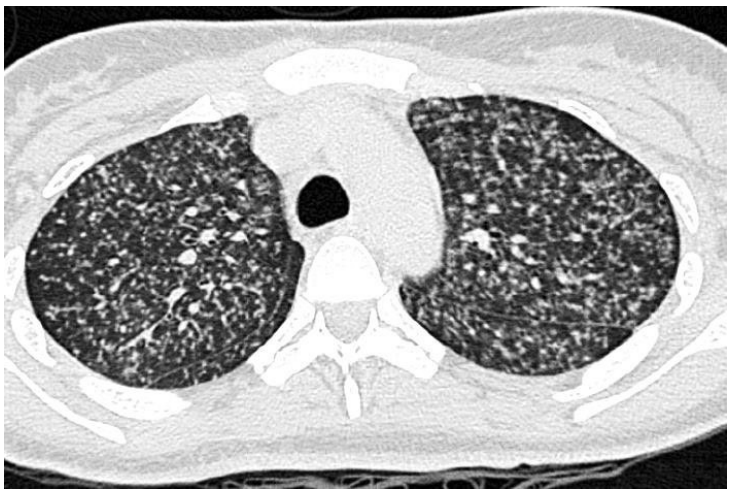

CXR shows a diffuse bilateral nodular pattern, with a random micronodular pattern on CT. This patient had miliary tuberculosis.

/ Reticulonodular Pattern on CXR

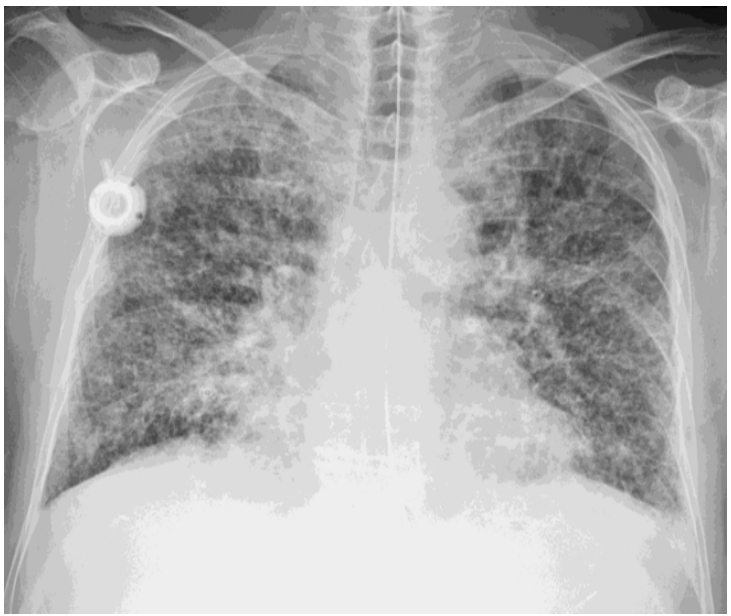

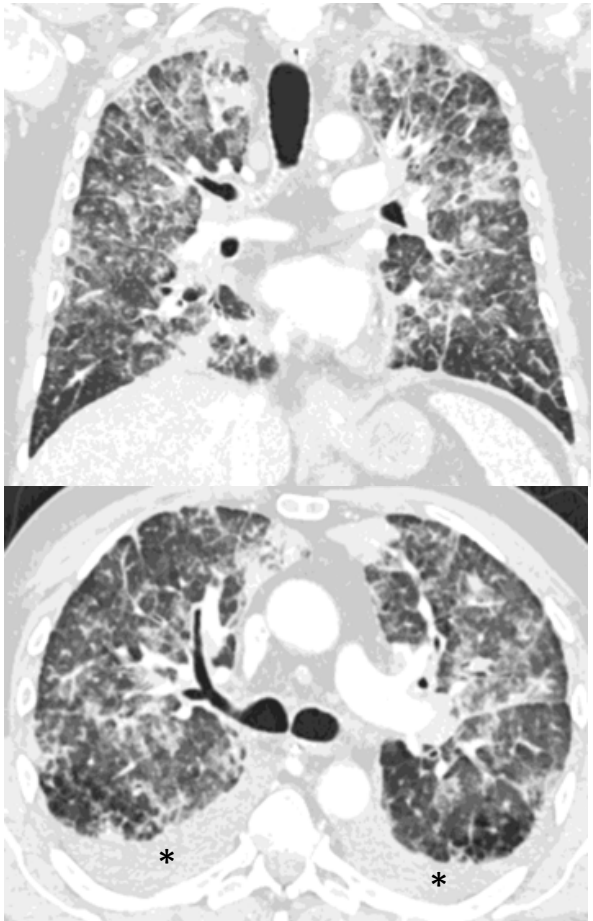

CXR shows a diffuse reticulo-nodular pattern. CT shows irregular inter- lobular reticulations, thickened bronchovascular bundles, patchy ground- glass opacifications and pleural fluid (*). This patient had lymphangitis carcinomatosis secondary to gastric cancer.

CHAPTER OUTLINE:

/ Patterns on CT Scans

The most common interstitial patterns on CT are intra- and inter-lobular reticulations (A), honeycombing (B), ground-glass opacification (C), consolidations (D) and micronodules (E).

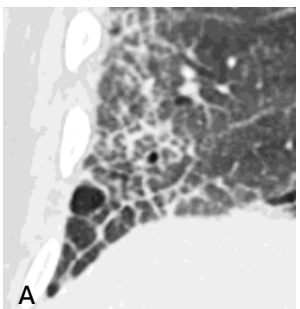

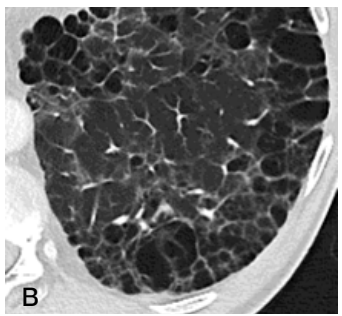

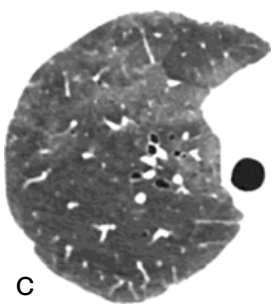

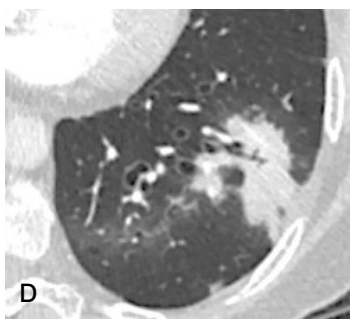

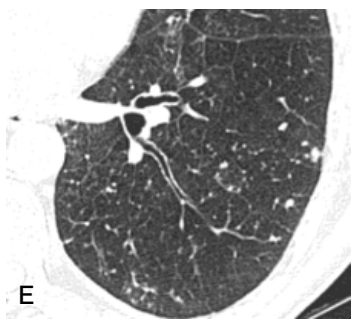

<!> ATTENTION

Several patterns (A-E) usually coexist in the same patient.

These patterns are not specific to interstitial lung diseases.

However, associated signs such as mosaic attenuation (F), cysts (purple arrow, G) or extra-pulmonary findings (e.g., pericardial (turquoise asterisks) or pleural (blue asterisks) effusion, H) are sometimes crucial in reaching the final diagnosis in chronic interstitial lung diseases.

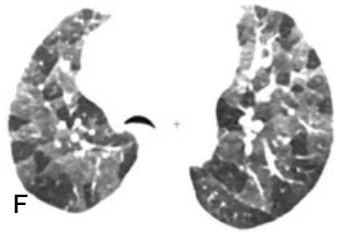

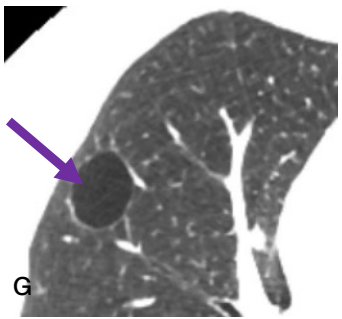

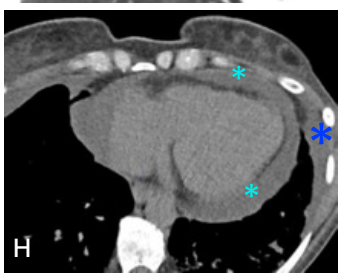

/ Chest Imaging

CHAPTER OUTLINE:

/ Nodular Opacification

Lung nodules are rounded opacities located in the pulmonary interstitium. They comprise pulmonary nodules (≤ 3 cm, yellow & green arrow) and pulmonary masses (> 3 cm, red arrow). Nodules < 6 mm in average diameter are called micronodules according to the Fleischner Society Glossary. Pulmonary nodules can be solitary or multiple.

Pulmonary nodules are often detected incidentally on CXRs or on CT.

CXRs have a limited value for nodule detection and characterisation. CT is superior to CXR for the detection of lung nodules.

On CXRs, pulmonary nodules are well-defined lesions of soft tissue density, surrounded by lung parenchyma that tends to be normally aerated.

<!> ATTENTION

The prevalence of lung cancer increases with the size of the nodule (< 1% in nodules < 5 mm; 1% - 30% in nodules > 5 mm and < 10 mm; 30-80% in nodules > 10 mm)

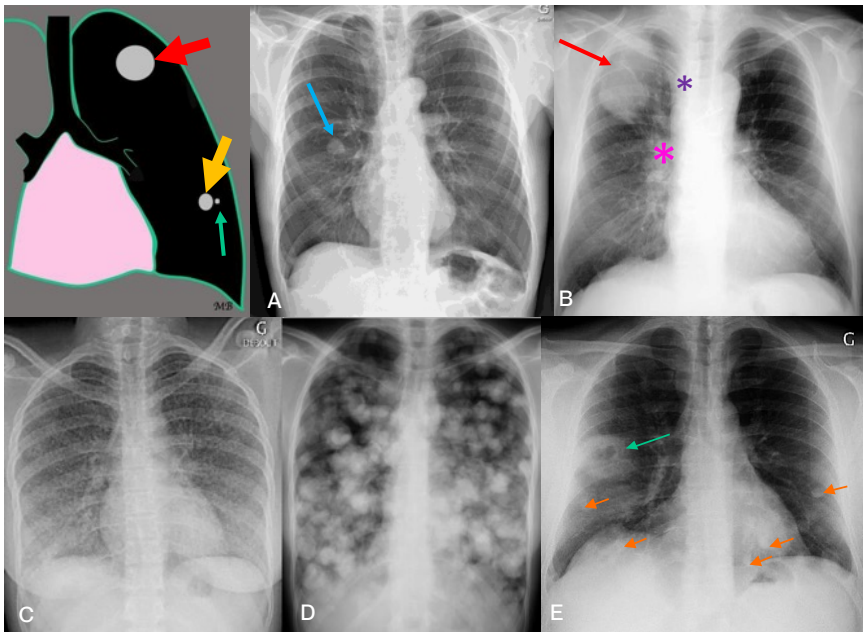

Lung nodules and masses. A. Solitary lung nodule ((blue arrow)hamartoma). B. Lung mass ((red arrow)lung cancer, squamous cell carcinoma) with enlarged paratracheal stripe (purple asterisk) and hilar enlargement (pink asterisk) due to lymph node metastases. C. Multiple micronodules in miliary tuberculosis. D. Metastatic follicular thyroid cancer with pulmonary nodules of varying size. E. Multiple nodules (orange arrows) and a cavitary mass ((green arrow)=gas-filled mass with thick borders) in a patient with granulomatosis with polyangiitis (GPA, formerly called Wegener's granulomatosis).

/ Solitary Pulmonary Nodule (SPN)

Solitary pulmonary nodule (SPN) = well-defined lung lesion < 30 mm in size surrounded by lung parenchyma and/or visceral pleura. SNPs have a rounded or oval shape and no linear shape. There is no associated lymphadenopathy, pneumonia or atelectasis.

SPNs can be solid ((green arrow) i.e., they obscure pulmonary vascular structures on CT), subsolid (= GGO without obscuring pulmonary vessels). Subsolid nodules can be further divided into nonsolid ((blue arrow) GGO only) and partly solid nodules ((orange arrow) GGO & solid part). The differential diagnosis of SPNs ranges from benign lesions to lung cancer. Recognition of early stages of lung cancer is essential for prognosis.

>▪< FURTHER KNOWLEDGE

- Key factors to assess the malignant potential of a SPN include nodule size, growth and morphology.
- Malignancy likelihood increases with nodule size and nodule growth rate. Malignancy prevalence in SPN < 5mm is < 1% and in SPN > 10 mm it is about 15%.
- Benignity features include perifissural location, triangular morphology, fatty content and central or pop-corn calcifications.
- Features suggesting malignancy include spiculated or lobulated borders, pleural indentation, vascular convergence, bubble-like lucencies, subsolid morphology and cystic airspace with mural nodule.
- To assess morphologic features of SPN, thin section CT with mediastinal and lung window settings is a must.

<∞> REFERENCE

Snoeckx A et al. Evaluation of the solitary pulmonary nodule: size matters, but do not ignore the power of morphology. Insights Imaging. 2018 Feb;9(1):73-86. doi: 10.1007/s13244-017-0581-2. Epub 2017 Nov 15. PMID: 29143191; PMCID: PMC5825309.

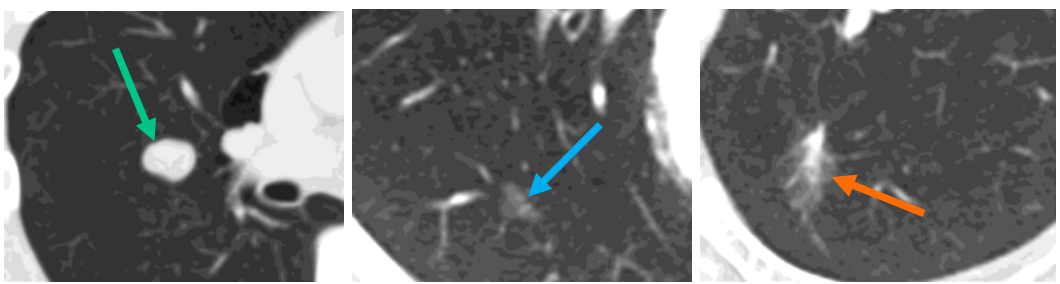

Benign features (1)

- Benign patterns of calcification include central, diffuse, popcorn and laminated patterns, which are typically seen in granulomas and hamartomas. However, if patients have a known primary malignant tumour, e.g., osteosarcoma or gastro- intestinal (GI) cancer, these calcification patterns should not be regarded as benign as osteosarcoma metastases can have diffuse calcification patterns whereas GI cancer metastases can have central or popcorn calcifications.

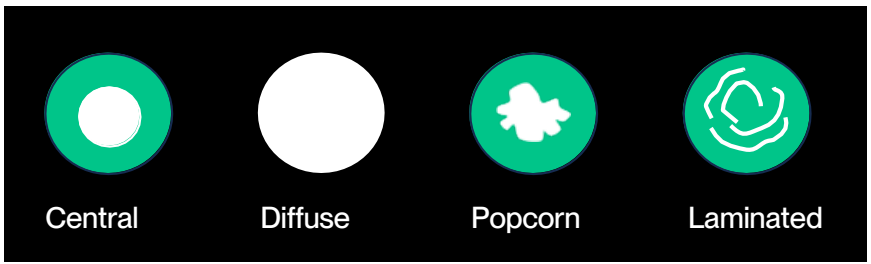

- Calcified granulomas (green arrows) as a response to healed infection are the most common cause of pulmonary nodule calcification. Calcification size is usually 2 - 5mm. Calcification location is typically central or diffuse. Often, calcified granulomas are associated with hilar nodal calcification. Images A (lung window) and B (soft tissue window) were obtained in the same patient with a benign calcified granuloma.

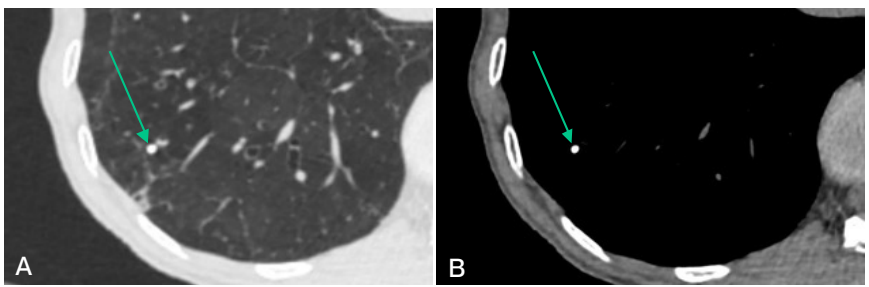

Benign features (2)

- Perifissural location (green arrows, A) and triangular shape (pink arrows, A and D) corresponding to intrapulmonary lymph nodes.
- Fatty content (orange arrows, B, E and F).
- Pop-corn calcifications (blue arrows) typical of chondroid hamartomas (C and F).

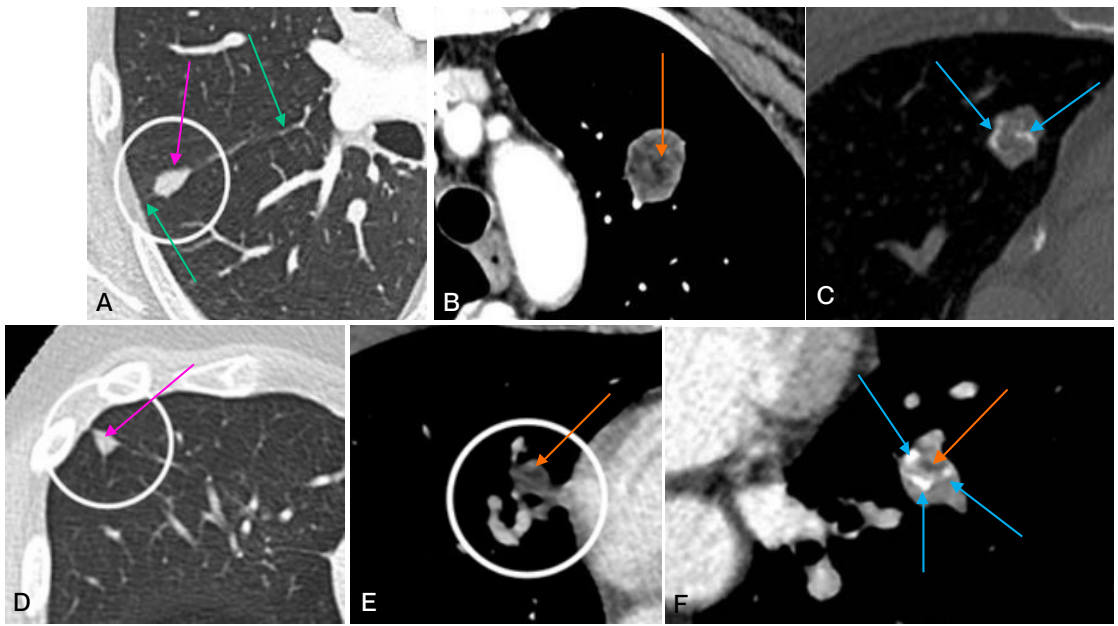

Images reproduced from: Snoeckx A et al. Evaluation of the solitary pulmonary nodule: size matters, but do not ignore the power of morphology. Insights Imaging. 2018 Feb;9(1):73-86. doi: 10.1007/s13244-017-0581-2.

Features rather suggesting malignancy

- Scarce dot-like, rather peripheral calcifications (blue arrow) → A
- Spiculated margins (turquoise) → A and F
- Lobulated margins (yellow arrow) → B
- Subsolid nodule (red arrow) → C
- Part-solid (light purple circle) → E
- Cavitation ((orange arrow) in the absence of an infectious cause or in not immunocompromised patients) → D
- Retraction of pleura/ fissure (pink arrow) → E
- Bubble-like lucencies (green arrow) → F

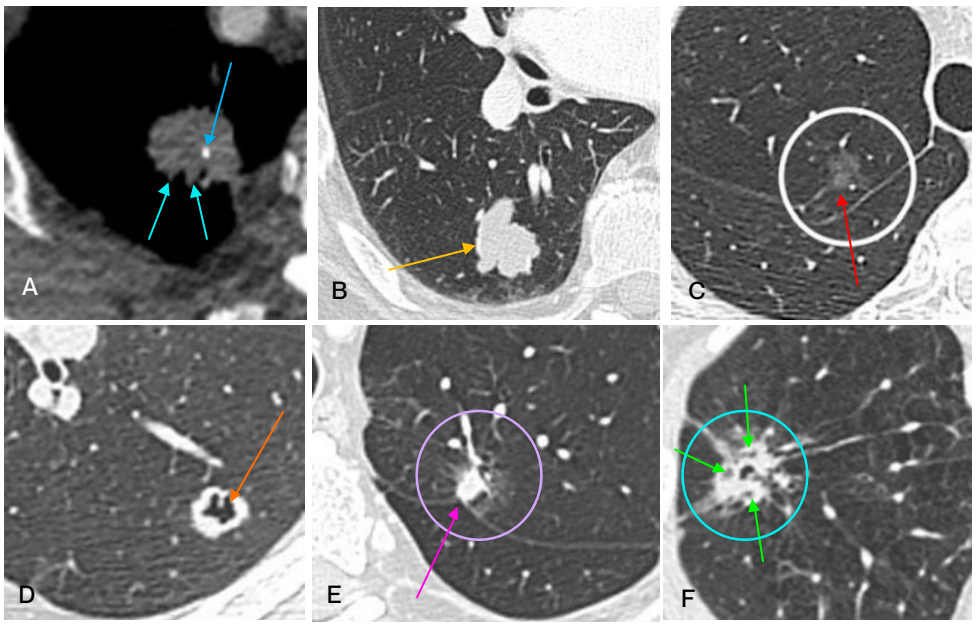

Images reproduced from: Snoeckx A et al. Evaluation of the solitary pulmonary nodule: size matters, but do not ignore the power of morphology. Insights Imaging. 2018 Feb;9(1):73-86. doi: 10.1007/s13244-017-0581-2.

To evaluate nodule growth, volumetry rather than measurement of lesion size needs to be done.

Volume Doubling Time (VDT)

- = time a growing nodule doubles its volume
- = major volumetric parameter for screening and follow-up of chest CT
- Principle:
  - Malignant nodules are more likely to have a **VDT < 400 days (red arrows)** whereas benign nodules tend to have a **VDT > 500 days (green arrows).**
  - Solid malignant nodules tend to grow faster than benign nodules.
  - Nevertheless, there is overlap between the growth rate of benign and malignant nodules.

<!> ATTENTION

Software-based volumetry VDT is a major parameter in CT-based lung cancer screening (see page 124)

As CT acquisition parameters, e.g., slice thickness and window width have a major influence on VDT measurements, they should be kept as similar as possible for follow-up scans

>|< COMPARE

Adenocarcinoma (VDT = 215 days)

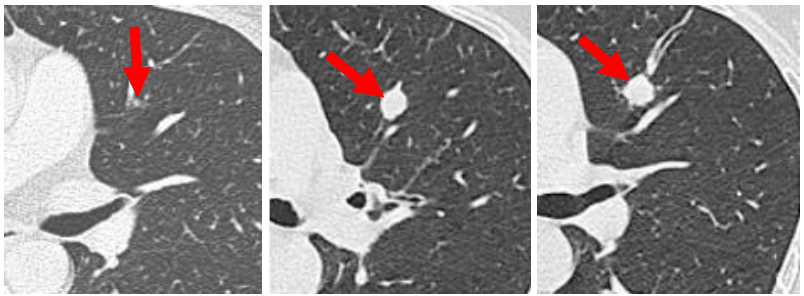

October 2019 January 2022 August 2022

Most likely benign SPN (VDT = 1020 days)

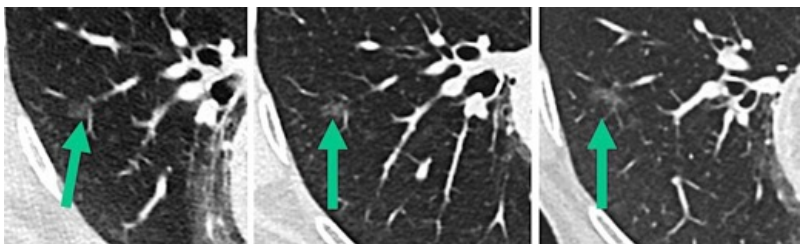

January 2020 January 2021 January 2024

<∞> REFERENCES

Hammer MM, Gupta S, Byrne SC. Volume Doubling Times of Benign and Malignant Nodules in Lung Cancer Screening. Curr Probl Diagn Radiol. 2023 Nov-Dec;52(6):515-518. doi: 10.1067/j.cpradiol.2023.06.014.

Anand Devaraj, Bram van Ginneken, Arjun Nair, David Baldwin. Use of Volumetry for Lung Nodule Management: Theory and Practice. (2017) Radiology. 284 (3): 630-644. doi:10.1148/radiol.2017151022

Chest Imaging

CHAPTER OUTLINE:

/ Follow-up of Incidentally Detected Pulmonary Nodules (PNs)

The Fleischner Society 2017 Guidelines for the management of incidentally detected pulmonary nodules prioritise minimising unnecessary follow- up imaging while ensuring timely detection of malignancy. These guidelines aim to balance the risk of overdiagnosis with the need for early detection of lung cancer.

Management is based on nodule type, nodule size, the presence of solitary versus multiple pulmonary nodules (SPN versus MPN), patient risk factors (e.g., smoking history, family history of lung cancer, fibrosis, emphysema, upper lobe location) and patient comorbidities. For solid nodules, follow-up intervals are determined by nodule size (< 6 mm, 6 - 8 mm, > 8 mm) or nodule volume (< 100 mm^3, 100 – 250 mm^3, > 250 mm^3), morphology, location and growth rate. For subsolid nodules, management further depends on CT appearance (GGO versus part solid), the recommended follow-up for part solid being longer than for solid nodules.

<!> ATTENTION

These guidelines do not apply to :

- / patients with known primary cancer (who are at risk for metastases)
- / patients with immunosuppression (who are at risk for infection)
- / lung cancer screening participants
- / patients < 35 years.

Most pulmonary nodules < 1 cm are not detected on CXRs, therefore low dose CT (LDCT) with 1 mm continuous thin sections, 2D coronal and sagittal reconstructions is recommended for follow-up. However, larger solid nodules visible on CXRs and considered as “low risk” can also be followed with CXR due to the lower radiation exposure and lower cost of CXRs compared to CT.

Biopsy under bronchoscopy or CT guidance and minimally invasive surgery with lung-sparing techniques are recommended in lesions that display CT or FDG PET CT findings strongly suggesting malignancy. Transthoracic CT guided biopsy is very effective in experienced hands; however, it can yield false negative results in part-solid nodules and in very small solid nodules. The choice of the most appropriate procedure for tissue sampling is made in the setting of multidisciplinary tumour boards.

<∞> REFERENCE

MacMahon H, Naidich DP, Goo JM, et al. Guidelines for Management of Incidental Pulmonary Nodules Detected on CT Images: From the Fleischner Society 2017. Radiology. 2017 Jul;284(1):228-243. doi: 10.1148/radiol.2017161659. Epub 2017 Feb 23. PMID: 28240562.

/ Lung Cancer

Lung cancer remains one of the leading causes of cancer-related morbidity and mortality worldwide, with significant public health implications. Smoking remains the primary risk factor (about 85% of cases), although other factors, e.g., exposure to second-hand smoke, environmental pollutants, workplace hazards (asbestos and chemicals), genetic predisposition and previous chronic lung diseases also play a role.

It is estimated that nearly 65% of all new lung cancer diagnoses are seen in former smokers or never smokers and 12% of new lung cancer cases are among never smokers.

Unfortunately, lung cancer is often diagnosed at an advanced stage, contributing to its high mortality rates. The prognosis varies depending on the histologic type of lung cancer, stage at diagnosis and patient's overall health. Non-small cell lung cancer (NSCLC) comprises most cases and generally has a poorer prognosis compared to small cell lung cancer (SCLC), which tends to be more aggressive but may respond better to chemotherapy and radiation therapy. Overall, only 25% of patients with lung cancer survive > 5 years.

Nevertheless, early diagnosis has been shown to dramatically improve survival, e.g., the NSCLC 2-year relative survival has increased by 5% - 6% for every stage of diagnosis in recent years. Furthermore, reduction in smoking and improved lung cancer detection and treatment have also reduced lung cancer mortality.

CT is the primary imaging modality for the detection and staging of lung cancer. It is used for the initial evaluation of suspicious nodules, masses or lymph-adenopathy, guiding further diagnostic interventions. PET CT is often utilised to precisely assess the extent of the primary tumour (improved separation of tumour from adjacent atelectasis and fibrosis compared to CT), to detect nodal metastases, distant metastases and synchronous second primary cancers (see page 23).

<∞> REFERENCE

Siegal DA, et al. Proportion of never smokers among men and women with lung cancer in 7 US states. JAMA Oncol. 2021 Feb 1; 7(2): 302-304. doi: 10.1001/jamaoncol.2020.6362.

Centers for Disease Control and Prevention. National Center for Health Statistics. CDC WONDER On-line Database, compiled from Compressed Mortality File 1999-2014 Series 20 No. 2T, 2016.

https://www.who.int/news-room/fact-sheets/detail/lung-cancer

Siegel RL, Miller KD, Fuchs HE, Jemal A. Cancer Statistics, 2021. CA Cancer J Clin. 2021 Jan;71(1):7-33. doi: 10.3322/caac.21654. Epub 2021 Jan 12. PMID: 33433946.

Hirsch FR, Scagliotti GV, Mulshine JL, Kwon R, Curran WJ Jr, Wu YL, Paz-Ares L. Lung cancer: current therapies and new targeted treatments. Lancet. 2017 Apr 1;389(10066):299-311. doi: 10.1016/S0140-6736(16)30958-8. Epub 2016 Sep 6. PMID: 27609408.

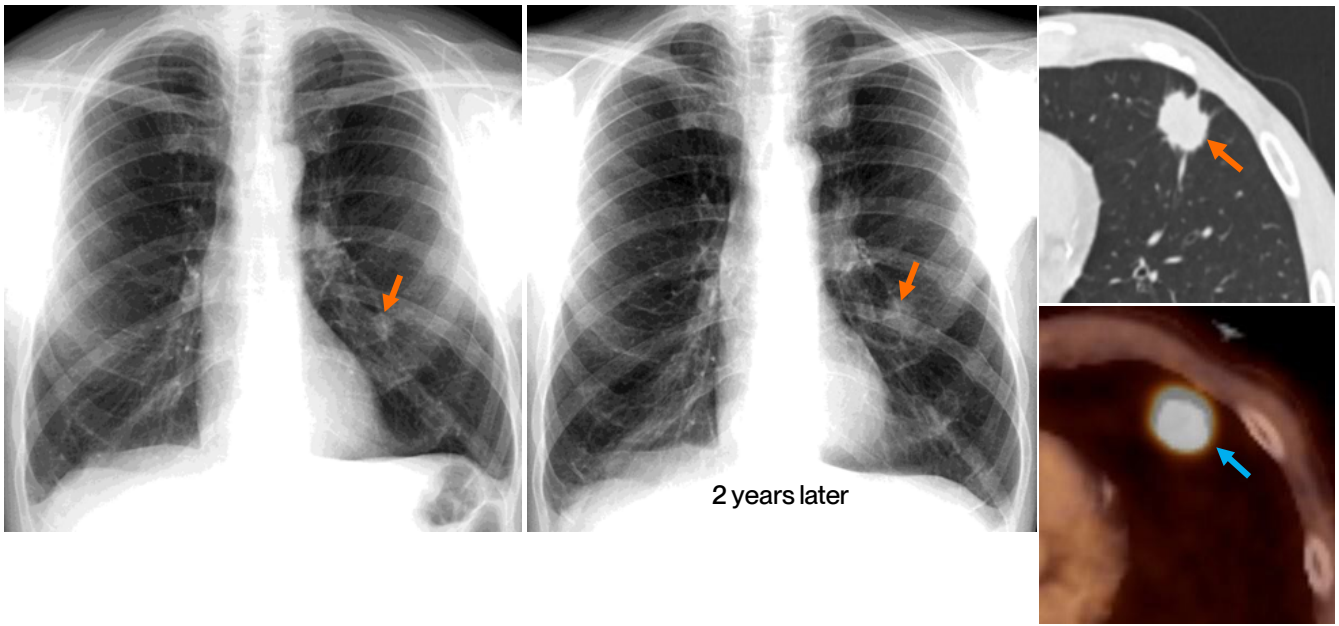

CXRs with a 2-year interval showing a growing lung nodule in the left lower zone (orange arrows). CT shows a spiculated lingular solid nodule (orange arrow), with a strong FDG hypermetabolism (blue arrow) on PET CT. Biopsy revealed lung adenocarcinoma.

Chest Imaging

CHAPTER OUTLINE:

PA and lateral CXRs (A and B) showing a large lung mass in the left upper lobe (orange asterisks). There is enlargement of the left hilum (green arrow), lateral bulging of the right mediastinal border (pink arrows) and absent right hilum overlay sign (turquoise circle) suggesting contralateral hilar involvement. Corresponding axial, coronal and parasagittal CT images with soft tissue settings (C-E) confirming the large (6.4 x 7.2 x 5 cm), solid, mostly necrotic lung mass (orange asterisks) in the left upper lobe with hilar (green arrow) and contralateral mediastinal involvement (pink asterisks). Confluent contralateral metastatic necrotic lymph nodes (pink asterisks)are shown in D. Biopsy revealed squamous cell carcinoma of the lung. Slight elevation of the left hemidiaphragm (yellow arrows) due to diaphragmatic palsy (proven by ultrasonography) caused by phrenic nerve invasion. CT further revealed a single extra-thoracic metastasis in the liver (not shown).

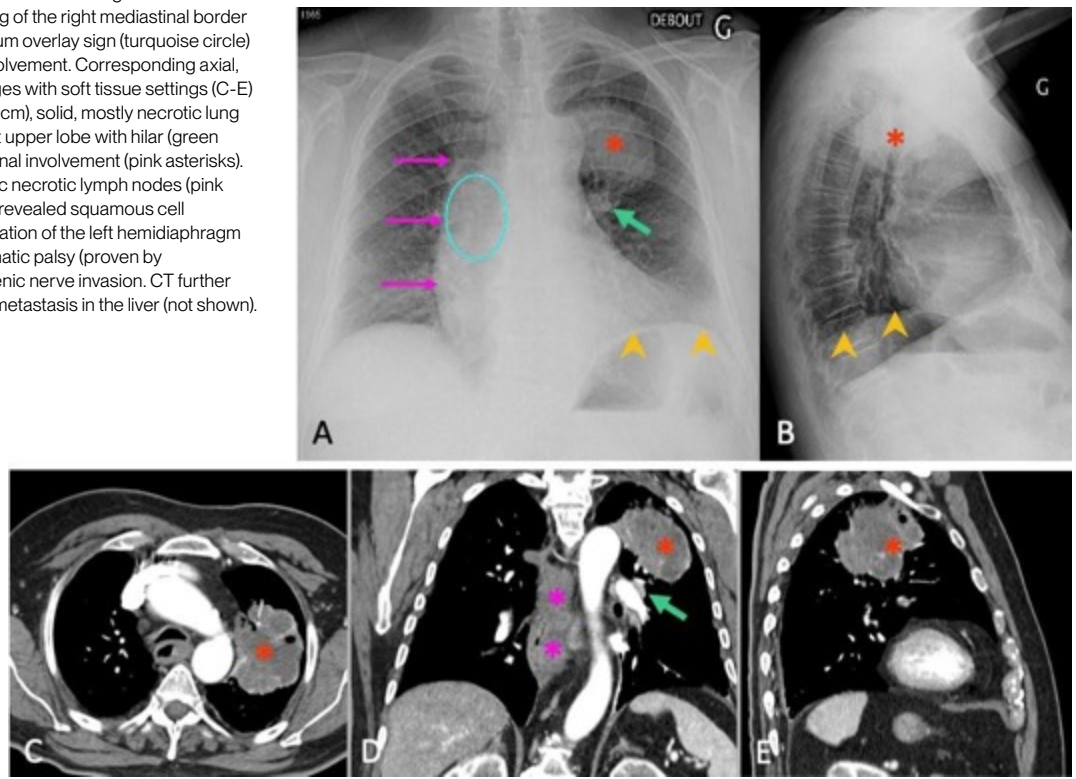

According to the TNM classification (8th edition), the multidisciplinary tumour board classified this tumour as T4N3M1b because:

- tumour size > 7 cm
- contralateral mediastinal nodal involvement
- single extra-thoracic metastasis (not shown).

> see next page.

CHAPTER OUTLINE:

/ Lung Cancer TNM Classification and the Multidisciplinary Tumour Board (MDTB)

The TNM classification of lung cancer = essential tool to accurately stage the disease.

TNM stands for **T**umour, **N**ode and **M**etastasis:

- the "T" category assesses the primary tumour size and extent of invasion into nearby structures, e.g., main bronchus, pericardium, phrenic nerve
- the "N" category refers to lymph node invasion (ipsilateral versus contralateral, hilar or mediastinal)
- the "M" category denotes the presence of metastases to distant sites, e.g., contralateral lung, liver, bones or brain

The TNM staging system is typically determined through a combination of clinical/endoscopic findings, histology, cross-sectional imaging (CT, PET CT or MRI scans) and sometimes surgical exploration.

Once the TNM stage is determined, it provides valuable guidance for selecting the most appropriate treatment (surgery, chemotherapy, radiation therapy, immunotherapy or a combination thereof).

The TNM staging also helps in predicting patient prognosis, guiding discussions regarding potential outcomes and supportive care needs.

Ultimately, the TNM classification system plays a crucial role in personalised treatment planning and optimising patient outcomes in lung cancer management.

The TNM classification of lung cancer is done based on all available information in the setting of specialised multidisciplinary tumour boards (MDTBs), which convene experts from various medical specialties to collaborate on individual patient cases, ensuring evidence- based treatment plans.

<!> ATTENTION

MDTBs increase treatment efficacy, reduce treatment-related morbidity and improve patient outcomes. They promote synergy among specialists, optimise resource utilisation and uphold personalised care as the cornerstone of modern oncology practice. With the increasing complexity of cancer care and rapid advancements in treatment modalities, the utilisation of multidisciplinary tumour boards is more crucial than ever.

Schematic drawing of a lung cancer MDTB partly created with the aid of chatgpt.com.

/ Chest Imaging

CHAPTER OUTLINE:

/ Lung Cancer Screening

Lung cancer screening of high-risk individuals (i.e., current or former smokers with a high number of pack years) aims to detect the disease at an early stage when treatment is more effective, thus reducing mortality rates.

>|< COMPARE

ADVANTAGES:

The primary screening technique is low-dose CT (LDCT) of the chest, which offers several advantages:

+ non-invasive and relatively quick, making it well-tolerated by patients
+ high sensitivity for the detection of lung nodules, allowing for the identification of potentially malignant lesions, enabling timely follow-up and further diagnostic evaluation to confirm or rule out cancer
+ LDCT lung cancer screening rather than CXR lung cancer screening has been shown to reduce lung cancer mortality rates

DISADVANTAGES:

Despite its benefits, LDCT screening for lung cancer has certain limitations and challenges:

– the risk of false-positive findings can lead to unnecessary anxiety and invasive procedures –distinguishing between benign and malignant nodules on LDCT scans can be challenging, necessitating additional tests such as biopsy or repeat imaging

– LDCT screening is associated with radiation exposure, albeit at a lower dose compared to standard CT scans - while the radiation risk is minimal, repeated screening over time may accumulate radiation doses

Implementing widespread lung cancer screening programs poses several challenges, such as:

/ identifying individuals who would benefit most from screening while minimising harm from overdiagnosis and unnecessary interventions
/ developing effective strategies for risk assessment and participant selection
/ ensuring access to high-quality screening facilities and expertise, particularly in underserved communities
/ addressing barriers such as cost, limited resources and participant awareness

<∞> REFERENCES

Siegal DA, et al. Proportion of never smokers among men and women with lung cancer in 7 US states. JAMA Oncol. 2021 Feb 1; 7(2): 302-304. doi: 10.1001/jamaoncol.2020.6362.

Centers for Disease Control and Prevention. National Center for Health Statistics. CDC WONDER On-line Database, compiled from Compressed Mortality File 1999-2014 Series 20 No. 2T, 2016. https://www.who.int/news-room/fact-sheets/detail/lung-cancer

National Lung Screening Trial Research Team; Church TR, Black WC, Aberle DR, Berg CD, Clingan KL, Duan F, Fagerstrom RM, Gareen IF, Gierada DS, Jones GC, Mahon I, Marcus PM, Sicks JD, Jain A, Baum S. Results of initial low-dose computed tomographic screening for lung cancer. N Engl J Med. 2013 May 23;368(21):1980-91. doi: 10.1056/NEJMoa1209120. PMID: 23697514; PMCID: PMC3762603.

Sands J, Tammemägi MC, Couraud S, Baldwin DR, Borondy-Kitts A, Yankelevitz D, Lewis J, Grannis F, Kauczor HU, von Stackelberg O, Sequist L, Pastorino U, McKee B. Lung Screening Benefits and Challenges: A Review of The Data and Outline for Implementation. J Thorac Oncol. 2021 Jan;16(1):37-53. doi: 10.1016/j.jtho.2020.10.127. Epub 2020 Nov 12. PMID: 33188913.

/ Multiple Pulmonary Nodules (MPNs)

As opposed to the SPN, which is often detected incidentally, multiple pulmonary nodules (MPNs) are most often seen in symptomatic patients, in patients with an underlying malignancy or in immunocompromised patients. Exceptions to this rule comprise multiple calcified granulomas in patients with previous tuberculosis or previous chicken pox pneumonia (see page 109).

The differential diagnosis of MPNs larger than 5 mm mainly includes metastases, septic emboli, fungal infections, autoimmune diseases (e.g., granulomatosis with polyangiitis, rheumatoid pulmonary nodules) and multiple arterio-venous malformations. Lung metastases most commonly arise from lung cancer, colorectal, kidney, pancreatic and breast cancer. Synchronous lung

<!> ATTENTION

Pulmonary metastases have the following imaging features:

- varying size
- mainly found in the lower lung zones and peripheral lung zones
- most often well-defined
- cavitation typically in squamous cell carcinoma
- calcification and pneumothorax typically in osteosarcoma
- in many cancers, metastases show increased FDG uptake on PET CT scans

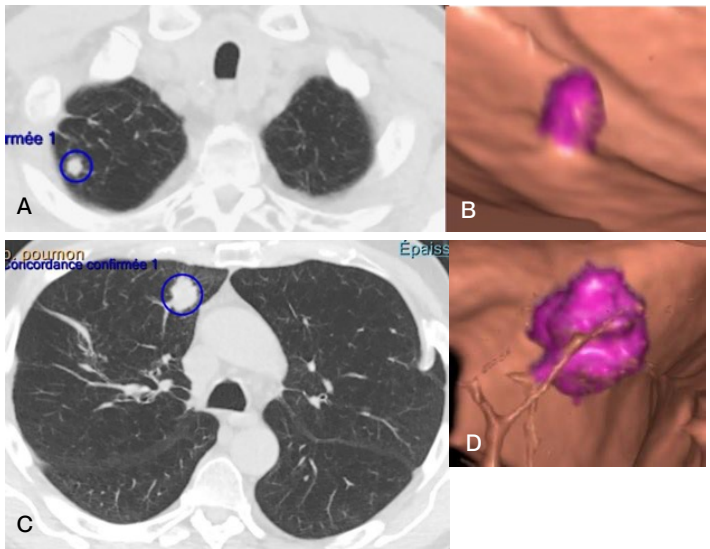

Lung metastases detected 2 years post treatment of a head and neck SCC. A right apical upper lobe nodule (A and B) and a right anterior upper lobe nodule (C and D) were seen. Images B and D correspond to volume rendering reconstructions using an automated software for volume calculation.

<∞> REFERENCE

Chen H, Stoltzfus KC, Lehrer EJ, Horn SR, Siva S, Trifiletti DM, Meng MB, Verma V, Louie AV, Zaorsky NG. The Epidemiology of Lung Metastases. Front Med (Lausanne). 2021 Sep 20;8:723396. doi: 10.3389/fmed.

CHAPTER OUTLINE:

Granulomatosis with polyangiitis (GPA, formerly known as Wegener's granulomatosis) is a non-caseating granulomatous vasculitis affecting the upper and lower respiratory tract, the kidneys, the central nervous system and the orbits. Although imaging findings vary, the most common pulmonary manifestations include multiple cavitary nodules or cavitary masses, pulmonary haemorrhage (which can manifest as alveolar consolidation ± cavitation) and pleural effusions.

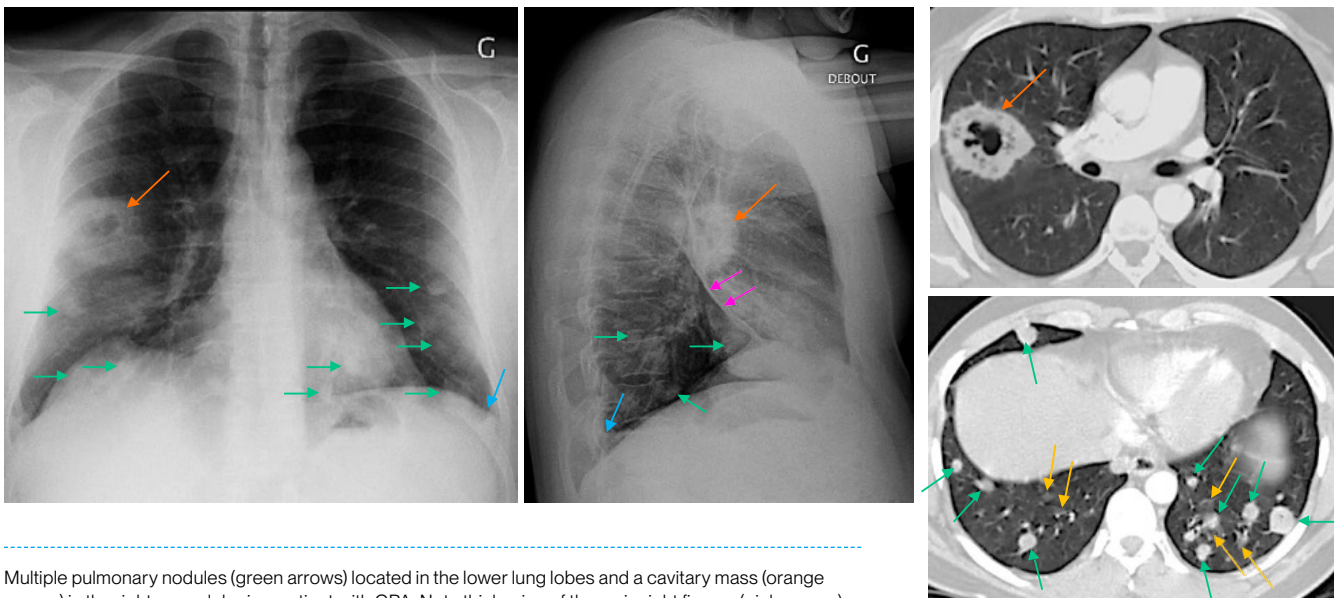

Multiple pulmonary nodules (green arrows) located in the lower lung lobes and a cavitary mass (orange arrows) in the right upper lobe in a patient with GPA. Note thickening of the main right fissure (pink arrows) due to interlobar pleural effusion. Pleural effusion also in the left posterior costophrenic recess (blue arrows). On CT, additional areas of GGO (yellow arrows) due to haemorrhage.

CHAPTER OUTLINE:

/ Atelectatic Opacification (Collapse)

Atelectasis = collapse of a complete lung or part of the lung (lobe, segment or specific subsegmental area) leading to an impaired 0_2 and $C0_2$ exchange and, therefore, to an intrapulmonary shunt.

<!> ATTENTION

The mechanisms by which atelectasis occurs include:

- obstruction → the alveolar air is absorbed distal to an obstructive lesion → as the ventilation is impaired and the perfusion is maintained, all the gas in the area affected by obstruction is absorbed → because the visceral and parietal pleura do not separate, there is significant traction and volume loss – causes include bronchial obstruction due to tumour, foreign bodies or mucous plugs (e.g., in COPD, asthma and cystic fibrosis).
- compression → a space occupying mass compresses the adjacent lung leading to alveolar collapse.
- relaxation → loss of contact between the visceral and parietal pleura (e.g., due to pleural effusion or pneumothorax) leads to alveolar collapse.
- contraction → scar tissue leads to lung contraction. Causes include destructive lung conditions, e.g., lung fibrosis, tuberculosis, after severe pneumonia forms, radiation pneumonitis.
- adhesion → surfactant deficiency or dysfunction (e.g., in neonates and ARDS) leads to an increased alveolar surface tension → alveolar collapse.
- gravity → gravity affects the distribution patterns of lung fluids and volume of alveoli – in the supine position, the dorsal lung alveoli physiologically display some partial atelectasis (dependent atelectasis).

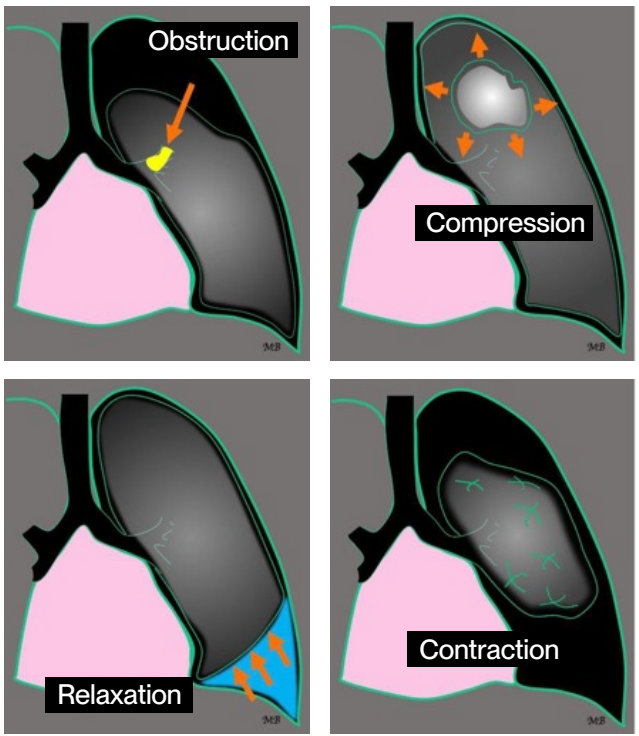

/ Radiologic Signs

Based on anatomical extent, atelectasis can be categorised as:

- / subsegmental → collapse of a part of a lung segment
- / segmental → collapse of a lung segment
- / lobar → collapse of an entire lobe
- / lung → complete lung collapses

Therefore, radiographic features will vary!

Signs of atelectasis on CXRs include homogeneous lung opacification (orange star), displacement of intterlobar fissures (green) towards the atelectasis, mediastinal shift (pink) towards the atelectasis (including displacement of mediastinal contents, e.g., trachea, heart) and hilum, ipsilateral hemidiaphragm elevation ((blue) which can have a peaked appearance), compensatory hyperinflation of the unaffected ipsilateral lung (with increased radiolucency and oligemia (turquoise star)) or hyperinflation of the contralateral lung (light pink line) and ipsilateral ribs closer together than contralateral ribs (yellow lines). Mediastinal shift, diaphragmatic elevation and closeness of ribs are seen only in the presence of substantial atelectasis.

<!> ATTENTION

Collapse of each individual lobe is associated with typical imaging features.

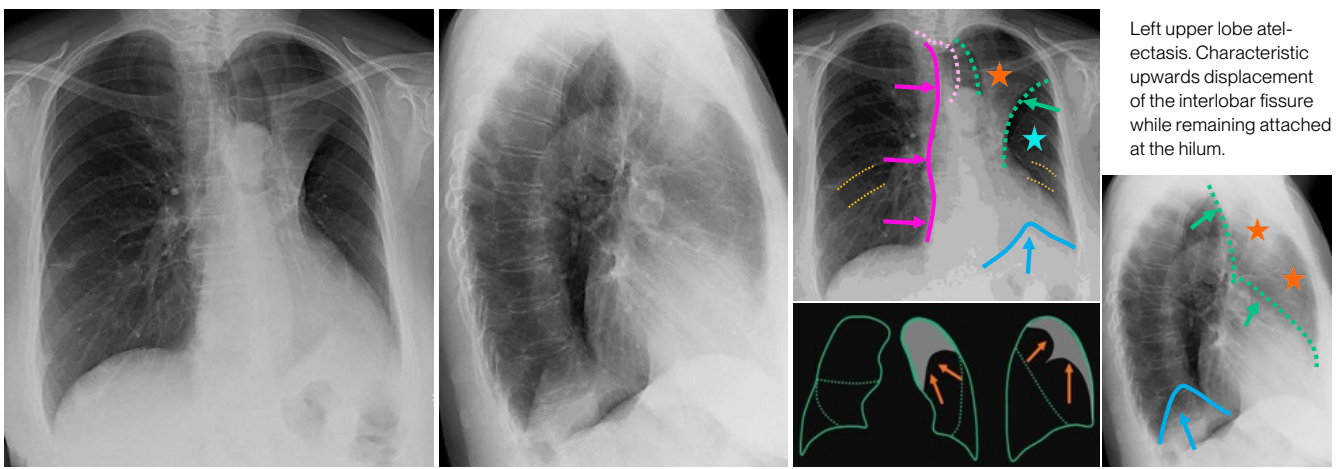

Left upper lobe atelectasis. Characteristic upwards displacement of the interlobar fissure while remaining attached at the hilum.

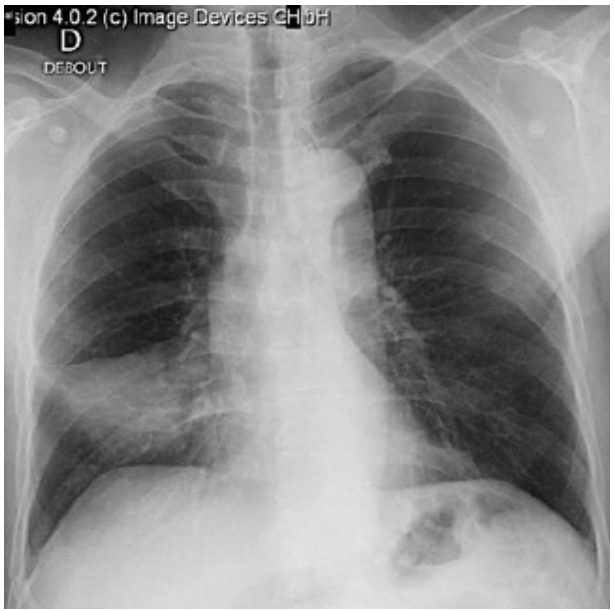

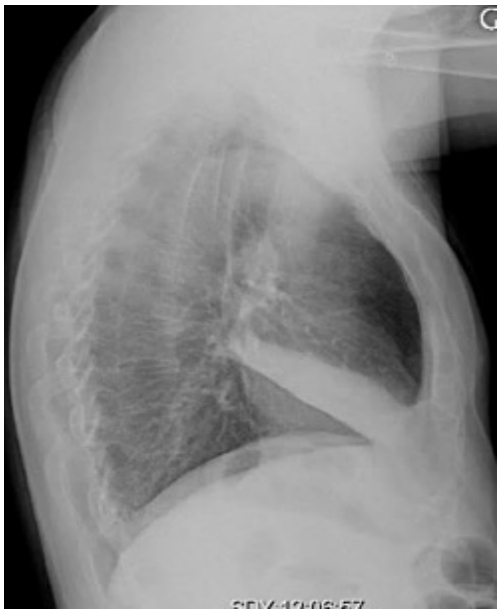

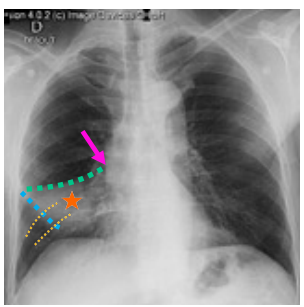

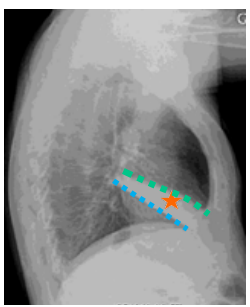

Classic signs of right middle lobe atelectasis as seen on CXR include homogeneous pulmonary opacification (orange stars), displacement of interlobar fissures towards the atelectasis (i.e., downwards displacement of the horizontal fissure (green lines) and upwards displacement of the oblique fissure (blue line)), displacement of the right hilum (pink arrow) towards the atelectasis, closeness of ipsilateral ribs (yellow lines).
Compare with the normal position of the interlobar fissures shown on page 32!

CHAPTER OUTLINE:

<!> ATTENTION

Complete lung collapse should not be confounded with a large pleural effusion. The direction of the mediastinal shift is crucial to distinguish between the two entities: shift towards the pathology in the collapsed lung and in the opposite direction of pathology in a large effusion.

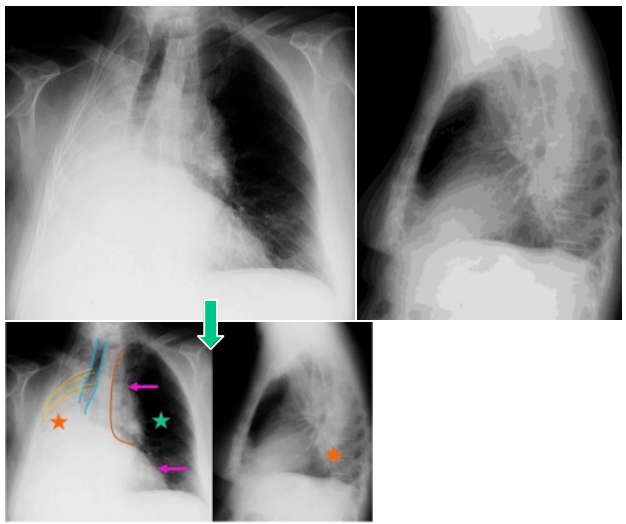

Right lung collapse caused by right main bronchus obstruction due to lung cancer. Homogeneous opacification (orange stars) of the right lung, displacement of the mediastinum (pink arrows) towards the right, deviation of the trachea to the right (blue lines), closeness of (yellow lines) ipsilateral ribs and compensatory hyperinflation of the left lung (radiolucency, oligemia (green star), herniation across the midline (brown line)). Retrocardiac opacity on the lateral CXR (orange star) corresponds to the collapsed lung (see normal lateral CXR on page 16).

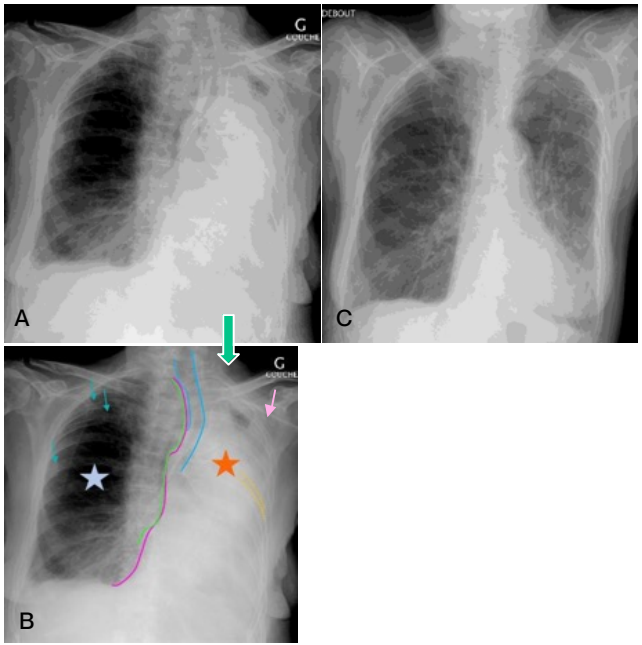

Near total left lung collapse caused by left main bronchus obstruction due to a mucous plug in a patient with cystic fibrosis (A, B).
Homogeneous opacification (oramge star) of most of the left lung, displacement of the mediastinum (pink line) to the left, trachea displacement (blue lines) to the left, closeness of (yellow lines) ipsilateral ribs and compensatory hyperinflation of the right lung (radiolucency, oligemia (light blue star) and herniation across the midline (green line)). CXR obtained the same day after endoscopic removal of the mucous plug (C) shows collapse disappearance. Note that the patient equally has old rib fractures (turquoise arrows). Central venous catheter (light pink line).

CHAPTER OUTLINE:

/ Increased Lucency (Hyperlucency)

/ Emphysema Definition and Types

Pulmonary emphysema = chronic lung condition characterised by enlargement of alveoli and destruction of alveolar wall without fibrosis, leading to air trapping and decreased lung function.

The imaging modality of choice is CT although CXR may reveal indirect signs of pulmonary emphysema.

On CXRs, pulmonary emphysema typically appears as hyperinflated lungs (yellow arrows) with flattened diaphragms (green arrows) and increased lung transparency (red asterisks) due to reduced tissue density. On CT scans, emphysema presents as areas of low attenuation (red asterisks), indicating air trapping and destruction of lung tissue, often accompanied by bullae or enlarged air spaces (blue asterisks). These imaging findings help diagnose and assess the severity of emphysema.

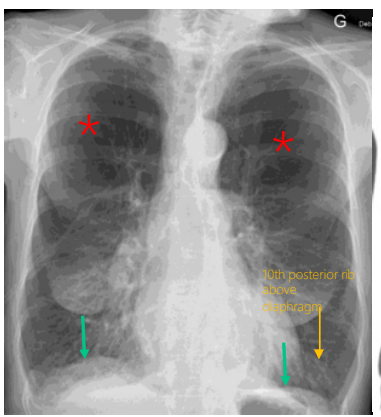

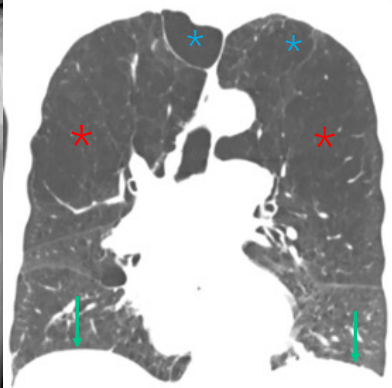

Based on its distribution, emphysema can be classified into:

- centrilobular > primarily affecting the central or proximal portions of the acinus, associated with cigarette smoking and commonly found in the upper lobes of the lungs.
- panacinar (panlobular) > involving the entire acinus, often associated with alpha-1 antitrypsin deficiency and mainly affecting the lower lobes.
- distal acinar (paraseptal) > predominantly affecting the distal portions of the acinus near the pleura and septa, commonly associated with smoking, bullae formation and pneumothorax, typically found in the lung periphery.

These different types may occur separately or coexist within an individual with emphysema and the distribution patterns can influence the clinical presentation and management of the condition.

/ Emphysema on CT

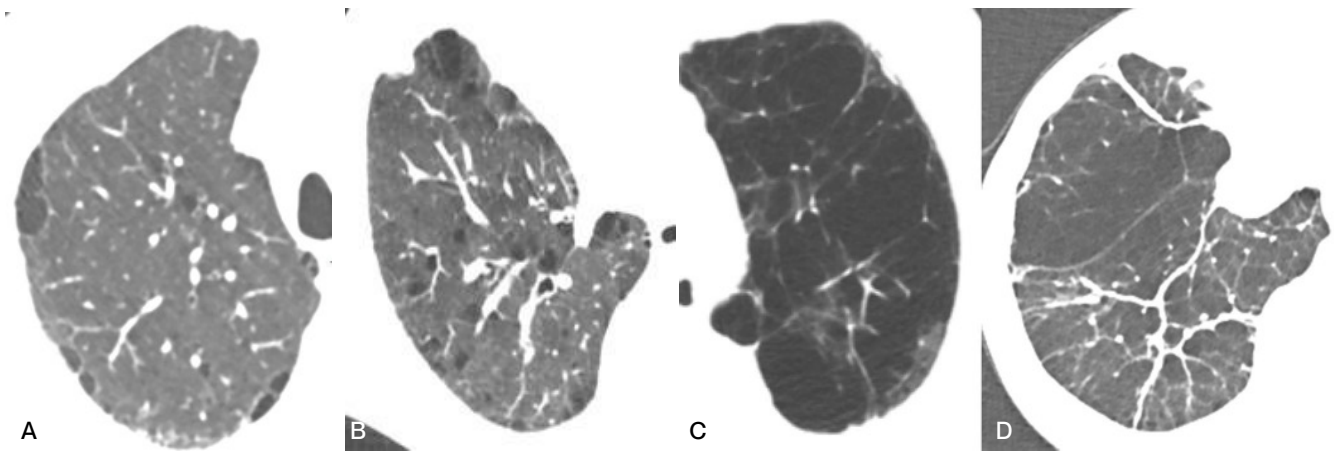

A. Mild paraseptal emphysema B. Mild centrilobular emphysema C. Advanced destructive centrilobular emphysema. D. Basal panlobular emphysema in a patients with Alpha-1-antitryspsin (A1AT) deficiency.

Pulmonary Oedema

CHAPTER OUTLINE:

/ Left Heart Failure

Pulmonary oedema = abnormal accumulation of fluid in the extravascular lung compartment, i.e., in the interstitium ± alveoli.

The pathophysiologic mechanisms leading to pulmonary oedema include

- increased pulmonary capillary hydrostatic pressure (left heart failure and fluid overload)
- abnormal leakage of fluid into alveoli due to damage of type II pneumocytes and endothelial cells in the alveoli

The most common cause of cardiogenic pulmonary oedema is left heart failure, which results in decreased cardiac output and increased pulmonary venous pressure.

The most common cause of non-cardiogenic pulmonary oedema are renal failure and ARDS (Acute Respiratory Distress Syndrome = acute lung injury with diffuse alveolar damage).

The pulmonary capillary wedge pressure (PCWP) is an important parameter used to evaluate cardiac function and to diagnose left heart failure and pulmonary oedema. It reflects the pressure exerted on lung capillaries by the blood in the left atrium during diastole. It is measured by inserting a catheter into the pulmonary artery (PA) and advancing the catheter until it wedges into a small PA branch. The PCWP provides an estimate of the pressure in the left atrium. The normal PCWP = 8 - 12 mmHg, the normal left atrial pressure = 5 - 10 mmHg. On a PA CXR, the upper lobe veins are smaller than the lower lobe veins because in an erect position effects of gravity are superimposed on the low pressure, low resistance vascular bed.

<!> ATTENTION

Features of left heart failure on CXRs include a continuum of imaging findings as follows:

- an increase of the left atrial pressure to 10 – 15 mmHg (PCWP = 13 – 18 mmHg) results in upper lobe venous diversion (synonym = venous cephalisation, redistribution) – cephalisation of pulmonary veins is an early sign of pulmonary oedema > see images on the next page
- an increase of the left atrial pressure to 16 – 22 mmHg (PCWP = 18 – 25 mmHg) results in interstitial pulmonary oedema with characteristic Kerley lines > see images on next pages
- finally, an increase of the left atrial pressure > 23 mmHg (PCWP > 25 mmHg) results in alveolar pulmonary oedema with characteristic alveolar opacities > see next pages
- pleural effusion and cardiomegaly are further features of left heart failure

<!> ATTENTION

Normal (PCWP = 8 - 12 mmHg) = Grade 0

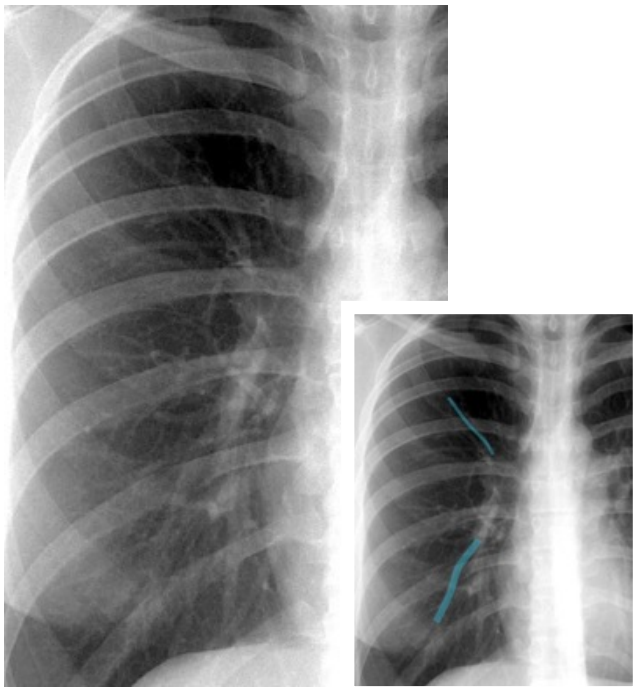

In the erect position, the upper lobe pulmonary veins have a smaller diameter than the lower lung veins, measured equidistant to the hilum.

Cephalisation of the pulmonary veins
(PCWP = 13 – 18 mmHg) = Grade 1 oedema

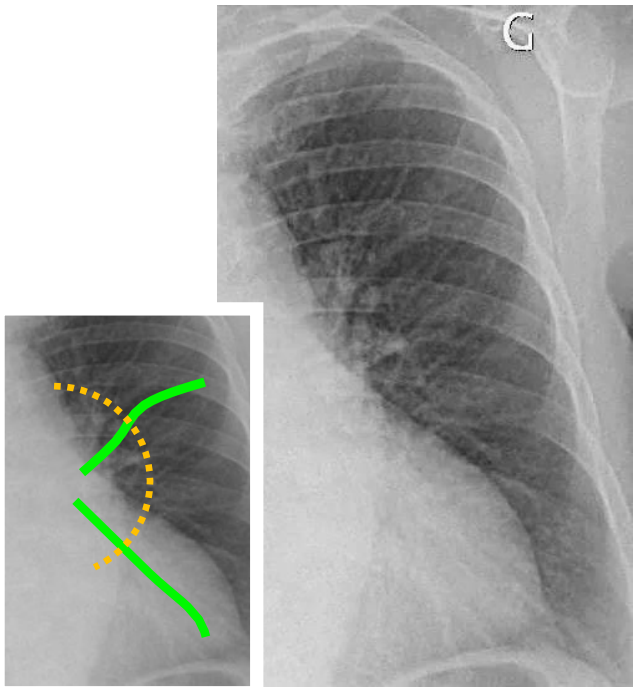

Cephalisation = the upper lobe pulmonary veins appear dilated as they branch away from the hilum. If the upper lobe veins have a similar or larger diameter than the lower lung veins, measured equidistant to the hilum, there is cephalisation.

CHAPTER OUTLINE:

Interstitial lung oedema (PCWP = 19 – 25 mmHg) = Grade 2 oedema
> transudate in the interstitium

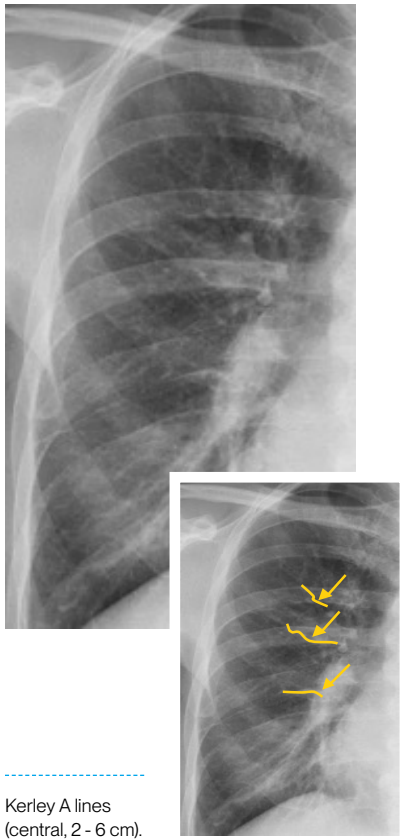

Kerley A lines (central, 2 - 6 cm).

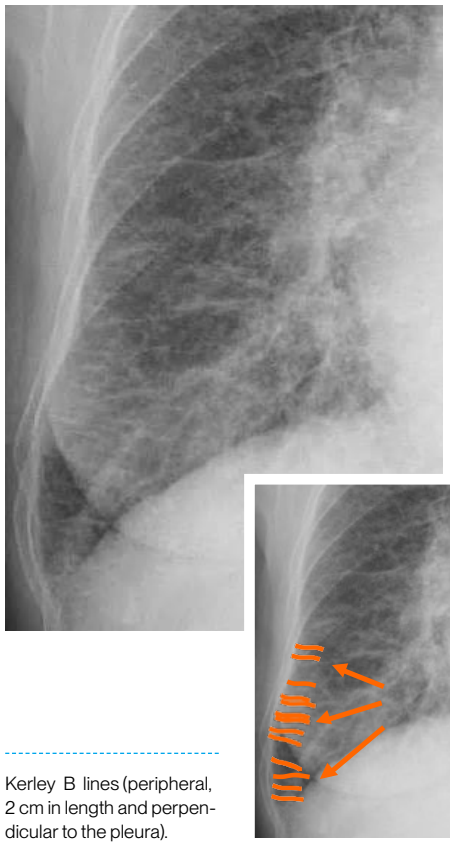

Kerley B lines (peripheral, 2 cm in length and perpendicular to the pleura).

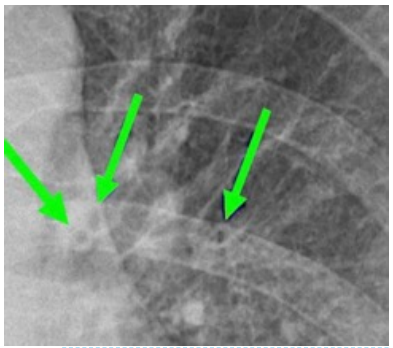

Peribronchovascular cuffing (green arrows) = fluid accumulation in the interstitial spaces around bronchi due to increased hydrostatic pulmonary circulation pressure > fluid leakage from capillaries into surrounding tissues. As a result, the bronchi appear surrounded by a thickened cuff on CXRs.

Grade 3 pulmonary oedema corresponds to alveolar oedema (PCWP > 25 mmHg).

On CXRs, alveolar oedema is characterised by:

- symmetrical distribution, i.e., both lungs are equally affected
- central predominance, i.e., oedema is more pronounced near the hilar regions of the lungs than towards the periphery
- gravity-dependent distribution, i.e., oedema tends to be more prominent in the lower half of the lungs, following the laws of gravity

These patterns can be explained by the mechanics of fluid pressure, with symmetrical distribution arising from pressure affecting both lungs, central predominance due to pressure starting from the heart and spreading outward and gravity dictating the distribution of blood volume and pressure within the lungs.

<!> ATTENTION

The central distribution on PA and AP CXRs of grade 3 pulmonary oedema leads to the typical "bat wing" or "butterfly appearance".

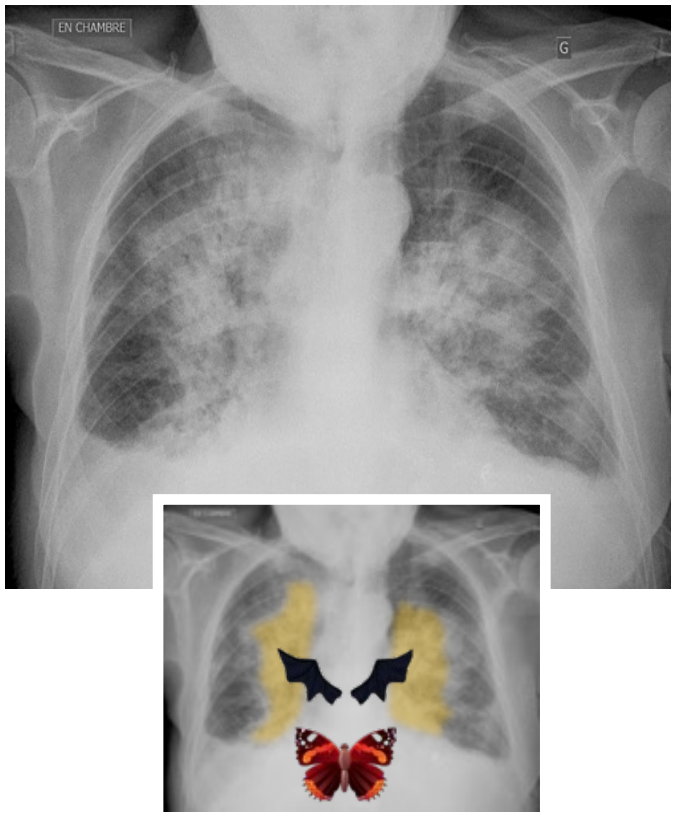

Chest Imaging

CHAPTER OUTLINE:

Increasing fluid pressure and volume in congestive heart failure, starting from the left atrium and progressing through the pulmonary vessels, interstitial and alveolar spaces results in pleural effusion.

Pleural effusions lead on CXRs to blunting of the costophrenic angles (red) and thickening of the oblique (light pink arrow) and horizontal (pink arrow) fissures.

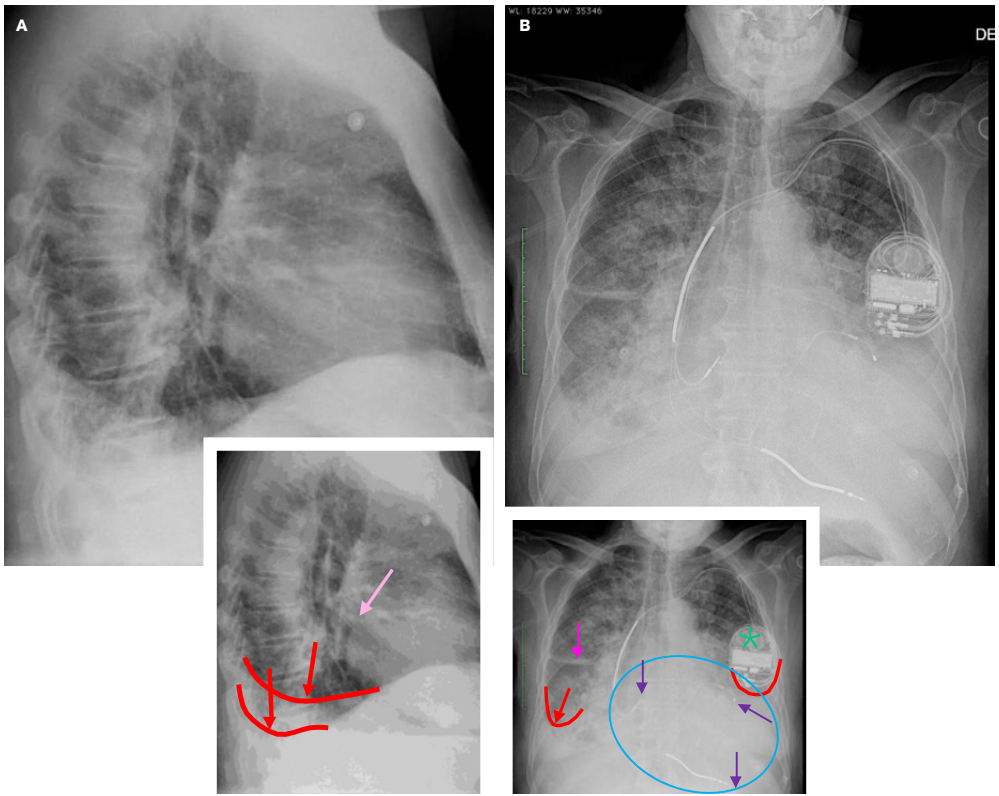

Lateral erect and AP CXRs in two different patients (A and B) with left heart failure , pulmonary oedema and pleural effusions in the costophrenic angles (red). Cardiomegaly ((blue circle) based on the position of the electrode tips (purple arrows) of the pacemaker (green asterisk), the heart size can be estimated on the PA CXR in patient B despite massive alveolar oedema). The cardiothoracic ratio is well above 0.5.

CHAPTER OUTLINE:

Pulmonary Hypertension

CHAPTER OUTLINE:

/ Pulmonary Hypertension (PH)

Pulmonary hypertension (PH) is characterised by increased pulmonary arterial pressure, structural changes in pulmonary circulation and the appearance of vaso-occlusive lesions.

PH is defined as mean pulmonary artery pressure > 20 mmHg. PH is called pre-capillary when the pressure in the left atrium (LA) is ≤ 20 mm Hg and pulmonary vascular resistance (PVR) is ≥ 3 Wood Units (WU, 1 Wood unit = 80 dynes × sec/cm^5). Otherwise (LA pressure > 20 mmHg and PVR < 3 WU), it is described as post-capillary.

There are 5 groups of PH depending on the aetiology:

- idiopathic or pulmonary artery disease (group 1)
- left heart disease (group 2)
- pulmonary parenchyma disease (group 3)
- chronic thromboembolic disease (group 4)
- various causes (group 5)

The clinical symptoms are nonspecific (dyspnoea, tiredness) and the diagnosis is often made late. The radiological assessment includes at least a CXR.

Depending on the clinical presentation cardiac ultrasound, chest CT, cardiac MRI and invasive pulmonary pressure measurement may be performed.

CXR may be normal or shows dilation of the pulmonary arteries (PA). It can also evidence right and/or left ventricular dilatation and parenchymal abnormalities suggesting a pulmonary cause of PH (group 3).

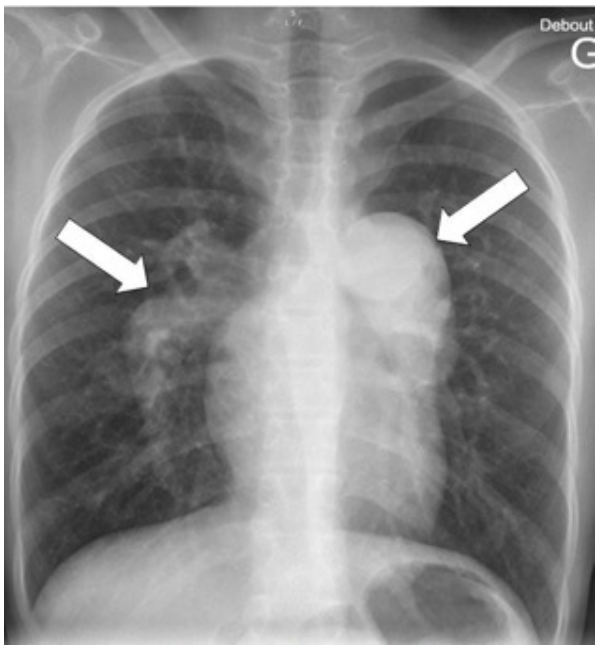

Significant dilation of the pulmonary arteries (arrows) on the PA CXR.

CT shows dilation of the right heart and PA. It may also detect the cause of PH, such as congenital heart malformations (group 1), lung parenchymal disease (group 3) or signs of chronic thromboembolic disease (CTED) (group 4).

Cardiac MRI can be useful to precisely analyse right ventricular function and may detect fibrosis at the insertion points of the right ventricle.

Group 1

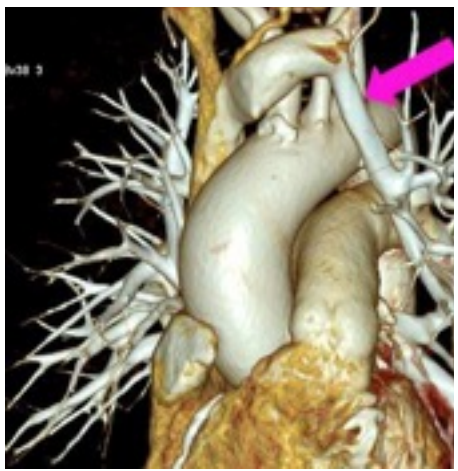

Abnormal pulmonary venous return of the left superior lobe (pink arrow).

Group 3

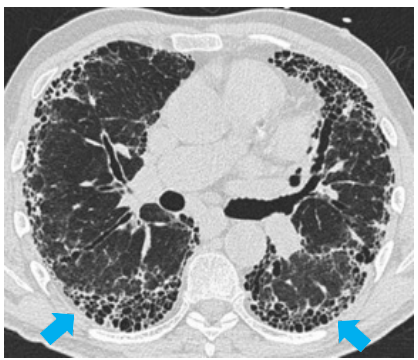

Pulmonary fibrosis with honeycomb lesions (blue arrows).

Group 4

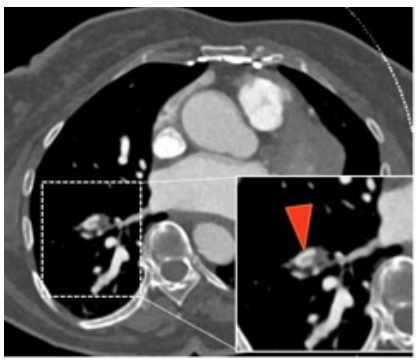

Organised thrombus (web lesion) within PA in a CTED (red arrow).

/ Take-Home Messages

- CXR is a quick, easily accessible and non-invasive exam enabling assessment of lung, mediastinal, pleural and chest wall diseases.
- Understanding the technical principles of CXR and a standardised reading approach are essential to reach the correct diagnosis.
- CT may overcome some of the limitations of CXR such as very subtle diseases and projection of other structures. It is primarily used:
  - to confirm or give a more detailed assessment of CXR findings
  - as a first line exam
  - in the case of a normal CXR
  - in the case of known limitations possibly false negatives of CXRs
  - to perform biopsy of selected lesions
- MRI is reserved to special cases, such as mediastinal diseases and is usually referred based on CT findings.
- Thoracic US might provide a quick first assessment at bedside and is useful for guiding interventional procedures.

References

- Lichtenstein DA. Ultrasound in the management of thoracic disease. Crit Care Med. 2007;35(5 Suppl):S250-S261. doi:10.1097/01.CCM.0000260670.67304.40
- Volpicelli G, Elbarbary M, Blaivas M, et al. International evidence-based recommendations for point-of-care lung ultrasound. Intensive Care Med. 2012;38(4):577-591. doi:10.1007/s00134-012-2513-4
- Abid I, Qureshi N, Lategan N, Williams S, Shahid S. Point-of-care lung ultrasound in detecting pneumonia: A systematic review. Can J Respir Ther. 2024 Jan 29;60:37-48. doi: 10.29390/001c.92182. PMID: 38299193; PMCID: PMC10830142.
- Jahanshir, A., Moghari, S.M., Ahmadi, A. et al. Value of point-of-care ultrasonography compared with computed tomography scan in detecting potential life-threatening conditions in blunt chest trauma patients. Ultrasound J 12, 36 (2020). https://doi.org/10.1186/s13089- 020-00183-6
- Sim AJ et al. A review of the role of MRI in diagnosis and treatment of early stage lung cancer. Clin Transl Radiat Oncol. 2020 Jun 6;24:16-22. doi: 10.1016/j.ctro.2020.06.002. PMID: 32596518; PMCID: PMC7306507.
- Koyama H, Ohno Y, Seki S, Nishio M, Yoshikawa T, Matsumoto S, Sugimura K. Magnetic resonance imaging for lung cancer. J Thorac Imaging. 2013 May;28(3):138-50. doi: 10.1097/RTI.0b013e31828d4234. PMID: 23549390.
- Farsad M. FDG PET/CT in the Staging of Lung Cancer. Curr Radiopharm. 2020;13(3):195-203. doi: 10.2174/1874471013666191223153755. PMID: 31868151; PMCID: PMC8206197.
- Kitajima, K., Doi, H., Kanda, T. et al. Present and future roles of FDG-PET/CT imaging in the management of lung cancer. Jpn J Radiol 34, 387–399 (2016). https://doi.org/10.1007/s11604-016-0546-2
- Groheux D, Quere G, Blanc E, Lemarignier C, Vercellino L, de Margerie-Mellon C, Merlet P, Querellou S. FDG PET-CT for solitary pulmonary nodule and lung cancer: Literature review. Diagn Interv Imaging. 2016 Oct;97(10):1003-1017. doi: 10.1016/j.diii.2016.06.020. Epub 2016 Aug 24. PMID: 27567555
- Felson B. Chest roentgenology. Philadelphia, Pa: Saunders, 1973.
- Goodman LR. Felson's principles of chest roentgenology, a programmed text. 5th edition. Elsevier 2020. ISBN-13 978-0323625678
- Jones J, Hacking C, Beames C, et al. Pleura. Reference article, Radiopaedia.org (Accessed on 01 Jun 2024) https://doi.org/10.53347/rID- 14507
- https://doi.org/10.1148/rg.2017160095
- Carter BW, Benveniste MF, Madan R, et al. ITMIG Classification of Mediastinal Compartments and Multidisciplinary Approach to Mediastinal Masses. Radiographics. 2017 Mar-Apr;37(2):413-436. doi: 10.1148/rg.2017160095. Epub 2017 Jan 27. PMID: 28129068.
- Jiao A, Nadim B, Hammer M, Jhala K. 3D Visual Guide to Lines and Stripes in Chest Radiography. Radiographics. 2023 Sep;43(9):e230017. doi: 10.1148/rg.230017. PMID: 37590159.
- WHO Classification of Tumours Editorial Board. WHO Classification of Thoracic Tumours. (2021) ISBN: 9789283245063

Chest Imaging

CHAPTER OUTLINE:

- Snoeckx A, Reyntiens P, Desbuquoit D, Spinhoven MJ, Van Schil PE, van Meerbeeck JP, Parizel PM. Evaluation of the solitary pulmonary
- nodule: size matters, but do not ignore the power of morphology. Insights Imaging. 2018 Feb;9(1):73-86. doi: 10.1007/s13244-017- 0581-2. Epub 2017 Nov 15. PMID: 29143191; PMCID: PMC5825309
- Hammer MM, Gupta S, Byrne SC. Volume Doubling Times of Benign and Malignant Nodules in Lung Cancer Screening. Curr Probl Diagn Radiol. 2023 Nov-Dec;52(6):515-518. doi: 10.1067/j.cpradiol.2023.06.014.
- Anand Devaraj, Bram van Ginneken, Arjun Nair, David Baldwin. Use of Volumetry for Lung Nodule Management: Theory and Practice. (2017) Radiology. 284 (3): 630-644. doi:10.1148/radiol.2017151022
- MacMahon H, Naidich DP, Goo JM, et al. Guidelines for Management of Incidental Pulmonary Nodules Detected on CT Images: From the Fleischner Society 2017. Radiology. 2017 Jul;284(1):228-243. doi: 10.1148/radiol.2017161659. Epub 2017 Feb 23. PMID: 28240562.
- Siegal DA, et al. Proportion of never smokers among men and women with lung cancer in 7 US states. JAMA Oncol. 2021 Feb 1; 7(2): 302-304. doi: 10.1001/jamaoncol.2020.6362.
- Centers for Disease Control and Prevention. National Center for Health Statistics. CDC WONDER On-line Database, compiled from Compressed Mortality File 1999-2014 Series 20 No. 2T, 2016.
- https://www.who.int/news-room/fact-sheets/detail/lung-cancer
- Siegel RL, Miller KD, Fuchs HE, Jemal A. Cancer Statistics, 2021. CA Cancer J Clin. 2021 Jan;71(1):7-33. doi: 10.3322/caac.21654. Epub 2021 Jan 12. PMID: 33433946.
- Hirsch FR, Scagliotti GV, Mulshine JL, Kwon R, Curran WJ Jr, Wu YL, Paz-Ares L. Lung cancer: current therapies and new targeted treatments. Lancet. 2017 Apr 1;389(10066):299-311. doi: 10.1016/S0140-6736(16)30958-8. Epub 2016 Sep 6. PMID: 27609408.
- Ong D, Cheung M, Cuenca P, Schauer S. Clinical Utility of Routine Chest X-Rays During the Initial Stabilization of Trauma Patients. South Med J. 2019 Jan;112(1):55-59.
- Winer-Muram HT. The solitary pulmonary nodule. Radiology. 2006;239 (1): 34-49. doi:10.1148/radiol.2391050343 - Pubmed citation
- National Lung Screening Trial Research Team; Church TR, Black WC, Aberle DR, Berg CD, Clingan KL, Duan F, Fagerstrom RM, Gareen IF, Gierada DS, Jones GC, Mahon I, Marcus PM, Sicks JD, Jain A, Baum S. Results of initial low-dose computed tomographic screening for lung cancer. N Engl J Med. 2013 May 23;368(21):1980-91. doi: 10.1056/NEJMoa1209120. PMID: 23697514; PMCID: PMC3762603.
- Sands J, Tammemägi MC, Couraud S, Baldwin DR, Borondy-Kitts A, Yankelevitz D, Lewis J, Grannis F, Kauczor HU, von Stackelberg O, Sequist L, Pastorino U, McKee B. Lung Screening Benefits and Challenges: A Review of The Data and Outline for Implementation. J Thorac Oncol. 2021 Jan;16(1):37-53. doi: 10.1016/j.jtho.2020.10.127. Epub 2020 Nov 12. PMID: 33188913.
- Hansell DM, Lynch DA, McAdams HP, Bankier AA. Images of Diseases of the Chest: Expert Consult. 5th edition.
- Aluja Jaramillo F, Gutierrez FR, Diaz Telli FG, Yevenes Aravena S, Javidan-Nejad C, Bhalla S. Approach to Pulmonary Hypertension: From CT to Clinical Diagnosis. Radiographics. 2018;38:357–73.
- Broncano J, Bhalla S, Gutierrez FR, Vargas D, Williamson EE, Makan M, Luna A. Cardiac MRI in Pulmonary Hypertension: From Magnet to Bedside. Radiographics. 2020;40:982–1002.

CHAPTER OUTLINE:

Test Your Knowledge

CHAPTER OUTLINE:

/ Test Your Knowledge

<?> QUESTION 1

Annotate the following anatomic structures:

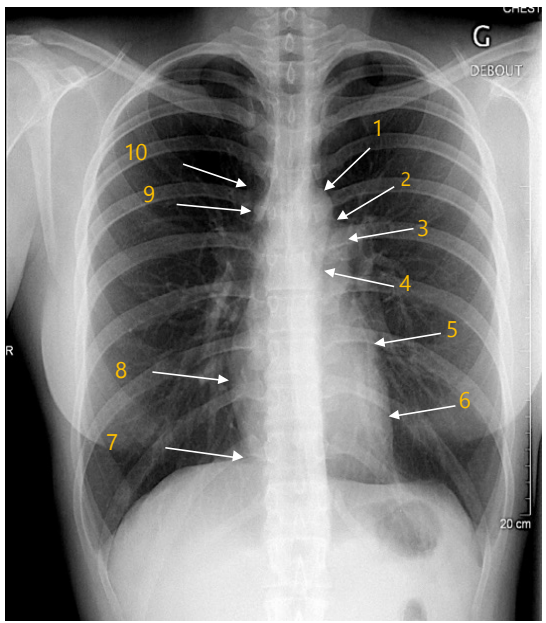

1 .....

2 .....

3 .....

4 .....

5 .....

6 .....

7 .....

8 .....

9 .....

10 .....

/ Test Your Knowledge

<?> ANSWER

1 Annotate the following anatomic structures:

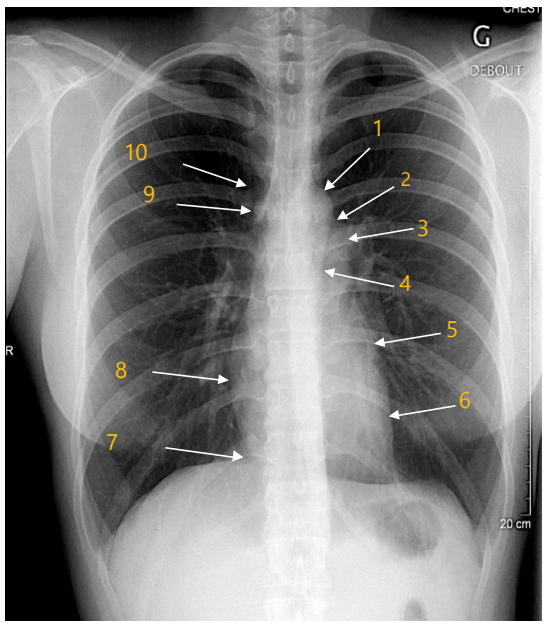

1 aortic arch
2 aortopulmonary window
3 pulmonary artery
4 descending aorta
5 left atrium
6 left ventricle
7 inferior vena cava
8 right atrium
9 azygos vein
10 superior vena cava

/ Test Your Knowledge

<?> QUESTION

2 Which statement(s) is/are true concerning this CXR?

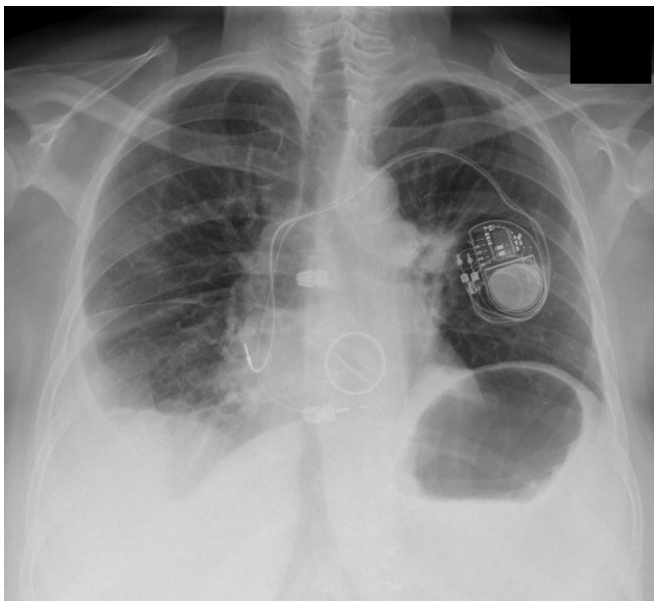

- ☐ This is an AP CXR
- ☐ The CXR is in maximum inspiration
- ☐ The CXR is in a strict anterior position
- ☐ The exposure is adequate

/ Test Your Knowledge

<?> ANSWER

2 Which statement(s) is/are true concerning this CXR?

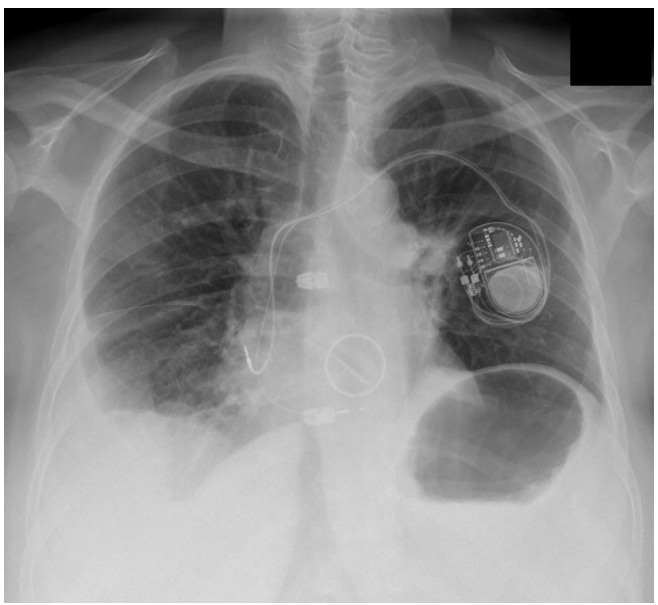

- ☐ This is an AP CXR
- ☐ The CXR is in maximum inspiration
- ☐ The CXR is in a strict anterior position
- ■ The exposure is adequate

/ Test Your Knowledge

<?> QUESTION

3 Among the following entities, which tumours typically occur in the anterior mediastinum? (several answers are possible)

- ☐ Thyroid cancer
- ☐ Lymphoma
- ☐ Neurogenic tumours
- ☐ Seminoma

/ Test Your Knowledge

<?> ANSWER

3 Among the following entities, which tumours typically occur in the anterior mediastinum? (several answers are possible)

- [x] Thyroid cancer
- [x] Lymphoma
- [ ] Neurogenic tumours
- [x] Seminoma

/ Test Your Knowledge

<?> QUESTION

4 Annotate the following mediastinal lines, stripes and structures:

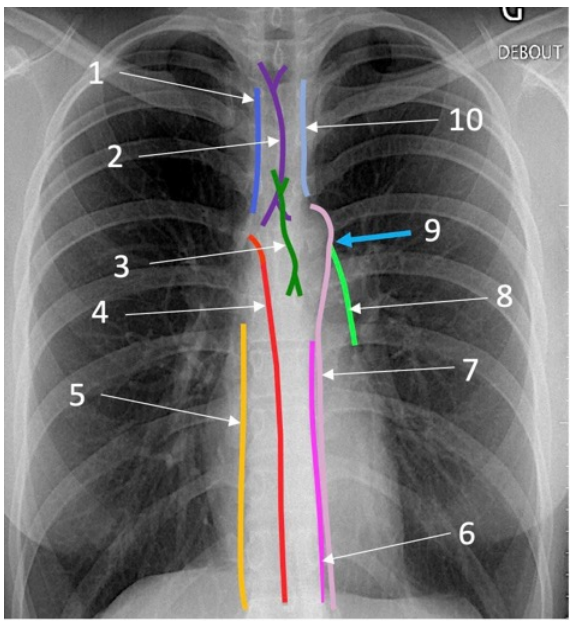

1 .....

2 .....

3 .....

4 .....

5 .....

6 .....

7 .....

8 .....

9 .....

10 .....

/ Test Your Knowledge

<?> ANSWER

4 Annotate the following mediastinal lines, stripes and structures:

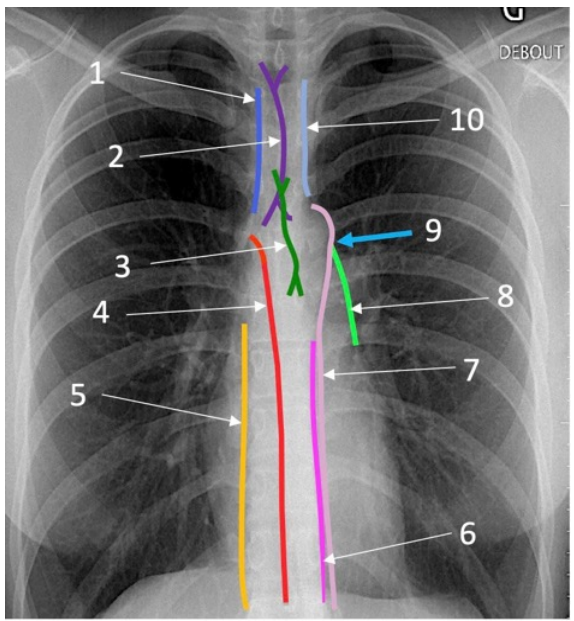

1 Right paratracheal stripe
2 Posterior junction line
3 Anterior junction line
4 Azygos oesophageal line
5 Right paravertebral line
6 Left paravertebral line
7 Para-aortic line
8 Aortic pulmonary stripe
9 Aortopulmonary window
10 Left paratracheal stripe

/ Test Your Knowledge

<?> QUESTION

5 Which type of lung opacification pattern corresponds to images A-D?

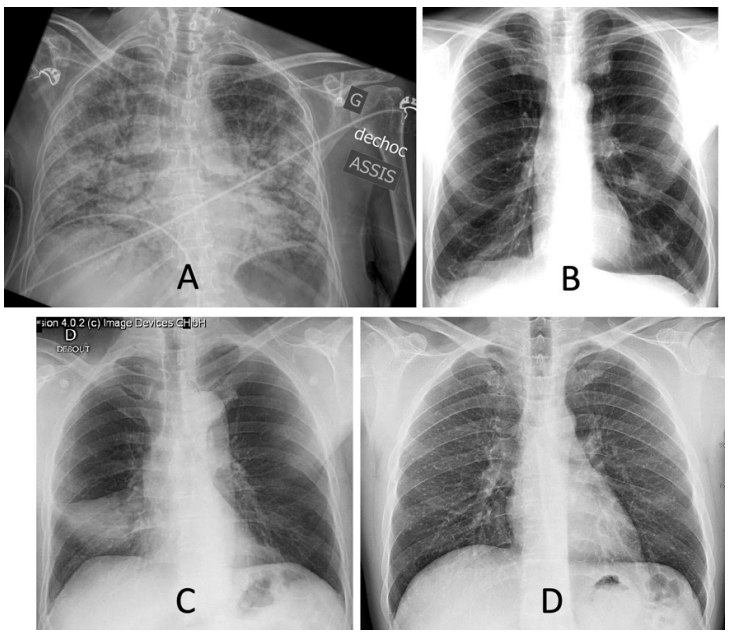

A .....

B .....

C .....

D .....

/ Test Your Knowledge

<?> ANSWER

5 Which type of lung opacification pattern corresponds to images A-D?

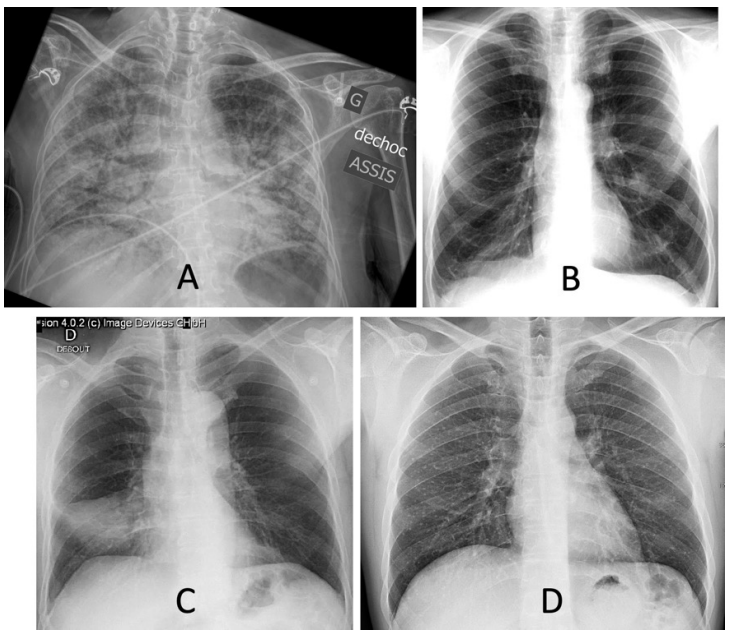

A Alveolar

B Nodule

C Atelectasis

D Interstitial (micronodular)

See pages 103-130 of this eBook chapter

/ Test Your Knowledge

<?> QUESTION

6 Which statement(s) is/are correct? This patient has...

- ☐ Loculated pleural effusions
- ☐ Cardiomegaly
- ☐ Intrapulmonary masses
- ☐ Right lower lobe atelectasis

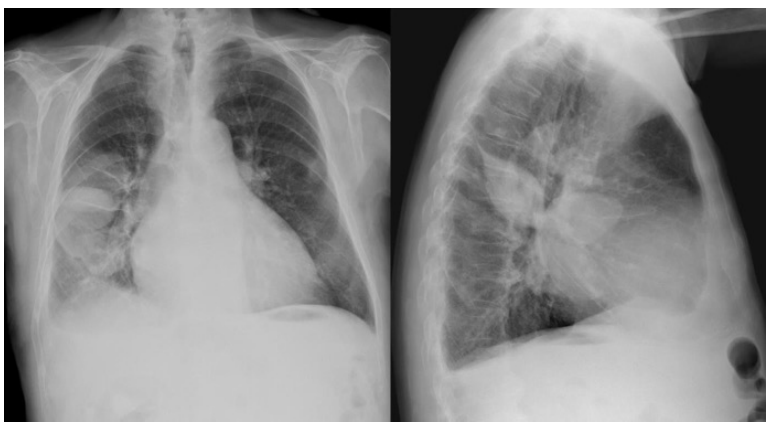

/ Test Your Knowledge

<?> ANSWER

6 Which statement(s) is/are correct? This patient has...

- ■ Loculated pleural effusions
- ■ Cardiomegaly
- ☐ Intrapulmonary masses
- ☐ Right lower lobe atelectasis

See pages 36 and 66 of the eBook chapter

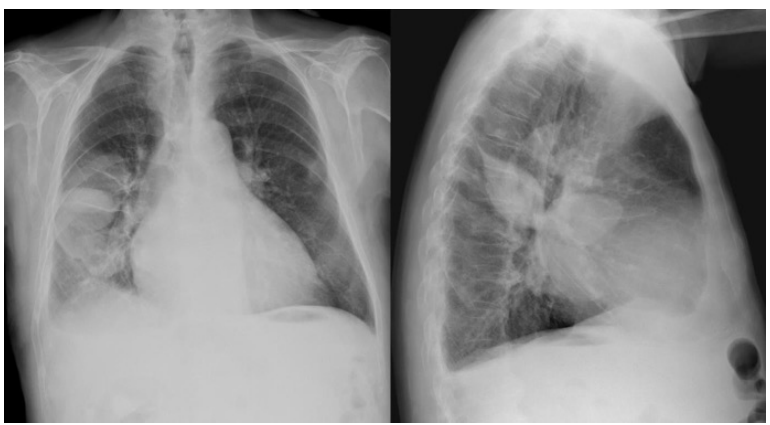

/ Test Your Knowledge

<?> QUESTION

7 Which statement(s) is/are true concerning this patient's imaging findings?

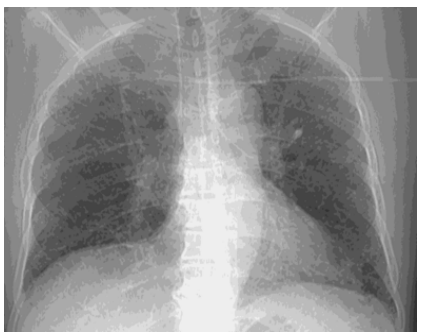

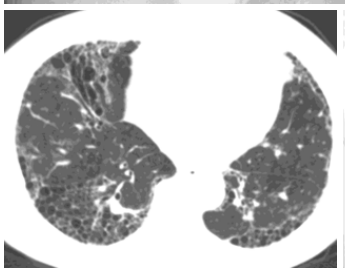

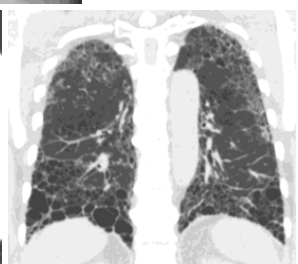

- ☐ The predominant pattern is nodular/micronodular
- ☐ The predominant pattern is honeycombing
- ☐ There are no signs of fibrosis/volume loss
- ☐ Connective-tissue disease related interstitial lung disease must be included in the differential diagnosis

/ Test Your Knowledge

<?> ANSWER

7 Which statement(s) is/are true concerning this patient's imaging findings?

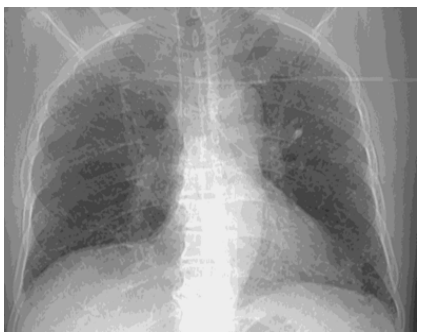

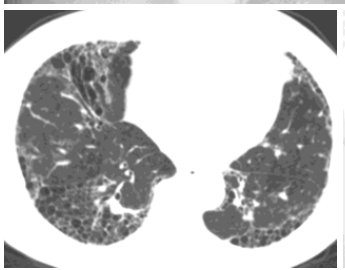

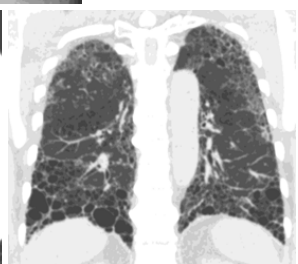

- ☐ The predominant pattern is nodular/micronodular
- ■ The predominant pattern is honeycombing
- ■ There are no signs of fibrosis/volume loss
- ☐ Connective-tissue disease related interstitial lung disease must be included in the differential diagnosis

See pages 109-112 of the eBook chapter

/ Test Your Knowledge

<?> QUESTION

8 Indicate to what pathophysiologic mechanisms seen in left cardiac failure correspond the following findings on a PA CXR?

- ☐ Venous cephalisation
- ☐ Peribronchial cuffing
- ☐ Kerley B lines
- ☐ Kerley A lines
- ☐ Alveolar opacification

/ Test Your Knowledge

<?> ANSWER

8 Indicate to what pathophysiologic mechanisms seen in left cardiac failure correspond the following findings on a PA CXR?

- ☐ Venous cephalisation
- ☐ Peribronchial cuffing
- ☐ Kerley B lines
- ☐ Kerley A lines
- ☐ Alveolar opacification

See detailed explanations on pages 134 – 138 of this eBook chapter

/ Test Your Knowledge

<?> QUESTION

9 Which statement(s) is/are correct?

- ☐ Solitary lung nodules are solid nodules without associated atelectasis, pneumonia or lymphadenopathy
- ☐ To evaluate nodule growth, volumetry rather than 2D measurement of lesion size is recommended
- ☐ The prevalence of lung cancer in solitary lung nodules larger than 10 mm in size is less than 10%
- ☐ A solitary lung nodule detected in a patient taking part in a lung screening programme should be followed according to the guidelines of the Fleischer Society

/ Test Your Knowledge

<?> ANSWER

9 Which statement(s) is/are correct?

- [x] Solitary lung nodules are solid nodules without associated atelectasis, pneumonia or lymphadenopathy
- [x] To evaluate nodule growth, volumetry rather than 2D measurement of lesion size is recommended
- [ ] The prevalence of lung cancer in solitary lung nodules larger than 10 mm in size is less than 10%
- [ ] A solitary lung nodule detected in a patient taking part in a lung screening programme should be followed according to the guidelines of the Fleischer Society

See pages 114, 118 and 119 of the eBook chapter

/ Test Your Knowledge

<?> QUESTION

10 Which of the following statements regarding pathology of the pleura and pleural cavity is/are correct?

- ☐ Typical signs of tension pneumothorax are displacement of the mediastinum towards the pneumothorax, elevation of the diaphragm and decreased distance between the ribs
- ☐ Pleural plaques can be detected on CXRs and are related to asbestos exposure
- ☐ CXR is the preferred imaging modality to depict pleural pathology
- ☐ Malignant mesothelioma is more common than pleural metastases

/ Test Your Knowledge

<?> ANSWER

10 Which of the following statements regarding pathology of the pleura and pleural cavity is/are correct?

- ☐ Typical signs of tension pneumothorax are displacement of the mediastinum towards the pneumothorax, elevation of the diaphragm and decreased distance between the ribs
- ■ Pleural plaques can be detected on CXRs and are related to asbestos exposure
- ☐ CXR is the preferred imaging modality to depict pleural pathology
- ☐ Malignant mesothelioma is more common than pleural metastases

See page 71 of this eBook chapter

Acknowlegments

This eBook chapter includes parts of a didactic course of the teaching programme for medical students at the University of Geneva entitled " Introduction to the Clinical Approach" (Unité d'Introduction à la Démarche Clinique, UIDC, 1ère année de master), as well as images from the course entitled "Learning in the Clinical Environment, Rotation Internal Medicine" (Apprentissage en milieu clinique rotation médecine interne). This course units, which I have developed over many years are being well received by medical students and junior residents.

I would herewith like to acknowledge the colleagues of the Academic Department of Radiology, Faculty of Medicine, University of Geneva, who have participated in presenting the above-mentioned chest radiology courses to medical students and/or who have added some of the clinical images over the years (in alphabetical order): Dominique Didier, Thomas De Perrot, Xavier Montet, Alexandra Platon, Pierre-Alexandre Poletti, Max Scheffler and Maria Isabel Vargas.

Minerva Becker

CHAPTER OUTLINE: